الجمهورية الجزائرية الديمقراطية الشعبية
وزارة التعليم العالي والبحث العلمي

University Setif 1 Ferhat ABBAS
Faculty of Nature and Life Sciences

جامعة سطيف 1 فرحات عباس
كلية علوم الطبيعة والحياة

Department of Biochemistry

N°: ……/SNV/2024

THESIS

Presented by

DJEHICHE Cheima

For obtaining the diploma of

DOCTORATE 3rd CYCLE

Field: Biological Sciences
Specialty: Biochemistry

Study of anti-inflammatory and immunomodulatory properties of *Ammodaucus leucotrichus*

Publically presented on 02/11/2024

Jury:

President	**Pr BAGHIANI Abderrahmane**	**Professor**	**Univ Setif 1**
Supervisor	**Pr ARRAR Lekhmici**	**Professor**	**Univ. Setif 1**
Co-supervisor	**Dr BENZIDANE Nadia**	**MCA**	**Univ. Setif 1**
Examiners	**Pr NECIB Youcef**	**Professor**	**Univ Constantine 1**
	Dr BAHI Ahlem	**MCA**	**Univ Constantine 1**
	Dr AMRAOUI Nacer	**MPA**	**Univ Setif1**

Laboratory of Applied Biochemistry

Dedicates

It is with God's help and grace that I have completed this modest work.

To my wonderful mom,

Who embodies infinite love and wisdom. Your immeasurable support and kindness illuminate each step of my journey with a gentle light.

To my father,

a model of perseverance and determination. Your strength and example have paved the way for a brilliant success.

To my dear husband Mehdi,

a companion in every moment. Your unwavering love is the solid pillar supporting my happiness every day.

To my dear parents-in-law,

for their warm welcome and sincere love. Your presence enriches my life in an infinite way.

To my beloved brother Amir,

a partner in childhood memories and a loyal friend. Your precious support is an invaluable gift, along with his sweet fiancée, Douaa.

To my sister Imene,

the radiant light of my life. Your optimism and joy are a constant source of inspiration.

To my sister-in-law Maroua,

gone but never forgotten. Her memory will forever be engraved in our hearts, may God welcome her in paradise.

To my lovely sister-in-law Safa and my brother-in-law Borhene.

Your presence adds a unique richness to our big family.

To the adorable little ones, Wijdene and Soulimen,

rays of sunshine brightening our days. Your innocence and happiness are priceless treasures.

This dedication, filled with sincere love, is a vibrant tribute to my family, united by unbreakable bonds that transcend the boundaries of life.

I love you all immensely.

Acknowledgments

First and foremost, I express my deepest gratitude to Allah the Almighty, who gave me the courage and determination to complete this work.

I extend my sincere thanks to Professor Lekhmici Arrar of University, Sétif 1 Ferhat Abbas, for agreeing to supervise me, for opening the doors of his laboratory and team to me, for his invaluable advice, and for sharing his expertise and competence throughout this research. I am also deeply grateful to myco-supervisor, Dr. Benzidane Nadia, for her guidance and invaluable assistance.

I would like to particularly thank the members of the jury for agreeing to evaluate this work and serve as examiners for this thesis:

I warmly thank Professor Abderrahmane Baghiani of the Department of Biochemistry at Ferhat Abbas University, Sétif 1, for welcoming me into his laboratory, for his availability and valuable advice, and for agreeing to chair the jury.

My sincere thanks also go to Professor Necib Youcef and Dr. Bahi Ahlem from the University of Frères Mentouri, Constantine 1, as well as Dr. Amraoui Nacer from University Sétif 1 Ferhat Abbas, for honoring me by serving as examiners for this thesis.

I would like to express my gratitude to my friend and sister, Dr. Djeghim Hanane, who supported me throughout the completion of this thesis.

Finally, I extend my heartfelt thanks to all my teachers and colleagues from the Department of Biochemistry and Cellular and Molecular Biology at the University of Constantine, particularly Dr. Teniou Soumia, Dr. Klibet Fahima, Dr. Zeghdar Moufida, and Dr. Moussaoui Samira. I also wish to thank the teachers from the Department of Biochemistry at the University of Sétif, especially Professor Nouredine Charef, for his help and advice, which were of great benefit throughout this work.

List of publications and communications

Publications

Djehiche, C., Benzidane, N., Djeghim, H., Tebboub, M., Mokrani, E. H., Mebrek, S., ... & Barhoum, A. (2024).Exploring the TherapeuticPotential of *Ammodaucusleucotrichus*SeedExtracts: A Multi-FacetedAnalysis of Phytochemical Composition, Anti-InflammatoryEfficacy, Predictive Anti-ArthriticProperties, and Molecular Docking Insights.Pharmaceuticals, 17(3), 385.

Djehiche, C., Benzidane, N., Djeghim, H., Tebboub, M., Mebrek, S., Abdelouhab, K., ... & Barhoum, A. (2024).*Ammodaucus Leucotrichus*SeedExtract as a PotentialTherapy in Animal Models of RheumatoidArthritisInduced by Complete Freund Adjuvant and Chicken Cartilage Collagen.AppliedBiochemistry and Biotechnology, 1-25.

Communications

Djehiche C, Benzidane N, Arrar L, 2022. Type ll collagen purified from chicken cartilage.1st International Electronic Conference on Processes,17-31 May 2022, online.

Djehiche C, Benzidane N, Djeghim H, Arrar L, 2022. Purification of type II collagen from chicken sternum. International Seminar on Organic and Pharmaceutical Chemistry, Skikda, 11-12 October 2022.

Djehiche C, Benzidane N, Djeghim H, Arrar L, 2022. Evaluation of the antiarthritic potential of *Ammodaucus leucotrichus in vitro.*1st International Seminar on Green Biotechnology and Food Security, Khenchela 16-17 Novembre 2022.

Djehiche C, Benzidane N,Djeghim H, Tebboub M, Mokrani ELH, Arrar L, 2023. In Vitro biological actuvity and molecular docking study of *Ammodaucus leucotrichus* .1st international seminar on the valorization of Biotechnological Research Results by Bioindustries, Constantine, 4-5 October 2023.

Djehiche C, Benzidane N, Djeghim H, Tebboub M, Arrar L, 2023.Alzheimer disease, TherapiesBased on *Ammodaucus leucotrichus*.1st National Seminar in Presential by-products of the Agri-Food Industry Valorization and Innovation, Oum-EL-Bouaghi, 30-31 Octobre 2023.

Djehiche C, Benzidane N, Djeghim H, Tebboub M, Arrar L, 2023. The effect of methanolic extract of Ammodaucus leucotrichus on arthritic rats.1st National Seminar on Present and Future Biomolecules, Algiers, 16 November 2023.

Djehiche C, Benzidane N, Djeghim H, Tebboub M, Arrar L, 2023. Phytochemical-basedtherapies for Alzheimer disease, Rheulatoid Arthritis and Diabetes. National Conference on Phytobiotehcnology, El-Taref, 17-18 December 2023.

Djehiche C, Benzidane N, Djeghim H, Tebboub M, Arrar L, 2023. Anti-arthriticEffect of *Ammodaucus leucotrichus in vivo.*4th International Conference on Food, Agriculture and animal sciences held in sivas/Turkey,27-29 April 2023.

Djehiche C, Benzidane N, Djeghim H, Tebboub M, Arrar L, 2024. Molecular docking studies of extracts and essential oils isolated from a medicinal plant of *Ammodaucus leucotrichus* as potential inhibitors of Rheumatoid Arthritis disease. 3th International Electronic Conference on Biomolecules, 23-25 April 2024, online, Basel, Switzerland.

الملخص

بحثت هذه الدراسة المعمقة في إمكانات مستخلصات بذور الكمون الصوفي *Ammodaucus Leucotrichus* كعامل علاجي لالتهاب المفاصل الرثوي. تم اختبار مستخلصات الميثانول والهكسان لدراسة خصائصها المضادة لالتهاب المفاصل الرثوي. أظهر مستخلص الميثانول قدرة كبيرة على تثبيط التربسين، وهو إنزيم يشارك في الالتهاب، بنسبة 85% عند تركيز 125 ميكروغرام/مل. وكان هذا متفوقًا بشكل ملحوظ على مستخلص الهكسان والدواء المضاد للالتهابات الشائع الاستخدام، ديكلوفيناك. من ناحية أخرى، أظهر مستخلص الهكسان قدرة ملحوظة على منع ترسب ألبومين المصل البقري، وهو بروتين نموذجي، بنسبة 90.4% عند تركيز 62.5 ميكروغرام/مل. تم إحداث التهاب المفاصل الروماتويدي في نماذج الفئران باستخدام طريقتين: التحصين باستخدام مساعد فروند الكامل ومحلول الكولاجين من النوع الثاني المشتق من غضروف الدجاج. تم تقييم الفعالية العلاجية للمستخلصات بجرعات مختلفة ومقارنتها مع الميثوتريكسيت، وهو علاج التهاب المفاصل الروماتويدي لدى البشر. أدت كل من المستخلصات والميثوتريكسيت إلى تحسين حركة الفئران، كما يتضح من زيادة مسافة المشي، وطول الخطوة، والمسافة داخل الخطوة، ومنطقة البصمة. كما أنها أثرت بشكل إيجابي على العلامات البيوكيميائية للالتهاب، مما أدى إلى زيادة تركيز الجلوتاثيون المضاد للأكسدة في المصل وتقليل تركيز المكمل C3 والمالوندیالدهید والميلوبيروكسيديز. وكشف التحليل الإضافي باستخدام قياس الطيف الكتلي للغاز عن وجود العديد من المستقلبات الثانوية في المستخلصات. في دراسات نظرية in silico حددت عدة مركبات ذات نشاط مثبط محتمل للتربسين: 2-هيدروكسي أسيتو هيدرازيد يظهر تأثيرات مثبطة متفوقة مقارنة بالديكلوفيناك. في الختام، توفر هذه الدراسة أدلة دامغة تشير إلى إمكانات مستخلصات بذور الكمون الصوفي كعلاج بديل واعد لالتهاب المفاصل الروماتويدي. تمهد النتائج الطريق لمزيد من البحث والتطوير في هذا المجال، مما قد يؤدي إلى خيارات علاجية جديدة للمرضى الذين يعانون من هذه الحالات المنهكة.

الكلمات المفتاحية: *Ammodaucus Leucotrichus*؛ الكولاجين؛ المساعد الكامل لفروند؛ التهاب المفصل الرثوي؛ تحليل GC-MS ؛ *in silico* ; التربسين.

Abstract

This comprehensive study investigated the potential of *Ammodaucus leucotrichus* seed extracts as a therapeutic agent for rheumatoid arthritis and joint inflammation. Methanol and n-hexane extracts were tested for their anti-inflammatory and anti-arthritic properties. The methanol extract demonstrated a significant ability to inhibit trypsin, an enzyme involved in inflammation, by 85% at a concentration of 125 µg/ml. This was notably superior to the n-hexane extract and the commonly used anti-inflammatory drug, diclofenac. On the other hand, the n-hexane extract showed a remarkable ability to prevent the denaturation of bovine serum albumin, a model protein, by 90.4% at a concentration of 62.5 µg/ml. Rheumatoid arthritis was induced in rat models using two methods: immunization with Freund's complete adjuvant and a solution of type II collagen derived from chicken cartilage. The therapeutic efficacy of the extracts was evaluated at varying doses and compared with methotrexate, a standard treatment for rheumatoid arthritis in humans. Both the extracts and methotrexate improved the mobility of the rats, as evidenced by increased walking distance, stride length, intra-step distance, and footprint area. They also positively influenced biochemical markers of inflammation, increasing the serum concentration of the antioxidant glutathione and reducing that of complement C3, malondialdehyde, and myeloperoxidase. Further analysis using gas chromatography-mass spectrometry revealed the presence of several secondary metabolites in the extracts. *In silico* docking studies identified several compounds with potential trypsin inhibitory activity: 2-hydroxyaceto hydrazide showing superior inhibitory effects compared to diclofenac. In conclusion, this study provides compelling evidence that suggests the potential of Ammodaucus leucotrichus seed extracts as a promising alternative therapy for rheumatoid arthritis and joint inflammation. The findings pave the way for further research and development in this area, potentially leading to new therapeutic options for patients suffering from these debilitating conditions.

Keywords: *Ammodaucus leucotrichus*; Collagen II; Complete Freund Adjuvant; Rheumatoid arthritis; GC–MS analysis; *in silico*; trypsin.

Résumé

Cette étude approfondie a examiné le potentiel des extraits de graines d'*Ammodaucus leucotrichus* en tant qu'agent thérapeutique contre la polyarthrite rhumatoïde et l'inflammation des articulations. Les extraits de méthanol et de n-hexane ont été testés pour leurs propriétés anti-inflammatoires et antiarthritiques. L'extrait méthanolique a démontré une capacité significative à inhiber la trypsine, une enzyme impliquée dans l'inflammation, de 85 % à une concentration de 125 µg/ml. Celui-ci était nettement supérieur à l'extrait de n-hexane et au médicament anti-inflammatoire couramment utilisé, le Diclofénac. D'autre part, l'extrait de n-hexane a montré une capacité remarquable à empêcher la dénaturation de l'albumine sérique bovine, une protéine modèle, de 90,4 % à une concentration de 62,5 µg/ml. La polyarthrite rhumatoïde a été induite chez des modèles de rats à l'aide de deux méthodes : l'immunisation avec l'adjuvant complet de Freund et avec une solution de collagène de type II dérivée du cartilage de poulet. L'efficacité thérapeutique des extraits a été évaluée à différentes doses et comparée au méthotrexate, un traitement standard de la polyarthrite rhumatoïde chez l'être humain. L'extrait de methanol et le méthotrexate ont amélioré la mobilité des rats, comme en témoignel'augmentation de la distance de marche, de la longueur des foulées, de la distance intra-pas et de la surface de l'empreinte. Ils ont également influencé positivement les marqueurs biochimiques de l'inflammation, augmentant la concentration sérique du glutathion antioxydant et réduisant celle du complément C3, du Malodialdéhyde et de la myéloperoxydase. Une analyse plus approfondie par chromatographie en phase gazeuse et spectrométrie de masse a révélé la présence de plusieurs métabolites secondaires dans les extraits. Des études d'amarrage *in silico* ont identifié plusieurs composés ayant une activité potentielle d'inhibition de la trypsine : le 2-hydroxyacéto hydrazide présentant des effets inhibiteurs supérieurs à ceux du Diclofénac. En conclusion, cette étude fournit des preuves convaincantes suggérant le potentiel des extraits de graines *d'Ammodaucus leucotrichus* en tant que thérapie alternative prometteuse pour la polyarthrite rhumatoïde et l'inflammation des articulations. Les résultats ouvrent la voie à de nouvelles recherches et développements dans ce domaine, conduisant potentiellement à de nouvelles options thérapeutiques pour les patients souffrant de ces maladies débilitantes.

Mots clés : *Ammodaucus leucotrichus* ; Collagène II ; Complete Freund Adjuvant; Arthrite rhumatoïde; Analyse GC-MS ; In *silico* ; Trypsine.

Table List

List of Figures

List of Abbreviations

AIA: Adjuvant-Induced Arthritis

ACPA: Anti-Citrullinated Protein Antibodies

BSA: Bovine Serum Albumin

bFGF: Basic Fibroblast Growth Factor

CAT: Catalase

CFA: Complete Freund's Adjuvant

COX: Cyclooxygenase

DAMPs: Danger-Associated Molecular Patterns

DMARDs: Disease-Modifying Antirheumatic Drugs

EPA: Eicosapentaenoic Acid

ECM: Extracellular Matrix

EDTA: Ethylenediamine Tetraacetic Acid

FRAP: Ferric Reducing Antioxidant Power

GC-MS: Gas Chromatography-Mass Spectrometry

GPx: Glutathione Peroxidase

GM-CSF: Granulocyte-Monocyte Colony-Stimulating Factor

H&E: Hematoxylin and Eosin

HLA: Human Leukocyte Antigen

iNOS: Inducible Nitric Oxide Synthase

ICAM: Intercellular Adhesion Molecule

IC50: Inhibitory Concentration

IFNs: Interferons

IL: Interleukin

JAK/STAT: Janus Kinase/Signal Transducers and Activators of Transcription

LT: Leukotrienes

LOX: Lipoxygenase

LFA-1: Lymphocyte Function-Associated Antigen 1

M-CSF: Macrophage Colony-Stimulating Factor

MDA: Malondialdehyde

ME: Methanolic Extract

MTX: Methotrexate

MAPK: Mitogen-Activated Protein Kinase

NEDD: N-1-Naphthylethylenediamine Dihydrochloride

NADPH: Nicotinamide Adenine Dinucleotide Phosphate

NFκB: Nuclear Factor Kappa B

NFAT: Nuclear Factor of Activated T Cells

OECD: Organisation for Economic Cooperation and Development

PAD : Peptidyl Arginine Deiminase

PAF : Platelet-Activating Factor

PDGF : Platelet-Derived Growth Factor

PAMPs : Pathogen-Associated Molecular Patterns

PMNs: Polymorphonuclear Neutrophils

PGE2 : Prostaglandin E2

PG : Prostaglandins

RNS : Reactive Nitrogen Species

ROS : Reactive Oxygen Species

RANKL: Receptor Activator of NFκB Ligand

SPMs: Specialized Pro-Resolving Mediators

SD : Standard Deviation

SAIDs: Steroidal Anti-Inflammatory Drugs

SOD : Superoxide Dismutase

SFL : Synoviocyte Fibroblasts-Like

TNF : Tumor Necrosis Factor

Table of content

RESULTS AND DISCUSSION

Introduction

Introduction

Autoimmune diseases (AD) arise from the immune system's inability to accurately distinguish between "self" and "non-self," leading to organ- or systemic-specific inflammation. Rheumatoid arthritis (RA), a prominent autoimmune disorder, is characterized by inflammatory changes in joint synovial tissue, cartilage, bone, and occasionally extra-articular locations. Inflammatory cytokines result from interactions between synovial-like fibroblasts (FLS), macrophages, and infiltrating lymphocytes. The inflammatory microenvironment can disrupt the balance between osteoclast-mediated bone resorption and osteoblast-mediated bone production, contributing to bone deterioration. RA's pathophysiology and refractory challenges are influenced by factors like aging, smoking history, immunogenicity, and genetic polymorphisms.

Current pharmacological interventions for RA, including non-steroidal anti-inflammatory drugs (NSAIDs), immunosuppressive glucocorticoids, and disease-modifying antirheumatic drugs (DMARDs), while effective, come with significant adverse effects.Given the substantial disability rate (43–48%) and a disease progression time of 5–10 years, there is a critical need for alternative treatments. This study shifts its focus to functional medicinal plants as potential alternatives.

The use of medicinal plants in treating rheumatoid arthritis has gained attention due to their therapeutic benefits and fewer side effects compared to conventional medications. Plants like Turmeric, Boswellia serrata, Willow bark, Ginger, Devil's Claw, and Cat's Claw have shown anti-inflammatory, analgesic, and immunomodulatory properties, however, further research is needed to establish precise mechanisms and dosages for optimal therapeutic benefits in RA treatment.

The genus *Ammodaucus* belonging to the Apiaceae family, has only one species, *Ammodaucus leucotrichus Coss. & Durieu*. This aromatic and medicinal plant, distributed in North Africa and tropical Africa, is recognized for its therapeutic compounds. Commonly known as Kammûnes-sofi or "Moudrayga" in Algeria, *Ammodaucus leucotrichus* has been traditionally used for various illnesses.

This study addresses the limitations of current anti-inflammatory treatments for RA by exploring the potential of *Ammodaucus leucotrichus* extracts. Using specific solvent systems like methanol and n-hexane, the study analyzes the anti-inflammatory and anti-arthritic properties of *Ammodaucus leucotrichus* seeds. Techniques such as gas chromatography-mass spectrometry (GC-MS) identify phytochemical constituents. In vitro assessments include protein denaturation assays and proteinase inhibitory activity assays targeting trypsin. The study further explores the in vivo antiarthritic effects of *Ammodaucus leucotrichus* extracts in animal models induced with collagen and complete Freund's adjuvant (CFA).

A crucial aspect of the study involves molecular docking studies *in silico*, evaluating the binding affinity of key compounds with trypsin, a vital enzyme in rheumatoid arthritis processes. The interaction of phytocompounds with human enzymes is examined through binding affinity assessment and PASS conceptual prediction, complemented by ADME/T studies for comprehensive comprehension.

This research aims to provide a groundbreaking therapeutic approach with fewer adverse effects for individuals with arthritis. By exploring the potential of *Ammodaucus leucotrichus* seed extracts, the study contributes to the quest for novel and more efficient treatments for rheumatoid arthritis, addressing challenges associated with conventional medications.

BIBLIOGRAPHIC SYNTHESIS

1. Immunomodulation

The immune system is a sophisticated, dynamic physiological system that relies on a network of connections created by thousands of cells and molecules to carry out its essential duties (Rankin *et al.,* 2018). The immune system serves as a defense mechanism and is vital to survival. It is also intimately linked to pathology and nearly every known illness, including inflammation, cancer, infection, autoimmune disorders, obesity and aging (Soares *et al.,* 2017). The onset of various diseases is usually accompanied by hypoactivation or hyperactivation of the immune system. Some diseases, most frequently autoimmune disorders and allergies, are brought on by viruses or by the immune system becoming overactive (Saferding *et al.,* 2020).

The impact of immunomodulatory biomaterials, both inorganic and organic, provides insight into their future disease treatment strategies (Figure 1). Inorganic biomaterials refer to materials with inorganic substances as the main body (Tang *et al.,* 2012). Organic materials commonly used in the biomedical field refer to biomaterials based on carbohydrates, nucleic acids, lipids, proteins, synthetic polymers, etc (Rezvantalab *et al.,* 2018).

1.1. Inorganic nanomaterials

Inorganic nanomaterials are the most popular in the biomedical field. They generally have more stable physicochemical properties and better controllability than organic materials. They have been widely used in the treatment of cancer, infection, acute kidney injury (AKI), orthopedic and neurological diseases (Fernandes *et al.,* 2020). Some inorganic nanomaterials have been used as immunoadjuvants to help build an immunotherapy platform. For example, studies have shown that gold nanoparticles, fullerene derivatives or graphene oxide

derivatives can act as nanoadjuvants by promoting local inflammation to combat viral infections and tumors (Xu *et al.*, 2016).

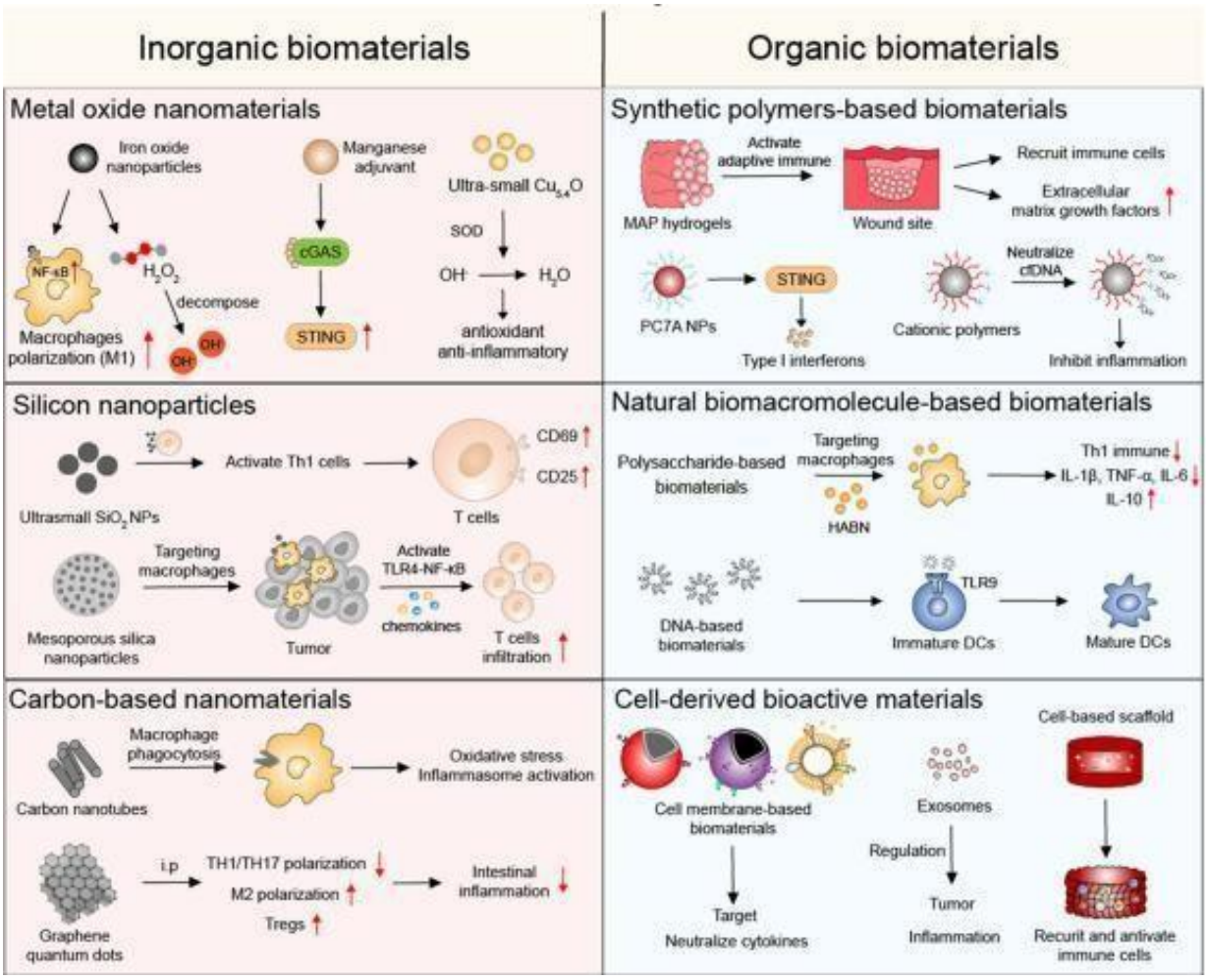

Figure 1: Inorganic and organic biomaterials with immunomodulatory functions (Dai *et al.*, 2022). **NPs**: Nanoparticles, **SiO2**: Silicon Dioxide, **DC**: Dendritic Cells, **TLR4-NF-kB**: Toll-like Receptor 4 and Nuclear Factor kappa B, **HABN**: hyaluronic acid (HA)-bilirubin (BR), **STING**: Stimulator of Interferon Genes, **cGAS**: Cyclic GMP-AMP Synthase, **M1/M2**: Reference to M1 and M2 Macrophage Polarization.

1.2. Organic biomaterials

Many organic biomaterials exhibit immunomodulatory properties when in contact with biologics organisms. Organic biomaterials with immunomodulatory functions can be divided

into synthetic polymeric materials, materials with natural biomacromolecules and bioactive materials of cellular origin (Adu-Berchie *et al.*, 2020).

1.2.1. Synthetic polymeric materials

Polymers have been altered as functional polymers in the last few decades for anti-inflammatory, anti-infection, and tissue regeneration (Gaharwar *et al.*, 2020). For example, Griffin *et al.* (2021) found that a degradable gel scaffold composed of microporous annealed particles (MAP) could activate the adaptive immune response (Figure 2, 3).

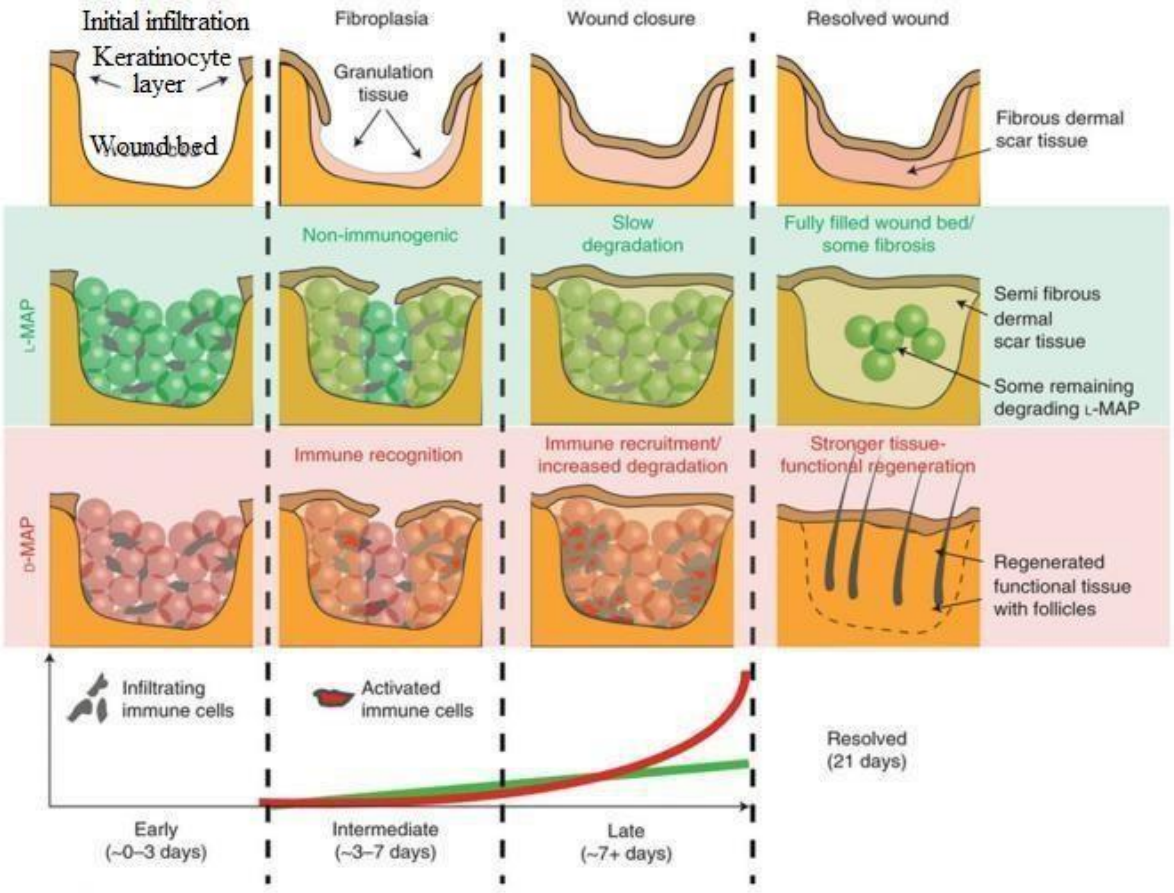

Figure 2: The use of L- or D-MAP in wound healing models. In the case of d-MAP, the hydrogel activates the adaptive immune system, leading to tissue remodeling and skin regeneration as the adaptive immune system degrades the D-MAP scaffold (Dai *et al.*, 2022)

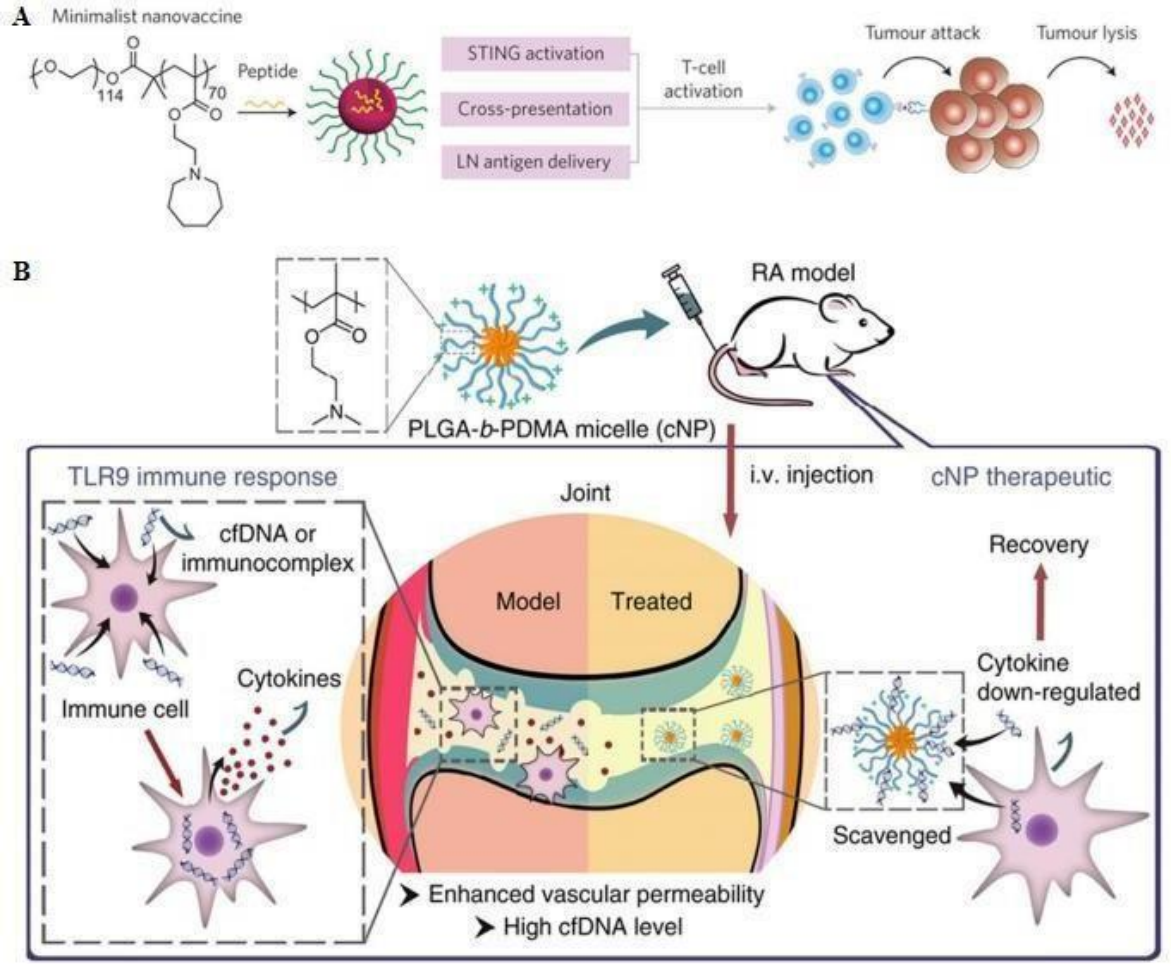

Figure 3: Schematic representation of the minimalist design of the PC7A nanovaccine (A). (B) Cationic nanoparticles have high free DNA binding capacity, which can effectively inhibit the activation of TLR9 and inhibit the inflammatory response of rheumatoid arthritis. Reproduced with permission (Dai *et al.*, 2022).

In order to target lymph nodes for antigen presentation and to activate the STING pathway to encourage the release of type I interferons, Luo *et al.* (2017) created methacrylate-based acid-responsive nanoparticles (PC7A), (Figure 3A). Specific immunomodulatory effects can be attained by customizing the nanoparticle structure and selectively altering the shape, size, charge, and surface functionalization of the nanoparticles (Kamaly *et al.*, 2012). For instance, Liang *et al.* (2018) showed that cationic nanoparticles (cNPs) made from the diblock copolymer of PLGA and PDMA may remove cell-free DNA (cfDNA) and then suppress the

activation of monocytes and fibroblast-like synovial cells found in primary synovial fluid (Figure 3B). Rheumatoid arthritis (RA) sites exhibit increased vascular permeability and large quantities of cellular free DNA. Studies have also demonstrated that cfDNA can be absorbed by cationic polymers and reduce the inflammation brought on by acute liver injury, and treat systemic lupus erythematosus (SLE), (Holl *et al.* 2016).

1.2.2. Natural biomacromolecule-based biomaterials

Biomacromolecules, which are naturally occurring substances that make up living things (such as polysaccharides and nucleic acids), typically display high biological activity and have specific immunomodulatory purposes (He *et al.*, 2020). These natural biomacromolecules pass on their immunomodulatory properties to the biomaterials they are based on, which have been extensively utilized in the development of immunotherapeutics for a variety of diseases (Taylor *et al.*, 2021). Lentinan, poria polysaccharide, and other fungal polysaccharides, in particular, have the power to boost immunity and anticancer activity. Han *et al.* (2021) created an inulin gel based on polysaccharides that can successfully control the intestinal flora, encourage the growth of symbiotic bacteria, and trigger the development of memory CD_8^+ T lymphocytes. Another naturally occurring biomaterial for biomedical engineering that goes beyond the typical genetic information storage is nucleic acid (figure 3).

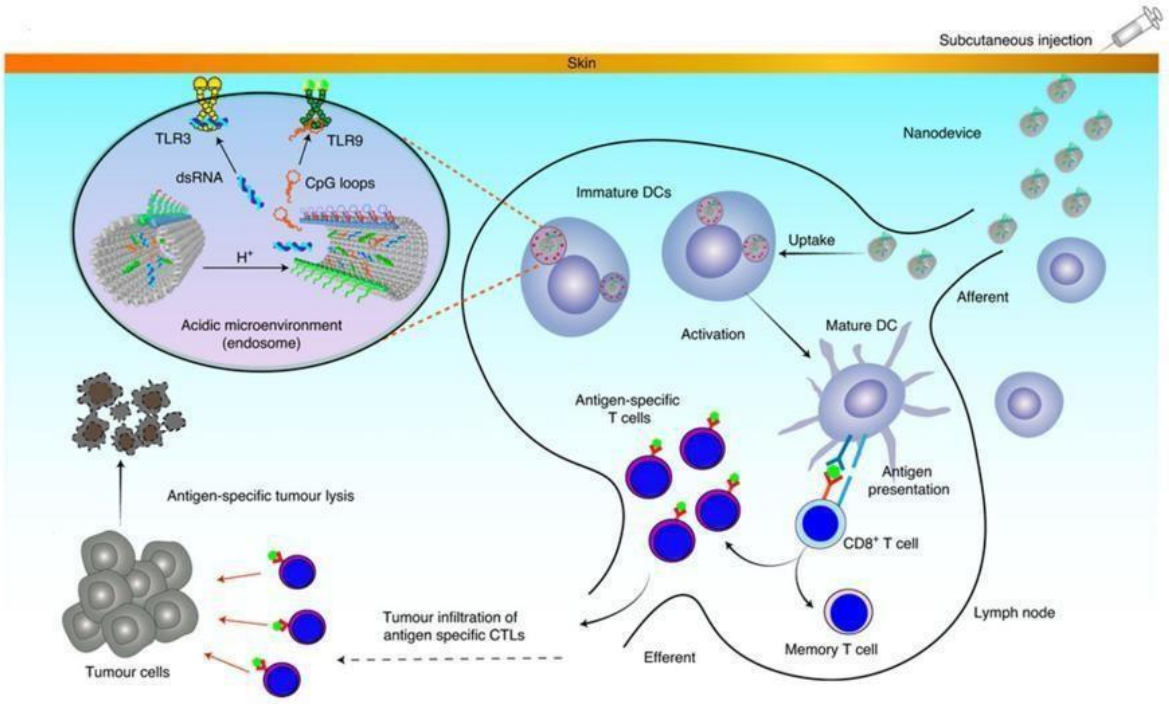

Figure 4: Schematic representation of the utilization of DNA nanodevices for efficient cancer immunotherapy (Dai *et al.,* 2022). **TLR9**: Toll-Like Receptor 9, **dsRNA**: Double-stranded RNA, **CpG**: Cytosine-phosphate-Guanine, **DCs**: Dendritic Cells, **CD8+ T cell**: Cytotoxic T-lymphocyte

1.2.3. Cell-derived bioactive materials

1.2.3.1. Cell membrane-based biomaterials

Numerous cell types, including red blood cells, immune cells, and cancer cells, which are often abundant in physiologically active proteins and phospholipids, can be used to create the cell membrane-based biomaterials (Pan *et al.,* 2021). For example, fusion cellular vesicles based on cell membranes can be employed to boost cancer immunotherapy or inhibit SARS-CoV-2 infection (Meng *et al.,* 2021). Rao *et al.* 2020 created a cell membrane-based nanodecoy by fusing monocyte membrane vesicles with genetically designed cell membrane vesicles that express the angiotensin-converting enzyme 2 (ACE2) receptor to reduce the cytokine storm brought on by viral infection (Figure 5). The nanodecoy can competitively

attach to viruses and neutralize cytokines through monocyte membrane receptors since SARS-CoV2 generally penetrates target cells through ACE2 receptors. This safeguards the host from SARS-CoV-2 infection (Hoffmann *et al.*, 2020).

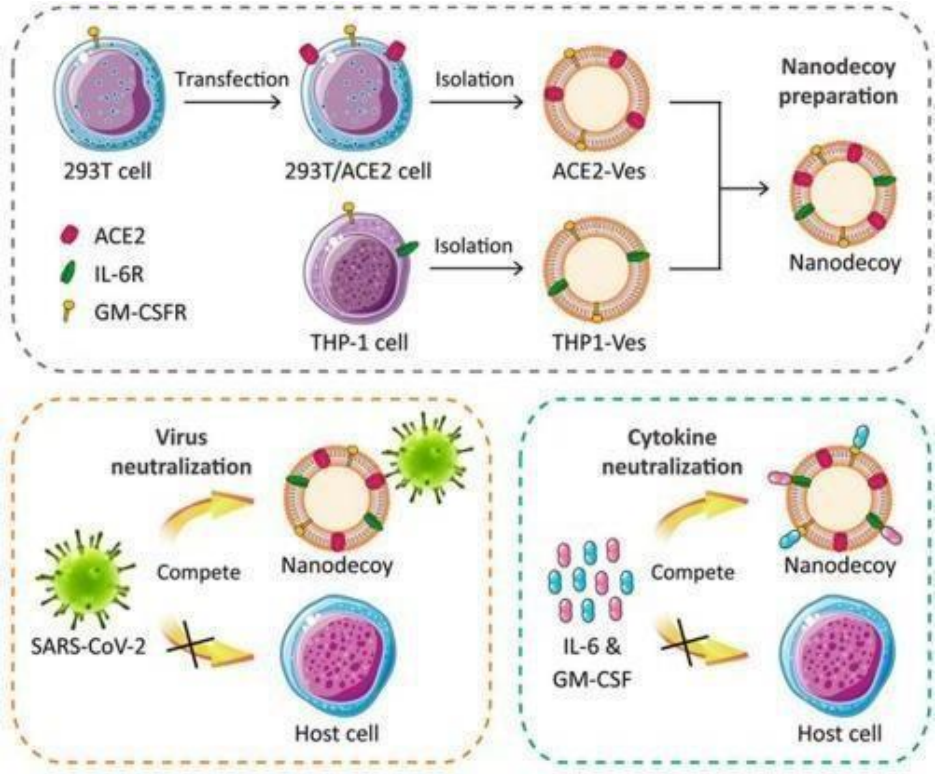

Figure 5: Preparation of anti-COVID-19 nanodecoys by fusing cellular membrane nanovesicles derived from genetically edited 293T/ACE2 and THP-1 cells. Nanodecoys fight COVID-19 infection by neutralizing SARS-CoV-2 and inflammatory cytokines (Dai *et al.*, 2022).

An efficient treatment plan is to create an immunosuppressive therapy platform to counteract the body's overactive immune response. Increased local concentrations of inflammatory cytokines occur in conjunction with neutrophil infiltration. In order to achieve this, Zhang *et al.* (2018) created a nanoparticle that is encapsulated in a neutrophil membrane with PLGA as internal support. This treatment for rheumatoid arthritis relies on the particular neutrophil-cytokine receptor combination to decrease inflammation (Figure 6).

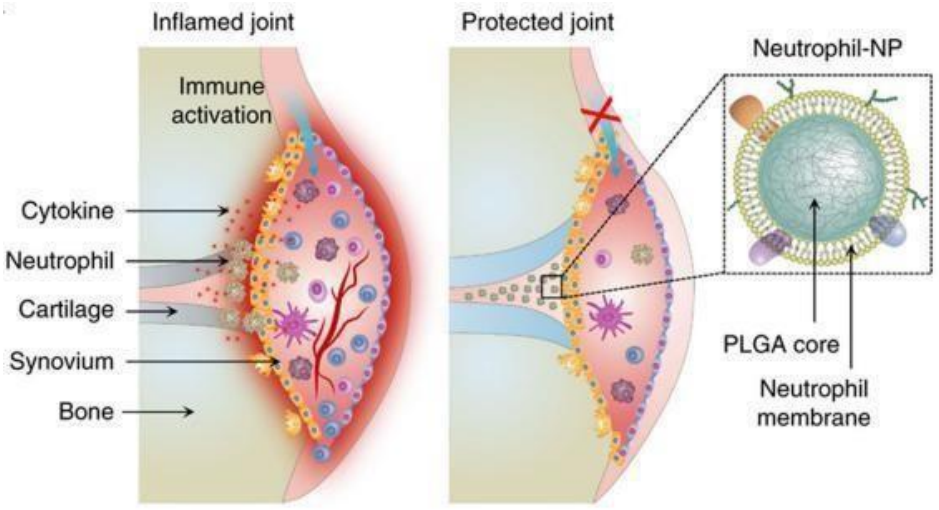

Figure 6. A schematic diagram of neutrophil membrane-coated nanoparticles inhibiting synovial inflammation and improving joint destruction in inflammatory arthritis (Dai *et al.,* 2022).

1.2.3.2. Exosomes

Extracellular vesicles called exosomes are loaded with proteins, lipids, fatty acids, and carbohydrate complexes (Zhang *et al.,* 2019). Different macrophage exosomes from various sources serve various biological purposes in various disorders, such as malignancies, inflammation, diabetes, or atherosclerosis (Shan *et al.,* 2021). They can be utilized to deliver drugs and also has immunomodulatory properties. Macrophage exosomes have the ability to boost T cell immunity. M1 macrophage exosomes can control M1 polarization of TAMs (Tumor-Associated Macrophages) to stop the growth of tumors (Gunassekaran *et al.,* 2021), and M2 macrophage exosomes (M2 Exos) have anti-inflammatory properties and can be utilized to treat atherosclerosis (Yang *et al.,* 2021).

2. Rheumatoid arthritis

The intricate interplay of numerous signaling pathways in rheumatoid arthritis (RA), result in the expression of different pro-inflammatory chemicals as cytokines, chemokines, and matrix metalloproteinases (MMPs). It makes it difficult to understand the RA criteria (McInnes & Schett, 2011). The phase of asymptomatic autoimmunity that follows a phase of disease risk is marked by archetypal autoantibodies that react with post-translationally changed proteins, frequently citrullinated antigens. Such antibodies to modified protein antigens (AMPA) are asymptomatic for years or even decades. Some patients eventually transition into a new stage and develop synovitis symptoms. An incorrect healing reaction, known as pannus development, occurs in the tissue at this stage of the disease. Pannus formation has damaging properties on its own and causes irreversible tissue damage to tendons, cartilage and bone (Weyand & Goronzy, 2021).

2.1. Pathophysiology of rheumatoid arthritis

The knowledge of RA and its systemic effects on the body is complicated by a confluence of biological indicators and environmental factors. Seropositive RA or seronegative RA are the two most common forms of RA in adults. Rheumatoid factor (RF) and antibodies to citrullinated protein antigens (ACPAs) found in blood tests suggest seropositive RA (Nordberg *et al.,* 2017). A useful diagnostic tool for individuals with early ACPAs can be found in approximately 67% of RA patients, and they provide information on the probability that the condition will proceed to RA. The ACPA-positive subgroup of RA has a more aggressive clinical phenotype than the ACPA-negative subgroup (Guo *et al.,* 2018).

By activating several cellular pathways, the mediators described below have a role in the pathophysiology of RA development (Ding *et al.,* 2023).

2.1.1. JAK-STAT pathway

One of the most important signaling pathways for cytokine signaling is JAK-STAT (Signal Transduction and Activator of Transcription), which is well known for how TNF-α rapidly induces the expression of the target genes. The JAK-STAT signaling system is abnormally active during RA (Angelini *et al.,* 2020). JAK family has four members JAK1, JAK2, JAK3, and TyK2 (tyrosine Kinase 2). STAT is a family of cytoplasmic proteins with both transcriptional activation and signal transduction functions. The STAT family includes STAT1-4, STAT5A, STAT5B, and STAT6. This pathway appears to be significant in aberrant of Rheumatoid Arthritis Fibroblast-like Synoviocytes (RA FLS) hyperplasia, synovial inflammation, and bone loss. It is implicated in a number of diseases (Emori *et al.,* 2020). JAK1 participates in the signaling process that occurs when certain cytokines, such as IFN- and IL-6, bind to create receptor complexes that activate JAK1 kinase and contribute to the pathogenesis of RA, vitiligo, and psoriasis (Abdou *et al.,* 2018). JAK3 engages in signaling pathways linked to IL-2, IL-4, IL-7, IL-9, IL-15, and IL-21 and is crucial for the development, expansion, and differentiation of T lymphocytes (Malemud *et al.,* 2018). Tyk2 can be triggered by IFNs, IL-6, IL-10, IL-12, and IL-23. Tyk2 is specifically inhibited in the therapy of RA (He *et al.,* 2019). STAT3 and STAT5 are activated downstream by JAK2. It is in charge of signaling *via* a number of receptors, including those involved in inflammatory and autoimmune reactions, like IL-6R, IL-12R, and IFN-R2.JAK2 expression is considerably higher in the synovial tissue of RA patients compared to healthy individuals (Monari *et al.,* 2009). Following therapy, there was a significant decrease in the levels of cytokines (IFN-, IL-12, and TNF-) as well as serum IL-2, IL-12, and p-Stat 3 in the synovial fluid of mouse models. In fact, CEP-33779 dramatically decreased a number of histological criteria that showed an improvement in arthritis, including synovial hyperplasia, vasculitis, matrix erosion, osteolysis, and osteogenesis (Stump *et al.,* 2011). These findings suggested that

JAK2 was implicated in the pathophysiology of RA and that JAK2 inhibition could treat RA by preventing cytokine production and T and B cell activation (Bousoik *et al.,* 2018). IFN-mediated signaling pathways allow STAT1 to participate in bodily functions. It is primarily triggered by cytokines like IL-6, IL-10, and IFN-γ. Only STAT2 is activated by IFN-λ and IFN-α/β. Through the interaction of STAT1 and the interferon regulatory factor 9 (IRF-9) to create a heterodimeric transcription complex of interferon-stimulated genetic factor (ISGF3), STAT2 has been demonstrated to be implicated in RA-associated inflammation (Blaszczyk *et al.,* 2015). Through the development of CD_4^+ T cells into Th17 and Th1 cells, STAT4 contributes to inflammation in RA by balancing the levels of IL-12 and IL-23 (Gao *et al.,* 2020). Since inhibiting STAT3 can enhance the activity of STAT5 and Foxp3, numerous studies have demonstrated that the effect of STAT5 may be opposite to that of STAT3. As a result, it could encourage Treg cell development and manage RA arthritis (Ju *et al.,* 2012).

2.1.2. NF-κB pathway

NF-κB activation in innate and adaptive immune cells may be responsible for inflammatory responses and the perpetuation of chronic inflammation in the RA synovium. NF-κB activation in T cells leads to signaling, activation and differentiation of inflammatory T cells, which produce inflammatory cytokines and maintain inflammation in the rheumatoid synovium. Impaired Treg function in RA patients may be related to Foxp3 downregulation and is due to the overexpression of inflammatory cytokines such as TNF-α in the RA microenvironment. In addition, B-cell proliferation and autoantibody production are closely linked to NF-κB-α activation. With regard to the regulation of innate immunity, deregulated activation of NF-κB in dendritic cells can lead to induction of cytokines that promote the differentiation of inflammatory T cells. These repetitive cycles can exacerbate the severity of the disease (Figure 7), (Nejatbakhsh Samimi *et al.*, 2020).

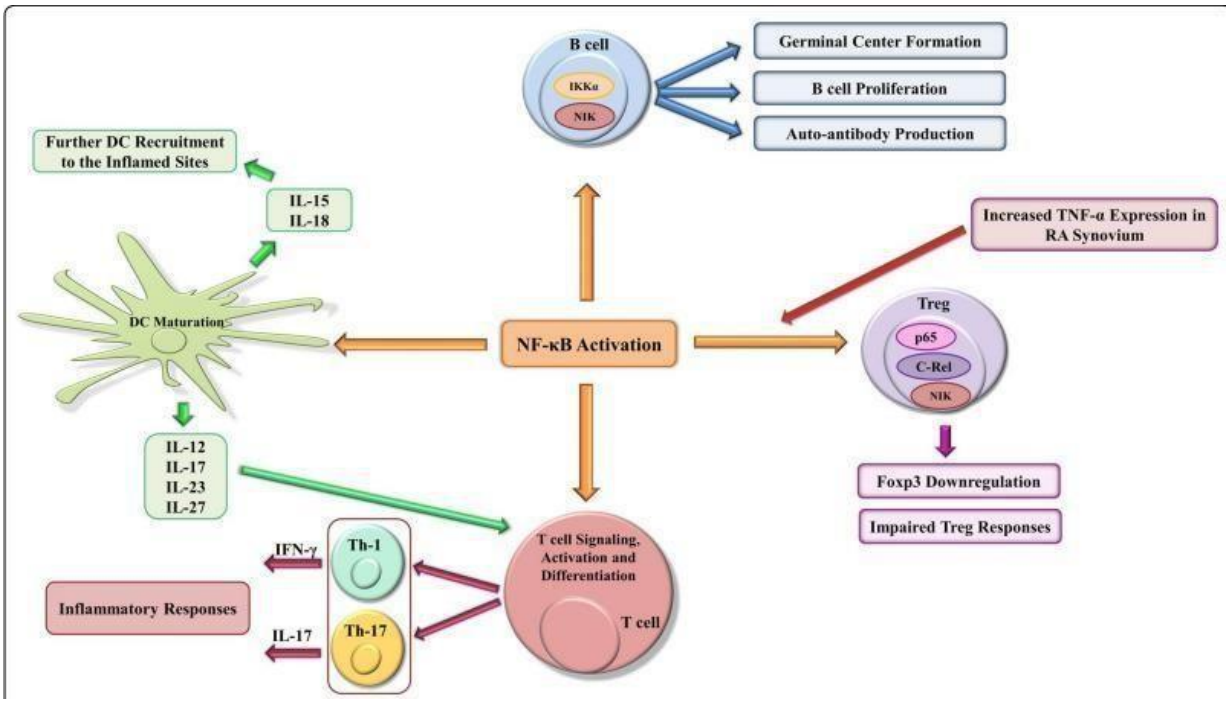

Figure 7: NF-κB activation perpetuates chronic infammation by targeting genes involved in inflammation during RA development.NF-κB: Nuclear factor kappa-light-chain-enhancer of activated B cells, PR: Rheumatoid Arthritis, Foxp3: Forkhead box P3, TNF-α: Tumor Necrosis Factor alpha (Nejatbakhsh Samimi *et al.*, 2020).

Activation of NF-κB in fibroblast synoviocytes regulates various cell-signaling processes, including decreasing apoptosis of fibroblast synoviocytes by increasing expression of anti-apoptotic factors and inhibition of P53 and Fas as apoptosis-regulating molecules. NF-κB activation can also affect the proliferation of FLS proliferation and lead to SLF (synovial lining fibroblasts) hyperplasia in RA synovium. In addition, FLS produce certain growth factors that lead to hyperplasia, inflammatory mediators such as inflammatory cytokines, which maintain chronic inflammation in the synovium, and various adhesion molecules which promote the migration of FLS to inflamed sites and enhance their invasive characteristics (Figure 8), (Nejatbakhsh Samimi *et al.*, 2020).

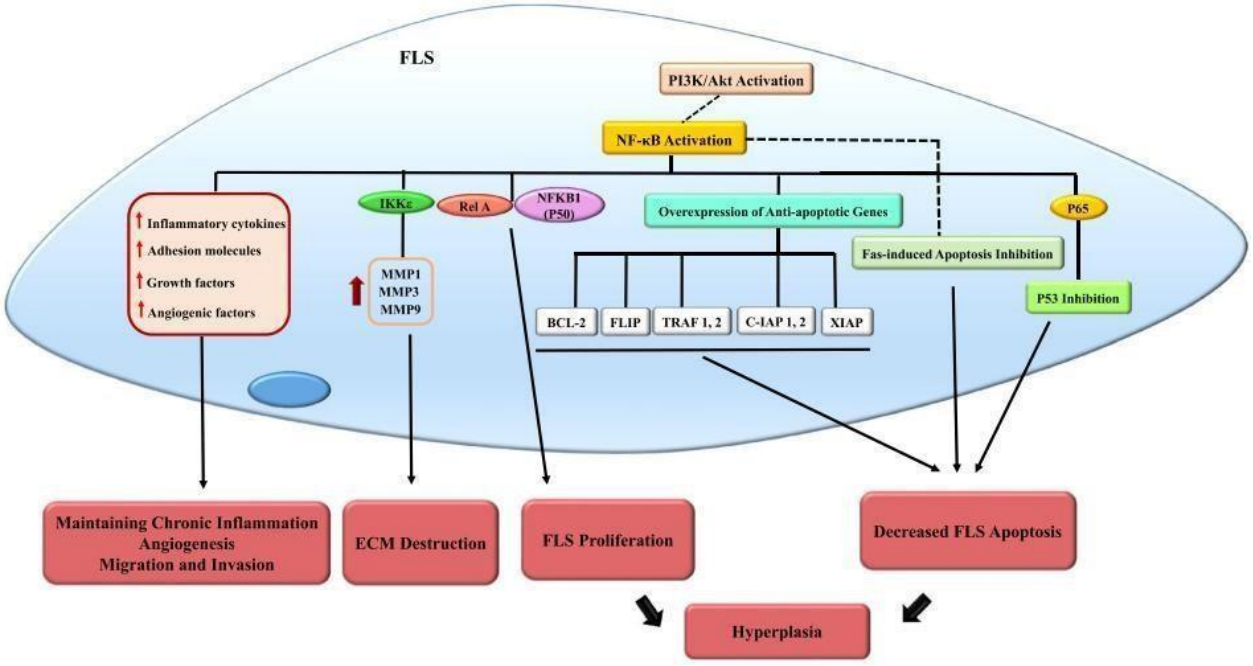

Figure 8: NF-κB activation in fbroblast-like synoviocytes regulates inflammatory responses in RA. RA: Rheumatoid arthritis, NF-κB: nuclear factor kappa B, FLS: Fibroblast-like synoviocyte, Fas: CD95 (Nejatbakhsh Samimi *et al.*, 2020).

2.1.3. MAPK pathway

The Mitogen-Activated Protein Kinase (MAPK) signaling pathway supports a number of cellular processes, including gene expression, metabolism, migration, survival, cell cycle progression, apoptosis, and differentiation, which are crucial to the pathological development of RA (Figure 9), (Ralph *et al.*, 2008). Its overactivation is highly associated with the breakdown of articular cartilage and the inflammatory hyperplasia of synovial tissue. As a possible target for treating RA and other immune-mediated chronic inflammatory disorders, MAPK controls the expression of several genes (Sujitha *et al.*, 2017). The three principal subfamilies of the MAPK pathway are c-Jun N-terminal kinase (JNK), extracellular kinase regulated signal-regulated kinase (ERK), and P38 MAPK (Whitaker *et al.*, 2021). The most significant MAPK family member associated with the inflammatory response in RA is P38, in a similar vein.

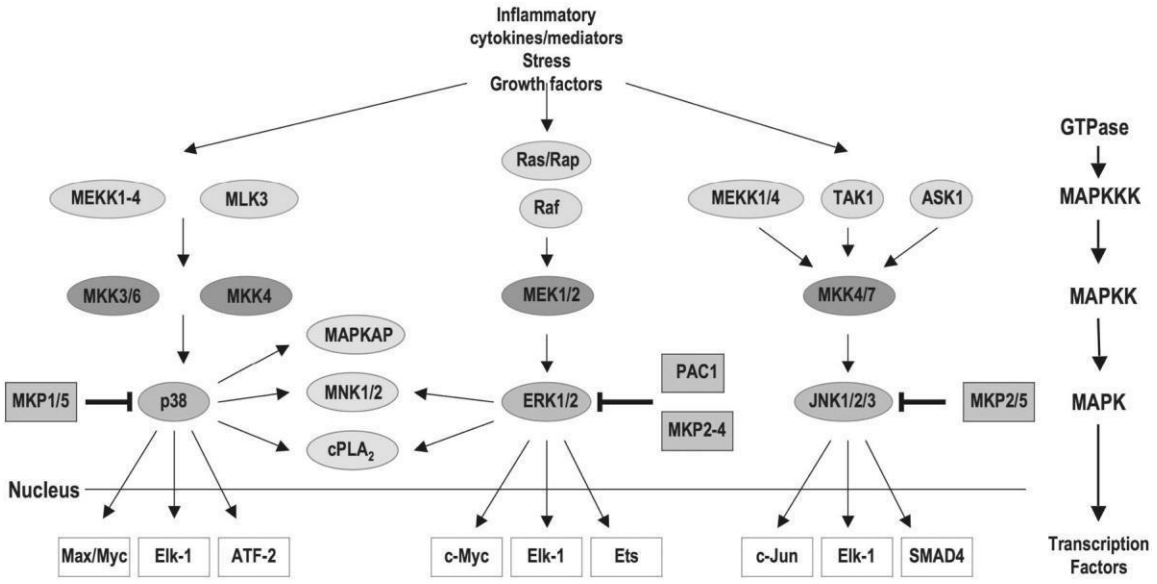

Figure 9: The ERK, JNK and p38 MAPK cascades (Thalhamer *et al.*, 2008).

MKK3 and MKK6 activate p38, which is abundantly expressed in the RA synovial tissue (Zhang *et al.*, 2021). The illness process in RA patients was aggravated by activation-induced phosphorylation of the p38 MAPK integrin, which blocked Fas-mediated cell death and caused a significant infiltration of T lymphocytes into the synovial region. An important pathogenic element in RA is the imbalance between Th1/Th2 cells. Inhibiting p38 activity can change the balance of natural CD4+ T cells, inhibiting the differentiation of cell types Th1/Th2, that is, to prevent their differentiation into Th1 cell variations. This can change the release of IL-2 and IL-4 as well as other cytokines. Th17, a newly identified subset of helper T cells, secretes and produces IL-17, an inflammatory cytokine, which gives it its name. It is also debatable how Th17/IL-17 affects the start and progression of RA (Samarpita *et al.*, 2021; Alam *et al.*, 2018).

2.2. Oxidative stress and RA

Various diseases, including metabolic, endocrine, neoplastic, granulomatous, infectious conditions, and other autoimmune disorders, have the potential to imitate rheumatoid arthritis

(RA), (Combe *et al.,* 2017). In a notable study conducted by Koster *et al.* (1986), a reduction in serum sulfhydryl group levels was observed in individuals with RA compared to a healthy control group, providing tangible evidence of oxidative stress in RA patients at that time, considering the role of sulfhydryl groups as peroxide scavengers. This finding aligns with the correlation between oxidative stress and RA, a chronic autoimmune disease characterized by inflammation (Fonseca *et al.,* 2019). Reactive oxygen species (ROS), generated during cellular oxidative phosphorylation and by activated phagocytic cells in oxidative bursts, surpass the normal buffering capacity, resulting in oxidative stress (Hitchon *et al.,* 2004). RA, as a representative of chronic inflammatory autoimmune diseases, is linked to oxidative stress, where the pool of ROS gradually increases due to increased production, reduced antioxidant defenses, or a combination of both, ultimately compromising redox signaling (Zamudio-Cuevas *et al.,* 2022). The precise mechanisms by which oxidative stress contributes to the initiation and perpetuation of local (within the joint environment) and systemic inflammation in RA, particularly at early stages, are not fully understood (Mobasheri, 2012). A meta-analysis from 2016, examining clinical trials involving individuals with RA to explore oxidative biomarkers as adjuncts in monitoring disease progression, uncovered a positive correlation between lipidperoxidation (assessed through serum levels of malondialdehyde: MDA) and disease activity (evaluated by the Disease Activity Score DAS-28). This discovery reinforces the proposition that oxidative stress and disease activity in RA are interconnected and progress together (Quiñonez-Flores *et al.,* 2016).

2.2.1 Mechanisms of oxidative stress and inflammation in rheumatoid arthritis

Oxidative stress plays a crucial role in initiating and perpetuating pathogenic mechanisms observed in systemic inflammatory conditions, including RA (Türk *et al.,* 2018). In physiological conditions, the production and clearance of reactive oxygen species (ROS) and

reactive nitrogen species (RNS) should ideally be maintained in a dynamic balance, as they exert pleiotropic effects on growth, differentiation, chemotaxis, and cell death (Phull *et al.*, 2018). They are also vital in defense mechanisms against pathogens (Smallwood *et al.*, 2018). However, under pathological conditions, such molecules, produced at high rates by articular neutrophils, monocytes, and macrophages, can damage various cell structures, including DNA, carbohydrates, proteins, and lipids (Batooei *et al.*, 2018), contributing to the establishment of oxidative stress (Figure 12). In affected joints, the most commonly found ROS/RNS include CO_2 (carbon dioxide), H_2O_2 (Hydrogen peroxide), -OH (Hydroxyl radical), NO- (Nitric oxide), ONOO- (Peroxynitrite), HOCl (Hypochlorous acid), and LOO- (Lipid peroxyl radicals), in addition to the reactive compound hydrogen sulfide (H_2S). Regarding the connection between pro-inflammatory cells and oxidative stress mediators, activated macrophages and T cells within the synovium, for instance, can stimulate the generation of ROS through the release of tumor necrosis factor TNF and IL-1, thereby intensifying synovitis (Hirvonen *et al.*, 2017).

One of the key pathways implicated in the pathogenesis of RA, characterized by high-grade inflammation, is directly linked to oxidative stress. In this context, proinflammatory cytokines play a role in activating the mitogen-activated protein kinase (MAPK), subsequently leading to the activation of NF-κB. This molecule, in turn, triggers the transcription of various genes associated with the maintenance of inflammation (Bordy *et al.*, 2018). Given that reactive oxygen species (ROS), primarily H2O2 (Phull *et al.*, 2018), can activate the NF-κB pathway, it becomes evident that oxidative stress is connected to the dysregulation of molecular signaling observed in the early stages of RA (Kaur *et al.*, 2021). Moreover, NF-κB may not only contribute to the increased production of IL-1 and TNF-α but could also be activated by these proinflammatory cytokines, establishing a positive feedback loop in a self-activation process with each other (Fonseca *et al.*, 2019), (Figure 10). Individuals with active RA, for

instance, exhibit elevated levels of ROS and reduced antioxidant capacity, ultimately leading to a more unfavorable oxidative status compared to healthy controls.

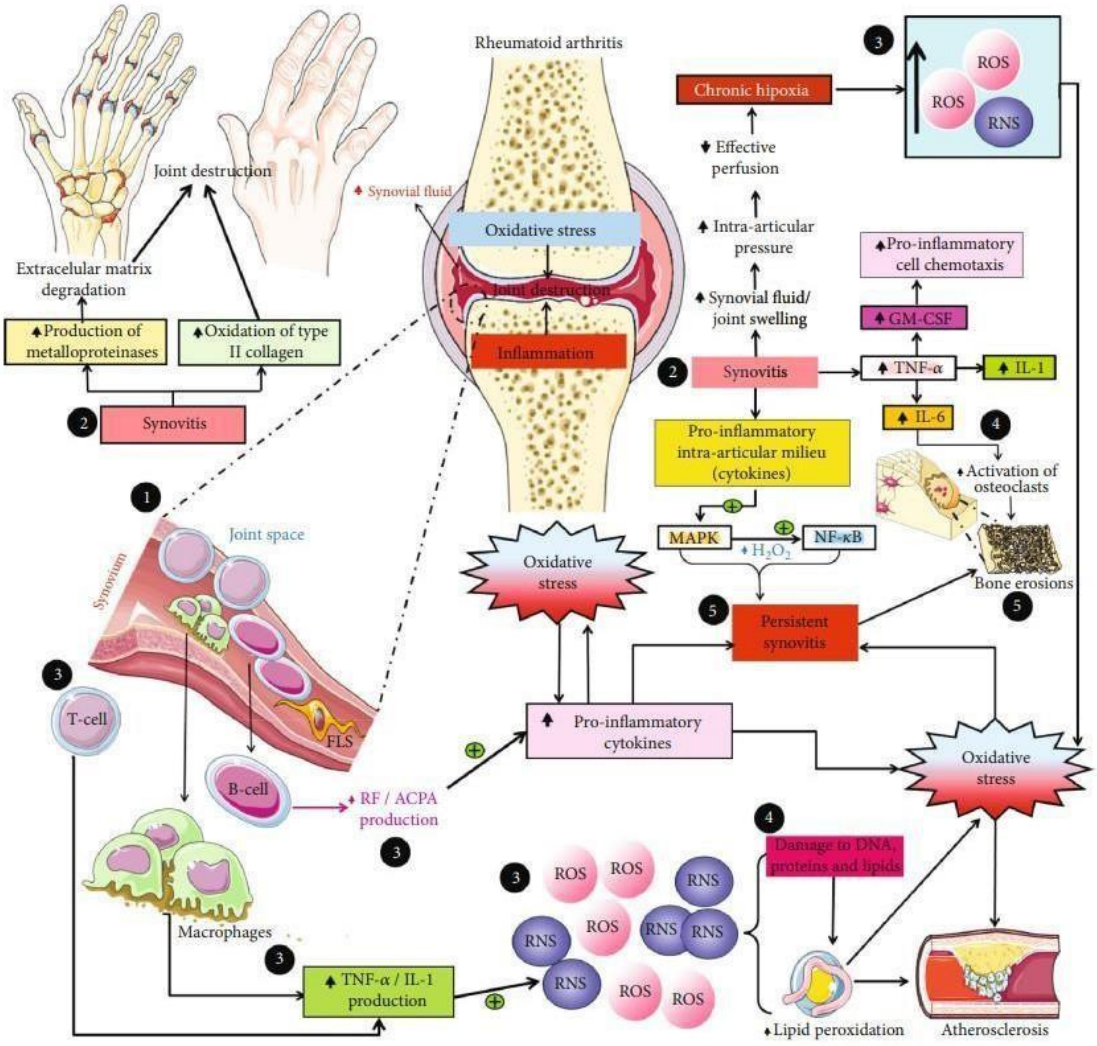

Figure 10: Cellular and molecular mechanisms of oxidative stress and inflammation in rheumatoid arthritis (Fonseca *et al.*, 2019)

As a consequence, higher levels of lipid peroxidation may be observed, either in the synovial fluid or in blood samples from RA patients (Phull *et al.*, 2018). Correspondingly, serum levels of MDA, a marker of lipid peroxidation, have been reported to show a positive correlation with proinflammatory cytokines in RA, while reactive oxygen metabolites (ROM) in blood samples are also found to be increased in RA patients and positively correlated with disease

activity (Bassu *et al.*, 2020). Regarding the impact of oxidative stress on specific cell types, ROS can trigger the apoptosis of chondrocytes, significantly contributing to the early-stage articular damage observed in RA (Phull *et al.*, 2018). Moreover, the dysregulation of autoreactive T lymphocytes, implicated in immune responses, may be associated with their exposure to an oxidative stress environment (Kaur *et al.*, 2021). Additionally, the proinflammatory intra-articular cascades may be heightened by the direct generation of ROS by local macrophages and by the local production of ACPA (Kaur *et al.*, 2021). Additionally, there is an increased production of matrix metalloproteinases, leading to extracellular oxidative damage (Phull *et al.*, 2018). The oxidation of collagen is particularly significant, as it heightens the immunogenicity of the extracellular matrix, contributing to the amplification of the loss of self-tolerance to extracellular components (Kaur *et al.*, 2021), (Figure 12). Equally intriguing, within the intracellular microenvironment, oxidative stress-induced somatic mutations in p53 within fibroblast-like synoviocytes (FLS) could play a role in synovial hyperplasia and the subsequent development of pannus. Pannus refers to the excessively proliferated synovial membrane characterized by invasive behavior and a richness of CD4+/T lymphocytes, directly contributing to cartilage destruction and bone erosions. This underscores the extensive range of oxidative damage observed in RA (Phull *et al.*, 2018).

2.2.2. Antioxidant intervention for rheumatoid arthritis

Antioxidant therapy emerges as a promising and innovative adjuvant or complementary strategy to more effectively manage disease activity (Dziąbowska-Grabias *et al.*, 2021). Therapies aimed at reducing oxidants and/or enhancing antioxidants show promise in treating various inflammatory diseases associated with oxidative stress (Liu *et al.*, 2021). Notably, different studies have highlighted the efficacy of various therapies as effective complementary

alternatives in controlling disease activity (Table 1), attributing their success to antioxidant effects and observing improvements in numerous disease activity parameters.

Table 1: Treatment of Rheumatoid Arthritis Transitioning from Conventional Methods to Supplemental Antioxidant Therapies (Dziąbowska-Grabias *et al.,* 2021).

Therapies antioxidant	**Oxidative effects**	**General clinical/biochemical effects**	**Authors /year**
N-acetylcysteine	Not measured	GH, VAS for the severity of pain, and HAQ scores were improved.	Batooei *et al.* (2018)
Synbiotic capsule supplements	Elevation of nitrite (indirect marker of NO) and GSH in plasma	Reduction in serum hs-CRP levels,mproved DAS-28 and VAS pain,	Zamani *et al.* (2017)
Pomegranate extract (Punica granatum L)	Increased concentrations of GPx; did not change MMP3, CRP, and MDA level	Reduced DAS-28 and HAQ	Ghavipour *et al.* (2017)
Ozone (rectal insu fflation) associated with MTX	Reduced anti-CCP levels and oxidative damage, increased antioxidant system; the increased levels of GSH were the only redox marker that correlated with all clinical variables (GSH vs. CRP, ESR, DAS-28, and HAQ-DI)	The clinical response to methotrexate (MTX) was enhanced by ozone.	Fernández *et al.* (2016)
Sesamin supplementation	Decreased serum levels of MDA and increased total antioxidant capacity	Improvement in anthropometric indices, lipid profile, and blood pressure	Abdollahzad *et al.* (2015)

DAS-28: Disease Activity Score Calculator for Rheumatoid Arthritis, MTX: Methotrexate , HAQ-DI: Health Assessment Questionnaire Disability Index, GSH: Glutathione, CRP:C-reactive protein, ESR:Erythrocyte Sedimentation Rate, CCP: Cyclic Citrullinated Peptide , MDA: Malondialdehyde, MMP: Matrix Metalloproteinases, GPx: Glutathione Peroxidases, GS: Glutathione Synthetase,VAS: Visual Analog Scale.

Additionally, a separate study suggested that the intake of antioxidants, including selenium, zinc, vitamin A, vitamin C, and vitamin E, may be beneficial in treating RA by increasing antioxidant levels in the body (Khadim *et al.,* 2023). Patients diagnosed with RA who underwent a 12-week treatment combining antioxidant vitamins A, E, and C with conventional DMARDs exhibited reduced levels of MDA and increased concentrations of

thiols, reduced glutathione (GSH), and vitamin C in their blood samples. Additionally, these patients demonstrated a decrease in the Rheumatoid Arthritis Disease Activity Index (RADAI), indicating that the antioxidant therapy efficiently improved both disease activity and the redox profile in this group (Jaswal *et al.,* 2003).

Supplementation therapy, often employed for its potential antioxidant benefits, encompasses various approaches. Notably, pomegranate (Punica granatum L), recognized for its rich flavonoid content with potent antioxidant properties, has demonstrated efficacy (Saparbekova *et al.,* 2023). Studies indicate that in RA patients, supplementation with pomegranate extract led to increased concentrations of glutathione peroxidase (GPx), a decrease in the Disease Activity Score (DAS-28), and improved serum oxidative status (Ghavipour *et al.,* 2017). Similarly, sesamin supplementation in RA individuals resulted in reduced MDA levels and enhanced total antioxidant capacity. Coenzyme Q10 supplementation, as another successful complementary therapy alongside conventional RA medications, was associated with decreased serum MDA and tumor necrosis factor-alpha (TNF-α) levels (Abdollahzad *et al.,* 2015). Probiotic therapy has also been described in individuals with RA. For instance, supplementation with synbiotic capsules containing Lactobacillus acidophilus, Lactobacillus casei, and Bifidobacterium bifidum has shown improvements, increasing nitrite concentrations (an indirect marker of nitric oxide NO) and GSH levels in the plasma (Zamani *et al.*, 2017).

2.3. Therapeutics and inhibition strategies in RA

The following outlines various therapeutic strategies and inhibition methods employed in the management of RA. Disease Modifying Anti-Rheumatic Drugs (DMARDs) and Glucocorticoids (GC) constitute the mainstay of RA treatment and have remained unchanged for an extended period (Huang *et al.*, 2021). Biological DMARDs Novel approaches are

under development and investigation, focusing on specific pathways linked to disease progression (Prasad *et al.,* 2023). Combination of conventional and targeted DMARDs may prove effective in addressing moderate to high RA activity in seronegative patients (Zampeli *et al.,* 2015). Supplementing Methotrexate with biologicals could be beneficial for cases where there is an inadequate response to Methotrexate (Solomon *et al.,* 2020). Gene therapy and mesenchymal stem cell therapy emerging therapeutic avenues are under investigation for the future (Watanabe *et al.,* 2021). Inhibition of miR-146a and miR-135a in RA patients, elevated miR-146a levels contribute to continuous TNF-alpha production. Downregulating miR-135a has shown to inhibit the proliferation, migration, and invasion of RA-FLS cells (Prasad *et al.,* 2023). Janus kinase inhibitors (JAKi) represent newer RA treatments that regulate cytokine responses by targeting intracellular signaling enzymes (Nash *et al.,* 2021).

3. Ammodaucus leucotrichus

3.1. Botanical description and classification

Ammodaucus leucotrichus Coss. & Dur. is a member of the *Apiaceae* botanical family, also known as Umbelliferae. *Apiaceae*, one of the largest plant families, encompasses approximately 300 genera and over 2500 species, distributed mainly in temperate regions worldwide and classified within the order *Apiales* (Mohammedi *et al.,* 2018). Within the *Apiaceae* family, *Ammodaucus leucotrichus* Coss. & Dur. stands as the singular species belonging to the genus *Ammodaucus*.

The classification of the plant is (Kralik, 1859):

Kingdom: Plantae

Phylum: *Streptophyta*

Class: *Equisetopsida*

Subclass: *Magnoliidae*

Order: *Apiales*

Family: *Apiaceae*

Genus: *Ammodaucus*

Species: *Ammodaucus leucotrichus*

A. leucotrichus is commonly identified as 'Kamune es sufi' or 'akâman' in several North African nations, referred to as "Moudrayga" in Algeria, and recognized as "Cumin chevelu" in the French language (Idm'hand *et al.,* 2020). *A. leucotrichus* is an aromatic small annual plant native to the Saharan and sub-Saharan regions of North Africa, including Morocco, Algeria, Tunisia, Egypt, and tropical Africa (Lenzi *et al.,* 2022). This glabrous plant reaches a height of 10–12 cm, featuring erect and finely striated stems branching from the base, with fleshy and finely divided leaves. The small flowers, characterized by five free white petals, are

grouped in umbels of two to four branches. The fruit is a diachene, measuring 8–10 mm in length and covered with dense white hairs (Figure 11). Typically, the species blooms between February and April, thriving spontaneously in wadis on sandy-gravelly soils under arid conditions with an annual rainfall not exceeding 100 mm. Currently, there is no available data on its propagation and conservation, and cultivation is not practiced (Sebaa *et al.*, 2018).

Figure 11. *Ammodaucus leucotrichus* in natural habitat (Idm'hand *et al.*, 2020)

3.2. Traditional uses

Ammodaucus leucotrichus is a plant extensively utilized in North African countries for culinary and medicinal purposes (Lenzi *et al.*, 2022). In Morocco, the plant's various parts, especially the fruits and seeds, are employed to address diverse health issues, including gastric-intestinal pains, otitis, hypotension, indigestion, cold, fever, pulmonary diseases, labor pains, anorexia, and cardiac diseases. It is also utilized in infantile diseases, with its fruits infused to alleviate digestive system problems (Idm'hand *et al.*, 2020). The seeds of *Ammodaucus leucotrichus* play a crucial role in preparations for ailments such as cystitis,

nephritic colics, kidney stones, diarrhea, emetic conditions, cough, anorexia, allergies, tachycardia, fatigue pains, helminthiasis, and gastroenteritis. In Algeria, where it is known as "Moudrayga or El massoufa," the plant is traded in local markets, especially in the Southern Algerian Sahara. Nomads collect seeds and leaves for various purposes, including the preparation of decoctions or infusions to address blood pressure, chest pain, liver and digestive system ailments, gastroenteritis, and diabetes. The Southern Algerian Sahara also sees the use of *Ammodaucus leucotrichus* leaves as a flavoring herb in teas, while its fruits serve as a spice in culinary preparations. The plant is consumed in decoction or infusion forms for therapeutic purposes, ranging from blood pressure regulation to the treatment of liver and digestive system ailments, gastroenteritis, and diabetes. Its fruits are widely employed as a sugar regulator for diabetics, and the seeds address various conditions such as stomach diseases, wound infections, cutaneous allergies, genital disorders, abdominal pains, scorpion stings, snakebites, and liver diseases. Furthermore, *A. leucotrichus* is used to alleviate allergy symptoms, diarrhea, indigestion, vomiting, spasms and colic, intestinal worms, fever, constipation, coughing, and anorexia. Alongside these uses, the plant is associated with aphrodisiac, emmenagogue, and abortive properties (Idm'hand *et al.,* 2020).

3.3. Phytochemistry

Various bioactive compounds have been identified in *Ammodaucus leucotrichus* through isolation from aqueous, acetone, methanolic, or ethanolic extracts (Khaldi *et al.,* 2019). These compounds encompass monoterpenes and their derivatives, sesquiterpenes and their derivatives, tannins, anthracenes compounds, sterols, triterpenes, reducing compounds, alkaloids, phenol acids, saponins, flavonoids, and coumarins. Key compounds such as perillaldehyde and limonene, along with novel guainolide lactone (ammolactone) and monoterpenoid 3-hydroxyperillaldehyde, methylperillate, borneolangelate, and γ-decalactone, have been identified (Ziani *et al.,* 2019). The presence of these metabolites highlights the

potential pharmaceutical applications, with terpenes as penetration enhancers, alkaloids as primary active ingredients, and flavonoids for various health benefits. Perillaldehyde, a major compound, finds applications in food preservation, cosmetics, perfumery, and the pharmaceutical industry (Idm'hand *et al.,* 2020). The table 2 provides a detailed overview of the isolated phytochemicals from different parts of the plant.

Table 2. phytochemicals isolated from different parts of *Ammodaucus leucotrichus* (Idm'hand *et al.*, 2020)

Compounds	**Part of the plant**
Thymol	Fruit
Cuminal	Seed
α-Terpineol	Seed, fruit
Terpen-1-ol	Fruit
trans-Verbenol	Fruit
trans-Carveol	Fruit
α-Copaene	Seed, fruit
β-Cubebene	Seed, fruit
β-elemene	Seed
Caryophyllene	Seed, aerial part
α-caryophyllene	Seed
α-selinene	Seed
α-Muurolene	Seed, fruit
δ-Cadinene	Seed, fruit
Spathulenol	Seed, fruit
Caryophylleneoxide	Seed
T-Muurolol	Seed, fruit
α-Curcumene	Seed
Bicyclogermacrene	Seed, fruit
β-Dihydroagarofuran	Seed
α-Cubebene	Fruit
ar-Curcumene	Fruit
α-Zingiberene	Fruit
β-Bisabolene	Fruit
γ-Cadinene	Fruit
GermacreneB	Fruit
β-Calacorene	Fruit
Germacrened-4-ol	Fruit
1-*epi*-Cubenol	Fruit
Chamazulene	Fruit
trans-α-Bergamotene	Fruit
α-Humulene	Fruit
β-Selinene	Fruit
α-Bulnesene	Fruit
10-*epi*-Cubebol	Fruit
τ-Cadinol	Fruit
β-Eudesmol	Fruit
11-Acetoxyeudesman-4-α-ol	Fruit
β-Caryophyllene	Seed
cis-β-Farnescene	Seed
trans-Muurola-3,5-diene	Seed
Isolongifolan-8-ol	Aerial part

Compounds	**Part of the plant**
GermacreneD	Seed, fruit
B-Selinene	Seed
Globulol	Seed, aerial part
α-Eudesmol	Seed, fruit
Longifolol	Seed, fruit
Ammolactone-A	Seed
α-Cadinol	Seed
α-Muurolol	Fruit
Terpinen-4-ol	Seed, fruit
1-Pentadecene	Fruit
1-Nonadecene	Fruit
Cuminaldehyde	Seed, aerial part, fruit
α-Campholenal	Seed
Benzaldehyde	Seed
Allylisovalerate	Seed, fruit
(*Z*,*E*)-Farnesol	Fruit
Methyleugenol	Seed, fruit
γ-Decalactone	Seed, fruit
cis-*p*-Mentha-2,8-dien-1-ol	Seed
AllocimeneB	Seed
p-Cymen-8-ol	Seed
cis-Pinocarveol	Seed
trans-Isocarveol	Seed
11-Acetoxyeudesman-4-a-ol	Seed
p-mentha-trans-2,8-dien-1-ol	Seed
cis-limonene oxide	Seed
Trans-p-mentha-1(7),8-dien-2-ol	Seed
Carvacrolmethylether	Fruit
3-Hydroxyperillaldehyde	Fruit
10-nor-Calamenen-10-one	Fruit
α-Terpinen-7-al	Fruit
γ-Terpinen-7-al	Fruit
Dehydro-Sabinaketone	Fruit
Trans-p-Mentha-2,8-dien-1-ol	Fruit
Cis-p-Mentha-2,8-dien-1-ol	Fruit
Trans-Limonene oxide	Fruit
Shybunol	Fruit
Caryophylleneacetate	Fruit
cis-*p*-mentha-trans-2,8-dien-1-ol	Fruit
Pyranton	Fruit
Rosifoliol	Fruit
z-5-Nonadecene	Fruit
α-copaen-11-ol	Aerial part

3.4. Biological activities and pharmacological properties

Extensive research has been conducted on *Ammodaucus leucotrichus* to explore its bioactive properties. Various extracts and isolated compounds have undergone thorough evaluation for their diverse biological activities, including antioxidant, antibacterial, antifungal, antidiabetic, anti-inflammatory, anticholinesterase, and cytotoxicity activities.

3.4.1. Antioxidant Activities

The antioxidant activities of *Ammodaucus leucotrichus* have been investigated by different researchers. Louail *et al.* (2016) assessed the antioxidant activity of the essential oil from the seeds, demonstrating its effectiveness by inhibiting β-carotene bleaching and linoleic acid hydroperoxide-derived attacks, outperforming Ascorbic acid. In contrast, Dahmane *et al.* (2017) found essential oils from the fruits to exhibit weaker antioxidant abilities against DPPH radicals and linoleic acid oxidation compared to standard antioxidants BHT and ascorbic acid. Sebaa *et al.* (2018) evaluated various extracts (essential oils, aqueous, and methanol) from *Ammodaucus leucotrichus* fruits, highlighting the methanol extract's superior antioxidant performance in both ferric reducing power and DPPH methods. This extract showed a notable free radical reduction capacity with a concentration range of 2 to 4 µg/ml. Additionally, an aqueous extract from the fruits exhibited potential antioxidant effects through the trapping of free radicals.

3.4.2. Antimicrobial activities

The essential oil extracted from *Ammodaucus leucotrichus* seeds demonstrated strong antimicrobial activity against various microorganisms, including Gram-positive bacteria (*Bacillus subtilis*), Gram-negative bacteria (*Escherichia coli*), and yeast species (*Candida albicans* and *Saccharomyces cerevisiae*), as well as fungi (*Aspergillus flavus* and *Penicillium*

expansum). The oil displayed significant inhibitory effects, with MIC values ranging from 0.37 to 0.92 mg/ml. Moreover, it exhibited noteworthy antibacterial activity against both Gram-negative and Gram-positive bacteria at doses of 1.29 mg/disc (Louail *et al.*,. 2016). The antifungal results indicated clear zones of growth inhibition against Aspergillus flavus and Penicillium expansum (Khaldi *et al.,* 2017). Additionally, other studies confirmed the broad-spectrum antibacterial and antifungal activities of extracts and fractions from *Ammodaucus leucotrichus* fruits. The essential oil also showed potent antifungal activities against various strains, such as *Candida albicans, Aspergillus niger*, and *Trichophyton rubrum*. Furthermore, the hydroethanolic extract and aqueous decoction from the aerial parts of *A. leucotrichus* exhibited moderate activity against both Gram-negative and Gram-positive bacteria. Overall, these findings highlight the plant's potential as a source of antimicrobial agents with diverse applications (Gherraf *et al.*, 2016; Mohammedi *et al.*, 2018).

3.4.3. Anticholinesterase activities

The aqueous, ethanolic, and essential oil extracts from the fruits of *Ammodaucus leucotrichus* Coss & Dur exhibit inhibitory effects against acetylcholinesterase (AChE), as reported by Boumezzourh *al.* (2023), with the essential oil showing the highest inhibitory efficacy, even at galantamine concentrations. Particularly, the essential oil achieves significant inhibition (78.07%) at a concentration of 0.75 mg/mL, surpassing positive controls. At 1 mg/mL, the essential oil displays the highest inhibition at 92.32%, followed by the ethanolic extract at 83.77%. A previous study by Sadaoui *et al.* (2018) highlights the strong acetylcholinesterase inhibitory activity of limonene, a component of the essential oil, with efficacy comparable to donepezil, a standard medication for Alzheimer's disease. In terms of anti-butyrylcholinesterase activity, all samples show strong inhibition, with perillaldehyde displaying the lowest IC50, followed by limonene and the essential oil. In summary, extracts

from *Ammodaucus leucotrichus*, especially the essential oil, demonstrate promising inhibitory properties against AChE, suggesting potential applications in Alzheimer's disease research.

3.4.4. Antidiabetic activities

Ammodaucus leucotrichus, a plant from the Apiaceae family, has been traditionally utilized in the North African Sahara for managing diabetes. Recent studies highlight its diverse pharmacological actions, particularly its antidiabetic properties (Idm'hand *et al.*, 2020). In a study on defatted hydroethanolic extract of *Ammodaucus leucotrichus* (DHEAM) seeds, significant antidiabetic and antihyperglycemic effects were observed in alloxan-induced diabetic mice. Orally administered DHEAM doses (100 and 200 mg/kg) for four weeks effectively regulated fasting blood glucose levels and improved overall health (Es-Safi *et al.*, 2020). Another investigation by El-Ouady *et al.* (2020) demonstrated the anti-diabetic activities of the aqueous extract of *Ammodaucus leucotrichus* fruits in streptozotocin-induced diabetic rats. The plant extract, administered orally at 10 mg/kg for 15 days, significantly reduced blood glucose levels and exhibited beneficial effects on liver histological structure and glucose tolerance. This research underscores the potential of *Ammodaucus leucotrichus* as a therapeutic option for diabetes.

3.4.5. Anti-inflammatory activities

Ammodaucus leucotrichus has gained recognition for its anti-inflammatory properties, particularly evident in the essential oil extracted from its fruits. In a study assessing the anti-inflammatory impact of the essential oil using a 100 mg/kg dose in a Carrageenan-induced hind paw edema mouse model, a significant anti-edematogenic response was observed (Es-Safi *et al.*, 2020). The defatted hydroethanolic extract of *A leucotrichus* also demonstrated noteworthy anti-inflammatory activity. Comparisons with diclofenac, a standard drug in this model, revealed similar inhibition percentages (18.7%, 21.6%, 19.4%, and 24.5%) of

Carrageenan-induced edema in groups treated with essential oils (Mohammedi *et al.*, 2018). Another investigation by Ziani *et al.* (2019) explored the anti-inflammatory properties of the hydroethanolic extract from the aerial parts of *Ammodaucus leucotrichus*. This study unveiled a reduction in the expression of inflammatory enzymes, such as iNOS, in LPS-activated murine macrophages, accompanied by a decrease in nitric oxide (NO) levels. These findings highlight the potential anti-inflammatory benefits of *Ammodaucus leucotrichus*, as evidenced by its essential oil and hydroethanolic extract (Ziani *et al.*, 2019). The plant comprises various bioactive chemical constituents, including monoterpenes, sesquiterpenes, tannins, anthracenes compounds, sterols, triterpenes, reducing compounds, alkaloids, phenol acids, saponins, flavonoids, and coumarins, believed to contribute to its medicinal properties, especially its anti-inflammatory effects (Idm'hand *et al.*, 2020).

3.4.6. Cytotoxicity activities

Ammodaucus leucotrichus has been identified for its cytotoxic properties. In a recent investigation, the standardized ethanolic extract of *A. leucotrichus* fruits and R-perillaldehyde, a monoterpenoid isolated from the fruits, were studied for their potential anticancer effects. The research explored genoprotective, proapoptotic, antiproliferative, and cytodifferentiating potentials on various human cell models. Specifically, genoprotective and proapoptotic activities were assessed on human lymphoblast cells (TK6) using the micronucleus test, while cytodifferentiation effects were examined on human promyelocytic cells (HL60) through the evaluation of differentiation markers (Lenzi *et al.*, 2022). Additionally, Ziani *et al.* (2019) investigated the cytotoxic activities of aqueous decoction and hydroethanolic extracts from aerial parts of *Ammodaucus leucotrichus*. Using the sulforhodamine B colorimetric assay, inhibitory growth activity was determined on four human tumor cell lines NCI-H460, HeLa, HepG2, and MCF-7. Hepatotoxicity was assessed using a primary culture of non-tumor liver

cells (PLP2) from freshly harvested porcine liver. The hydroethanolic extract exhibited lower GI50 values compared to decoction extracts, indicating a significant dose-dependent cytotoxic effect. MCF-7, HeLa, and NCI-H460 were identified as the most susceptible cell lines to the hydroethanolic extract of *A. leucotrichus*. These findings collectively suggest the potential anticancer and cytotoxic properties of *A. leucotrichus* extracts and compounds.

MATERIALS AND METHODS

1. Materials

1.1. Chicken sternal cartilage

Collagen (type II) was isolated from chicken cartilage obtained from butchers in the wilaya of Constantine, the cartilage was frozen until use.

1.2. Plant material

Ammodaucus leucotrichus seeds were collected from the Bechar region in the southwest of Algeria, during the summer of 2021. The authenticity of these seeds was verified by Professor Sabah Charmat from Ferhat Abbas University Setif 1, Algeria, and a voucher specimen was officially recorded with the reference number 220/SNV/DA/UFAS/21.

1.3. Animals

The male Wistar rats, weighing between 200 and 250 g, were purchased from the 'Institut Pasteur d'Algérie' in Algiers. They were housed in plastic cages within the Biotechnology Research Center for a period of seven days, adhering to standard animal facility conditions. These conditions included a 12-hour light and 12-hour dark cycle, a temperature of 23 ± 2°C, and continuous access to food and water before the commencement of the experiment.

2. Methods

2.1. Extraction of collagen II

Chicken sternal cartilage, stored at -20°C, underwent a rigorous cleaning process. This involved washing with distilled water and subsequent treatment with a methanol-chloroform solution (2/1 : v/v), for 5 minutes to eliminate non-collagenous proteins and lipids. The

procedure for preparing collagen-II was primarily based on the method by Akram & Zhang (2020), with minor adjustments (Figure 12).

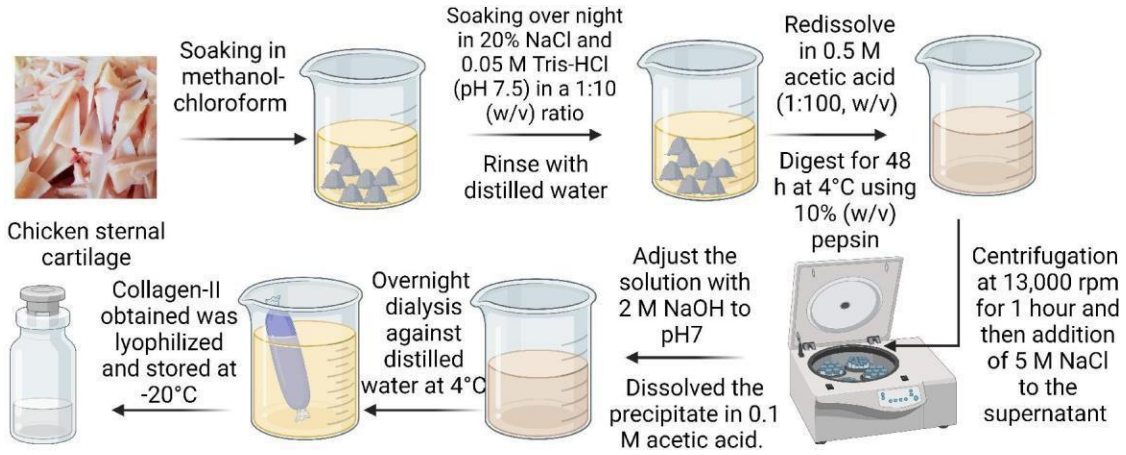

Figure 12: Schematic presentation showing: Type II Collagen from chicken cartilage.

The cartilage pieces were dissolved in a mixture of 20% NaCl and 0.05 M Tris-HCl (pH 7.5) in a 1:10 (w/v) ratio. This dissolution occurred overnight with stirring, followed by a rinse with distilled water. The resulting cartilage material was then stored at -20°C until needed. Subsequently, following the procedure by Khong *et al.* (2018), pepsin-soluble collagen-II was extracted with some modifications. The insoluble material was redissolved in 0.5 M acetic acid (1:100, w/v) and digested for 48 hours at 4°C using 10% (w/v) pepsin (EC 3.4.23.1; Spectrum Chemical, USA). The pepsin-solubilized collagen-II was subjected to centrifugation at 13,000 g for one hour. Gentle addition of 5 M NaCl to the supernatant under constant stirring achieved a final concentration of 0.8 M. To neutralize pepsin activity, 2 M NaOH was added to reach a pH of seven. The ensuing precipitate was collected and dissolved in 0.1 M acetic acid. After an overnight dialysis against distilled water at 4°C, the collagen-II obtained was lyophilized and stored at -20°C until use. To evaluate the purity of the purified collagen-II, characteristic UV spectra within the 190-280 nm range were examined based on the description by Sorushanova *et al.* (2019). Additionally, SDS polyacrylamide gel

electrophoresis (SDS-PAGE) with a 7.5% gel was employed (Laemmli, 1970). Before application, collagen-II powder was dissolved in 0.1 M acetic acid, involving placement in a SpeedVac vacuum concentrators for two hours at 35°C, and with overnight stirring at 4°C. This solution was then centrifuged for 20 minutes at 3000 rpm to eliminate any undissolved particles.

2.2. Extraction method

The collected *Ammodaucus leucotrichus* seeds underwent a series of preparation steps, including cleaning, air-drying, and subsequent grinding using an electric grinder to produce a fine powder. The methanol extraction was performed by macerating the obtained powder in methanol (CH_3OH, ≥99.8%, Sigma-Aldrich). A quantity of 500 g of powder was added to 5 L of methanol. The mixture was left to macerate for 7 days, following the method described by Arrar *et al.* (2013). The macerate was filtered through Whatman No. 4 paper, and the residue from the powder was subjected to a second and then a third maceration in methanol. The obtained filtrates were then vacuum-evaporated using a rotary evaporator at 40°C. Finally, the residue from evaporation was dried in an oven at 40°C. Resulting crude extract was stored in airtight containers and kept away from light until its use (Figure 13). Additionally, the delipidated extract was prepared from the crude extract using a separating funnel through successive washes with n-hexane (≥97.0%, Sigma-Aldrich). This process allows for the separation of the apolar fraction constituting the fatty part of the extract. The solvent from each of the two obtained phases was then evaporated at 40°C using a rotary evaporator, as described by Guemmaz *et al.* (2018).

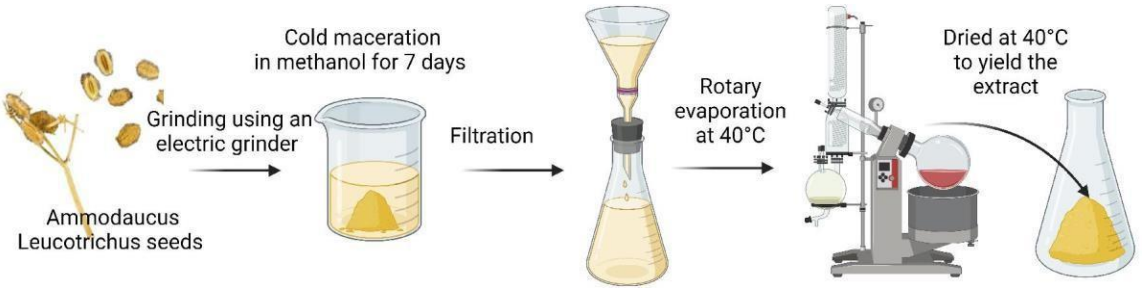

Figure 13: Schematic presentation showingextraction of polyphenols from *Ammodaucus leucotrichus* Seed.

2.3. Phytochemical analysis by GC-MS

The gas chromatography-mass spectrometry (GC-MS) analysis was conducted using a Hewlett-Packard 6890 system interfaced with a quadrupole mass spectrometer (model HP 5973), equipped with an HP5 MS capillary column (5% phenylmethyl siloxane in dimethylpolysiloxane, 30 m x 0.25 mm, 0.25 mm film thickness; PTAPC, BISKRA). The experimental setup included a helium carrier gas flow rate of 0.5 mL/min, a split ratio of 30, an electron ionization system with ionization energy of 70 eV, and a scan range of 30-550 atomic mass units. The GC-MS transfer line temperatures for the injector and detector were set at 250°C and 280°C, respectively, while the ion source temperature was maintained at 230°C. The column temperature was initiated at 60°C for 8 minutes, then increased gradually to 280°C at a rate of 2°C/min and held isothermal for 30 minutes. Injections comprised 0.2 mL of a n-hexane (HPLC grade 95%, Fisher Chemical) and methanol solution (HPLC grade, ≥99.9%, Sigma-Aldrich). Mass spectra were compared with the computer libraries Wiley 7N, National Institute of Standards and Technology (NIST) 02, and NIST 98 (NIST11 and Wiley 8) for compound identification (Abdi Bellau *et al.*, 2022)**.**

2.4. Toxicity assessment of extract

Male rats weighing between 200 and 250 g were assessed following the guidelines provided by the Organization for Economic Cooperation and Development (OECD) guideline 425 (2008). The rats were maintained for 14 days under standard conditions, including a regular 12-hour light/12-hour dark cycle, along with typical temperature and humidity levels. The rats were categorized into two groups: the treated group received a single oral dose of 2000 mg/kg of the extract, while the control animals were administered a 0.9% saline solution. Throughout the study, all experimental animals were closely monitored to record any clinical symptoms or behavioural changes.

2.5. Assay of protein denaturation inhibition

The in vitro anti-inflammatory effects of methanol and n-hexane extracts were examined through a protein denaturation assay, utilizing bovine serum albumin (BSA, pH 7, ≥98%, Sigma-Aldrich), as reported in the study by Karthik *et al.* (2013). A mixture of 0.2% BSA in Tris-HCl buffer (pH 6.8, >99%, Sigma-Aldrich) was combined with various concentrations of the extracts (250, 125, 62.5, 31.2, 15.62, 7.81,3 µg/ml) and the reference drug (Diclofenac, , 25 mg/ml). The sealed trays were subjected to 15-minute incubation at 37°C in an oven, followed by a 5-minute heating in a water bath at 70°C. Turbidity absorbance was measured at 660 nm using UV-vis spectrophotometer (VIS-7220G). The inhibition percentage (%) was calculated using the formula: % Inhibition = 100 x (1 – At)/Ac, where At is the absorbance of the test sample, and Ac is the absorbance of the control.

2.6. Assay of protease inhibition

The proteinase inhibitory activity analysis was carried out following a modified protocol reported in a study by Ahmad *et al.* (2020). The reaction mixture comprised 200 µl of the

tested extract at various concentrations (500, 250, 125, 62.5, 31.2 µg/ml), 200 µl of 25 mM tris-HCl buffer at pH 7,5 and 12 µl of 0.6 mg trypsin (1,000-2,000 units/mg solid, Sigma-Aldrich). After a 5-minute incubation at 37°C, 200 µl of 0.8% w/v ovalbumin (OVA, Sigma) was introduced to the mixtures, followed by a second incubation lasting 20 minutes. To stop the chemical reaction, 400 µl of a 35% v/v hydrochloric acid solution was added. The resulting solution underwent centrifugation (refrigerated centrifuge 3-30 KS, Sigma-Aldrich, Germany) at 5000 rpm for 5 minutes to collect the supernatant, and absorbance was measured at 280 nm using UV-vis spectrophotometer (VIS-7220G). Diclofenac served as the standard drug. The percentage of proteinase inhibition was calculated for each extract and standard using the formula: % Inhibition = 100 × (1 – At)/Ac, where At is the absorbance of the test sample, and Ac is the absorbance of the control.

2.7. *In vivo* anti-arthritic activities

2.7.1. Testing extract effect on collagen-II induced arthritis

Arthritis was induced in male rats weighing between 200 to 250 g, following the method described by Lei *et al.* (2020) with minor modifications. First, type II collagen (6 mg/ml) was dissolved overnight in 0.1 M acetic acid and then mixed with an equal volume of CFA to create a viscous solution with a final concentration of 3 mg/ml. The hind limbs of the rats were shaved and disinfected with a 70% (v/v) alcohol solution. For the initial immunization, 200 µl of the collagen-II-adjuvant emulsion (CII and CFA) were injected intradermally into each rat at three separate sites: 100 µl at the base of the tail, 50 µl in the left hind leg, and 50 µl in the right hind leg, while the rats were under light diethyl ether anesthesia. After 14 days, a second immunization took place with 100 µl of the emulsion (CII in incomplete Freund adjuvant) via intradermal injection. The rats were categorized into six groups, each consisting of 7 rats: Group I: The healthy group (negative control) received only 200 µl of 0.1 M acetic

acid. Group II: The CII-induced arthritis group served as the positive control. Group III: The CII-induced group received an oral treatment of 0.2 mg/kg MTX three times per week (Zhang *et al.*, 2019) until day 42. Groups IV-VI: In these groups, rats from the CII-induced group were orally treated with the extract at doses of 600 mg/kg/day (HD), 300 mg/kg/day (MD), or 150 mg/kg/day, respectively, starting from day 21.

2.7.2. Testing extract effect on CFA-induced arthritis

The CFA-induced arthritis model was based on a prior study (Aljumayi *et al.*, 2022) with minor adjustments. To induce rheumatoid arthritis, the rats were subjected to intradermal injections of 100 µl CFA in both the left and right hind legs under mild diethyl ether anesthesia. After a seven-day interval, a further intradermal injection of 50 µl of CFA was administered. The male rats, weighing between 200 to 250 g, were divided into six groups, each consisting of 7 rats: Group I: A normal group received 100 µl of 0.9% NaCl. Group II: The CFA group. Group III: The CFA group treated with MTX. Groups IV, V, and VI: These groups received *the* extract at three different does (150 mg/kg/day - LD, 300 mg/kg/day - MD, or 600 mg/kg/day - HD), respectively. Starting from day 14, the positive and negative control groups were maintained on the basal diet. In contrast, Groups IV, V, and VI received the basal diet along with doses of 150, 300, and 600 mg/kg/day of the extract, respectively. Group III was orally administered 0.2 mg/kg of MTX three times per week (Zhang et al 2019) until day 28 of the experiment.

2.7.3. Studied parameters of arthritis

2.7.3.1. Arthritic score

The arthritic score (AS) was assessed following the method by Sun *et al.* (2023). The scoring system was as follows: AS = 0 indicated no redness or swelling; AS = 1 represented redness

and swelling of the little toe joints; AS = 2 denoted redness and swelling of all joints and toes; AS = 3 signified redness and swelling below the ankle joint; AS = 4 indicated redness and swelling of all joints, including the ankle joint. The arthritis score for each rat was the sum of the scores for all joints.

2.7.3.2. Evaluation of arthritic rats gait

The disease progression in arthritic rats was monitored using a method developed by Gurram *et al.* (2022). This involved assessing the functional recovery of the animals from discomfort and pain by allowing them to walk on ink-absorbing paper, thereby imprinting their hind legs. Testing and Footprint Recording. The animals were evaluated in a confined corridor measuring 8.7 cm in width and 43 cm in length, with a dark shelter at one end. After two or three conditioning trials, during which the rats often paused to explore the corridor, the animals consistently walked towards the dark shelter at the end of the corridor (de Medinaceli *et al.*, 1982). Subsequently, the inked footprints on paper were scanned and analyzed to measure step length, intra-step distance, gait distance, and surface area. ImageJ software (Version 1.44; Wayne Rasband, National Institute of Health) was employed for these measurements.

2.7.3.3. Measurement of body, spleen, and thymus relative weights

The body weight of the rats was monitored once a week throughout the entire experimental period. It was calculated on days 0, 7, 14, 21, 28, 35, and 42 for each group in the first experiment involving collagen-induced arthritis, and on days 0, 7, 14, 21, and 28 for each group in the second experiment involving complete Freund's adjuvant-induced arthritis.

Additionally, under diethyl ether anesthesia at the end of both tests, the spleen, and thymus were harvested from each rat, and the relative weight (%) of each organ compared to the corresponding body weight of the rat was also determined using the following formula:

Relative weight of the organ=(Weight of the organ/Total body weigh)×100.The indices of these organs in arthritic control and treated animals were compared to those in the arthritic groups. The hind legs were used for additional analysis (Choudhary *et al.*, 2023).

2.7.3.4. Biochemical parameters

Blood sampling is performed by cardiac puncture into EDTA tubes at the time of animal sacrifice. The collected blood is kept at +4°C until centrifugation at 3000 rpm for 10 minutes. The plasma separated by centrifugation is then aliquoted into Eppendorf® microtubes and frozen at -20°C for the quantification of complement 3 (C3), glutathione (GSH), malondialdehyde (MDA), and the assessment of plasma myeloperoxidase (MPO) activity (Choudhary *et al.*, 2023).

A. Serum levels of C3

To determine the complement 3 (C3) levels in serum, an enzyme-linked immunosorbent assay (ELISA) was performed using the Mindray BS-240 Pro sequential analysis system (Cao *et al.*, 2023).

B. Reduced glutathione level

The concentration of reduced glutathione was determined using Ellman's approach 1959. Compounds with sulfhydryl groups turn yellow when DTNB is added. After adding 3 ml of 4% sulfosalicylic acid and 0.2 ml of supernatant to tubes, they were centrifuged at 2500 g for

15 minutes. Then, 0.2 ml of the supernatant was mixed with 1 ml of phosphate buffer (0.1 M, pH 7.4) and 0.4 ml of 10 mM DTNB. The absorbance at 412 nm was measured.

C. Serum levels of oxidative stress parameters

The analysis of plasma malondialdehyde (MDA) content was conducted to assess the level of lipid peroxidation in different experimental groups, following the method outlined by Guemmaz *et al.* (2018). A volume of 0.5 mL of 20% TCA (trichloroacetic acid) and 1mL of 0.67% TBA (thiobarbituric acid) was added to 0.5 mL of serum. The mixture was then incubated at 95°C for one hour. After incubation, the samples were cooled in an ice bath for 10 minutes. The MDA-TBA complex was then extracted by adding an equal volume of n-butanol. This mixture was vigorously vortexed and then centrifuged at 10000 rpm for 15 minutes. The supernatant was collected, and the absorbance was read at λ = 532 nm. The concentration of MDA was calculated using the molar extinction coefficient of the MDA-TBA adduct (156 $mM^{-1}x\ cm^{-1}$) and expressed in nmol/mL of serum (Guemmaz *et al.*, 2018).

Furthermore, the activity of plasma myeloperoxidase (MPO) was evaluated using the O-dianisidine method in the presence of H_2O_2, as described by Majid *et al.* (2023). A volume of 0.1 mL of each sample was mixed with 2.9 mL of phosphate buffer (50 mM, pH = 6) containing 0.167 mg/mL O-dianisidine Dihydrochloride and 0.1% hydrogen peroxide (H_2O_2). The absorbance of each sample was measured every minute for 3 minutes at λ = 470 nm.One unit of MPO activity corresponds to the degradation of one micromole of hydrogen peroxide (H_2O_2) per minute at 25°C. The calculated values are expressed in U/L using the formula: MPO (U/L) = (ΔA/min x 2832 U/L), where ΔA/min = (A3 – A2) / 2, A3 is the absorbance at three minutes, and A2 is the absorbance at one minute. The results are presented in U/L (Majid *et al.*, 2023).

2.7.3.5. X-ray assessment of rheumatoid arthritis severity

At the end of both experiments, the rats were euthanized, and their hind legs were preserved in 10% formalin for evaluating joint deterioration through X-ray radiography. The radiographic technique assessed the severity of joint deformities, and the radiographic images were scored. The modified Sharp/Van der Heijde system (Júnior *et al.*, 2020) was used for scoring. Each joint received a score for joint space narrowing and erosions. Joint space narrowing was scored from 0 to 4, with 0 indicating no narrowing, 1 representing minimal narrowing, 2 denoting a 50% loss of joint space, 3 indicating a 75% loss of joint space, and 4 illustrating complete joint space loss. The erosion score per joint ranged from 0 to 4, with 1 assigned if there was a discrete but clear presence of erosion and 2 or 3 if it was more extensive, based on the affected surface area of the joint. A score of 4 was given if the erosion was significant, or if there were multiple erosions adding up to a maximum. A score of 5 was assigned if there was complete joint collapse or if the entire joint surface was affected (Wang *et al.*, 2022).

2.7.3.6. Histopathological analysis of rat hind legs

The hind legs from each rat were promptly collected and fixed in a 10% formalin solution. Subsequently, they underwent decalcification in 15% HNO_3 over the course of one week. Following this, the legs were embedded in paraffin blocks after a series of immersion steps in alcohol and xylene using an automated process. The joint histological sections were then prepared for each leg and mounted on glass slides. Hematoxylin and Eosin staining were applied to the prepared slides once they had dried. This allowed for the observation of the morphology using a light microscope, enabling the detection and evaluation of histopathological changes within each group (Gao *et al.*, 2022).

2.8. *In silico* anti-arthritic activities

2.8.1. Molecular docking

To study the binding mechanisms of the 59 compounds identified in *Ammodaucus leucotrichus* seed extract, a molecular docking study was conducted targeting the active sites of trypsin. The 3D coordinates for the trypsin target (ID: 2PTN) were obtained from the Protein Data Bank (https://www.rcsb.org) and prepared for docking using the LeadIT 2.1.8 software package (www.biosolveit.com). Before the docking simulation, all water molecules were removed, and polar hydrogen atoms were introduced (Lasmari *et al.*, 2021). Any missing atoms were added, and formal charges were computed. Subsequently, the resulting structure underwent rigorous minimization before being exported as mol2 files (Boualia, I et al 2019). The 3D structures of the compounds were retrieved from the PubChem database (https://pubchem.ncbi.nlm.nih.gov/) and prepared for docking simulations using Schrodinger's Maestro version 11.3 LigPrep module (Release, 2015). This module streamlines the generation of all tautomeric forms, protonation states at pH=7.4±1, and enantiomers for each ligand (Demmak *et al.*, 2019). Molecular docking calculations were executed using FlexX 2.1.8, employing an incremental ligand construction approach (Rarey *et al.*, 1996). The fragment selection was set in automatic mode, and the standard algorithm for fragment placement was utilized. Phytocompounds in the extract were ranked using the FlexX scoring function, providing scores in terms of ΔG (Gibbs free energy) measured in kJ/mol.

2.8.2. Prediction of potential protein targets and drug-likeness analysis

To estimate the biological activity of the 59 compounds detected in the methanol extract, the PASS Online tool (way2drug.com/passonline/predict.php) was employed, achieving an average accuracy of over 95%. The structures of the compounds were uploaded in "mol"

format to PASS Online, yielding Pa (probability to be active) and Pi (probability to be inactive) values (Zhu *et al.*, 2020). Further assessments of the bioavailability, pharmacokinetic, and toxicity properties of hydroxyacetic acid hydrazide were conducted using SwissADME, BOILEDEgg (Swiss ADME), and ProTox-II (ProTox-II - Prediction of TOXicity of chemicals (charite.de))

2.9. Statistical analysis

The obtained results are presented as the mean ± standard deviation, with n = 3 for in vitro analysis and n = 7 for the in vivo study.Statistical analysis was conducted using one and two-way ANOVA, followed by Tukey's post hoc test for multiple comparisons. The statistical calculations were performed using SPSS Statistics 26.0 (IBM, USA), and statistical figures were generated using GraphPad Prism (version 10, GraphPad Software, USA). Probability values less than 0.05 were considered statistically significant.

RESULTS AND DISCUSSION

1. Extraction and purity of type II collagen

The successful extraction of collagen-II is essential to ensure the reliability of the animal models used in our study. This purity is crucial because it enables the induced arthritis in these models to closely mimic the human condition, thus facilitating a precise evaluation of the antiarthritic properties of the extracts we are testing. To assess the purity, molecular weight, and structural characteristics of the collagen II obtained from chicken sternum cartilage (CII), UV absorption spectrum analysis and SDS-PAGE (Sodium Dodecyl Sulfate Polyacrylamide Gel Electrophoresis) were used. Figure 14 shows the UV absorption spectrum of collagen II, which displays two distinct absorption peaks at approximately 225 nm and 280 nm. The peak at 225 nm is associated with the absorption of aromatic amino acids, primarily tryptophan, within the protein. The peak at 280 nm corresponds to the absorption of UV-light by the peptide bond in the protein's backbone (Naito *et al.*, 2022). This unique peak arises due to the relatively low concentration of tyrosine residues within collagen-II, estimated at approximately 8.0-9.7 per 1000 amino acid residues. Moreover, the SDS-PAGE analysis offered further confirmation of the exceptional purity of the collagen and its marker size in the range of 15-180 kDa. It distinctly showed the presence of the specific α1 and α2 chains, which are hallmark features of collagen-II, alongside a β chain. This unequivocally validates that the collagen sample is, indeed, collagen-II, and underscores the high level of purity achieved during the extraction process.

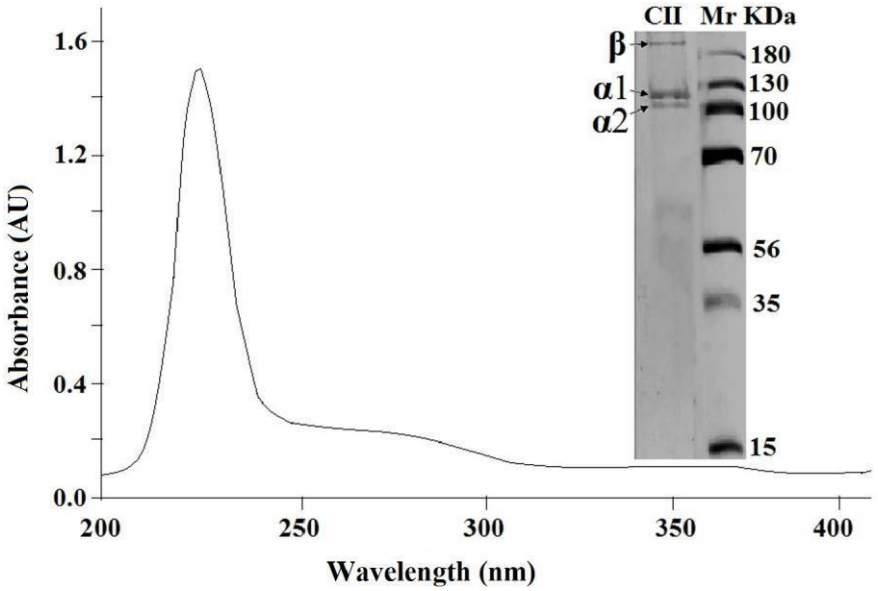

Figure 14: UV absorption spectrum and SDS-PAGE of collagen-II obtained from chicken sternum cartilage (CII). Mr: Molecular weight markers (15-180KDa).

2. GC-MS analysis of the extracts

The GC-MS analysis performed on methanol and n-hexane extracts revealed that approximately 59 and 58 secondary metabolites, respectively (annex 1 & 2). The validation of phytochemicals included considerations such as peak area, molecular weight, retention time, PubChem CID, and secondary metabolite formula, detailed in Table 2. These secondary metabolites, falling into distinct categories such as Ketones, Amino Alcohols, Hydrazide Derivatives, Pyranone Derivatives, Furfural Derivatives, Aldehydes, Phenol Derivatives, Sulfonate Esters, Cycloalkanols, Carboxylic Acids, Tricyclic Sesquiterpenes, Sesquiterpene Alcohols, Heterocyclic Compounds, Steroids, Spiro Compounds, Organosilicon Compounds, Tricyclic Alcohols, Phenone Oximes, Bicyclic Terpenes, Terpene Alcohols, Phthalate Esters, Siloxanes, Sugar Derivatives, Nitrobenzofurans, Cyclopropane Derivatives, Fatty Acids, Saturated Hydrocarbons, and Terpene Esters, are recognized for their biological and pharmacological significance.

Table 3: Comparative analysis of phytochemicals in the methanol and n-hexane extracts: peak area percentages from the GC-MS analysis and therapeutic effect on RA based on previous studies.

Class	Methanol extract	Peak area (%)	N-Hexane extract	Peak area (%)	Therapeutic impact
Ketones	2-Pentanone, 4,4-dimethyl-	1.36	4-Isopropenylcyclohexanone, (S)-(-)-(4-Isopropenyl-1-cyclohexenyl)methanol, (1R,7S,E)-7-Isopropyl-4,10-dimethylenecyclodec-5-enol	0.31	Positive effect (Ciaffi *et al.*, 2021;Torequl *et al.*, 2022; Zhou, C et al 2024)
Amino Alcohols	1-Propanol, 2-amino-, (.+/-.)-	0.57	Not present	0.00	Positive effect (Azizov et al 2021; Baoqi *et al.*, 2022)
Hydrazide Derivatives	Hydroxyacetic acid, hydrazide; 3-Hydroxy-3-methyl-butyric acid, hydrazide	1.91	Not present	0.00	Positive effect (Xu *et al.*, 2022)
Pyranone Derivatives	4H-Pyran-4-one, 2,3-dihydro-3,5-dihydroxy-6-methyl	0.20	Not present	0.00	Positive effect (Ciaffi *et al.*, 2021)
Furfural Derivatives	5-Hydroxymethylfurfural	0.87	Not present	0.00	Positive effect (Ciaffi *et al.*, 2021)
Aldehydes	1-Cyclohexene-1-carboxaldehyde, 4-(1-methylethenyl)-	0.35	3-Cyclohexene-1-carboxaldehyde, 1-Cyclohexene-1-carboxaldehyde, 4-(1-methylethenyl)-	3.07	Not Tested
Phenol Derivatives	Thymol	0.25	Phenol, 2,6-dimethoxy-4-(2-propenyl)-	0.79	Positive effect (Khan *et al.*, 2021)
Sulfonate Esters	2-Butene-1,4-diol, methanesulfonate t-butoxycarbonylaminoacetate	0.13	Not present	0.00	Positive effect (Torequl *et al.*, 2022)
Cycloalkanols	Cyclopentanol	0.19	Not present	0.00	Not Tested
Carboxylic Acids	1-Cyclohexene-1-carboxylic acid, 4-(1-methylethenyl)-; Formic acid, undecyl ester	0.48	Dodecanoic acid, Propanoic acid, 2-(tricyclo[3.3.1.13,7])	0.40	Positive effect (George et al 2020; Zeng *et al.*, 2021; Babaahmadi *et al.*, 2023)
Tricyclic Sesquiterpenes	5-Oxatricyclo[8.2.0.04,6]dodecane, 4,12,12-trimethyl-9-methylene-, (1R,4R,6R,10S)-	0.55	Not present	0.00	Positive effect (Yang *et al.*, 2022)
Sesquiterpene Alcohols	Isospathulenol, Thunbergol, 7,8-Epoxylanostan-11-ol, 3-acetoxy-, 1H-Cycloprop[e]azulen-7-ol, decahydro-1,1,7-trimethyl-4-methylene-, [1ar-(1a.alpha.,4a.alpha.,7.beta.,7a.beta.,7b.alpha.)]-, Methyl 16-R/S-hydroxy-cleroda-3,13(14)-Z-dien-15,16-olide	2.39	Isospathulenol, 1H-Cycloprop[e]azulen-7-ol, decahydro-1,1,7-trimethyl-4-methylene-, [1ar-(1a.alpha.,4a.alpha.,7.beta.,7a.beta.,7b.alpha.)]-, Methyl 16-R/S-hydroxy-cleroda-3,13(14)-Z-dien-15,16-olide	2.87	Not Tested
Heterocyclic Compounds	2,2-bis(oxidanylidene)-1,5-dihydroimidazo[4,5-c][1,2,6]thiadiazin-4-one	0.19	Not present	0.00	Not Tested
Steroids	3beta-Trimethylsiloxy-5alpha,6alpha-epoxycholestane	0.43	Not present	0.00	Not Tested

Spiro Compounds	Spiro[5.6]dodecan-7-one, Spiro[5.5]undeca-1,7-diene	0.45	5,5-diethyl-4-methyl-6-spiro[2.3]hexan	1.05	Not Tested
Organosilicon Compounds	Silane, trichlorododecyl	0.38	Not present	0.00	Not Tested
Tricyclic Alcohols	3-Isopropyl-6,7-dimethyltricyclo[4.4.0.0(2,8)]decane-9,10-diol	0.97	3-Isopropyl-6,7-dimethyltricyclo[4.4.0.0(2,8)]decane-9,10-diol	3.96	Positive effect (Liu, Y et al 2021)
Phenone Oximes	4'-Hydroxybutyrophenone oxime	0.22	Not present	0.00	Positive effect (Schepetkin *et al.*, 2021)
Bicyclic Terpenes	Bicyclo[2.2.1]heptane, 2-ethylidene-1,7,7-trimethyl-; 8-Isopropyl-1,5-dimethyltricyclo[4.4.0.02,7]dec-4-en-3-one	1.08	Not present	0.00	Not Tested
Terpene Alcohols	2,4,7,14-Tetramethyl-4-vinyl-tricyclo[5.4.3.0(1,8)]tetradecan-6-ol; Bicyclo[4.4.0]dec-2-ene-4-ol, 2-methyl-9-(prop-1-en-3-ol-2)-; Tetradecanoic acid, 5,9,13-trimethyl-, methyl ester; Tetradecanoic acid; 9,12-Octadecadienoic acid (Z,Z)-, methyl ester; 9-Octadecenoic acid, methyl ester, (E)-	15.23	9,12-Octadecadienoic acid (Z,Z)-, methyl ester; 9-Octadecenoic acid, methyl ester, (E)-	6.99	Positive effect (Kavitha *et al.*, 2017)
Phthalate Esters	Phthalic acid, tetradecyl trans-dec-3-enyl ester; Phthalic acid, butyl hept-4-yl ester	2.42	Not present	0.00	Not Tested
Siloxanes	Cyclononasiloxane, octadecamethyl-	0.33	Not present	0.00	Not Tested
Sugar Derivatives	1,2,3,4,5-Penta-O-acetyl-D-xylitol	0.27	Not present	0.00	Not Tested
Nitrobenzofurans	1,3-Isobenzofuranone, 5-nitro-	0.64	Not present	0.00	Not Tested
Cyclopropane Derivatives	Cyclopropanebutanoic acid, 2-[[2-[[2-[(2-pentylcyclopropyl)methyl]cyclopropyl]methyl]cyclopropyl]methyl]-, methyl ester	0.71	Not present	0.00	Not Tested
Fatty Acids	Tetradecanoic acid; 9,12-Octadecadienoic acid (Z,Z)-; 9-Octadecenoic acid; Octadecanoic acid; Hexadecanoic acid, methyl ester; n-Hexadecanoic acid; Heptadecanoic acid	51.14	9,12-Octadecadienoic acid (Z,Z)-; 9-Octadecenoic acid; Octadecanoic acid; Hexadecanoic acid, methyl ester; n-Hexadecanoic acid	61.10	Positive effect (Gnanasundaram *et al.*, 2017; Najah & Alshawish, 2023)
Saturated Hydrocarbons	Tetracontane	0.68	Heptane, 3-methyl-; Hexane, 3-methyl-; Hexane, 2,2-dimethyl-; Heptane	1.68	Not Tested
Terpene Esters	trans-(R,R)-chrysanthemyl (R)-2-methylbutanoate; Kauren-19-yl-acetate	2.48	Not present	0.00	Not Tested

The difference in chemical structure and solvation power between the two solvents, n-hexane and methanol, arises from their distinct polarities (Usman *et al.*, 2023). In contrast, methanol,

being a more polar solvent, enhances the extraction of a broader range of compounds, encompassing both polar and moderately polar substances (Zhou *et al.*, 2024). This difference is evident in the peak area percentages of various compound classes. Notably, certain compound classes crucial in influencing rheumatoid arthritis, such as amino alcohols, hydrazide derivatives, pyranone derivatives, furfural derivatives, sulfonate esters, cycloalkanols, tricyclic sesquiterpenes, heterocyclic compounds, steroids, organosilicon compounds, phenone oximes, bicyclic terpenes, phthalate esters, siloxanes, sugar derivatives, nitrobenzofurans, cyclopropane derivatives, and terpene esters, are conspicuously absent in the n-hexane extract.

Analyzing the results from Table 2, the methanolic extract is characterized by dominant fatty acids (51.14%), followed by terpene alcohols (15.23%) and terpene esters (2.48%). In contrast, the n-hexane extract also exhibits a dominance of fatty acids (61.10%), a lower percentage of terpene alcohols (6.99%), and the presence of tricyclic alcohols (3.96%). The presence of n-hexadecanoic acid, identified in both extracts, aligns with its known anti-inflammatory effects. Previous studies suggest that n-hexadecanoic acid demonstrates anti-inflammatory effects by inhibiting various inflammatory mediators, including phospholipase A2, prostaglandins E2, IL-6, IL-1, TNF, and nitric oxide synthase. Additionally, it exhibits hypocholesteromic, nematicidal, and pesticidal effects (Aparna *et al.*, 2012; Sheela *et al.*, 2013). The fatty acids identified in this plant align with findings from earlier research (Akbar *et al.*, 2020). Another noteworthy compound is cyclohexene-1-carboxaldehyde, 4-(1-methylthenyl)-, commonly known as perillaldehyde. This chemical, with the molecular formula $C_{10}H_{14}O$ and a molecular weight of 150.22 g/mol, has been newly identified in both methanolic extracts, registering a peak area of 0.35%, and in the n-hexane extract, where it attains a peak area of 3.02%.

3. *In vitro* anti-arthritic effect of the extracts

3.1. Protein denaturation assay

The anti-inflammatory properties of methanol and n-hexane extracts were assessed using *in vitro* protein denaturation and protease activity (crucial factors in chronic inflammatory conditions like RA) inhibition assays. Protein denaturation, which is associated with inflammation, was evaluated using a BSA denaturation assay. The strongest BSA denaturation inhibition was obtained with the n-hexane extract at 62.5 µg/ml: 90.36% versus 51.36% for diclofenac (the reference drug) at the same concentration (Figure 15). Conversely, the methanol extract exhibited a modest effect, while the n-hexane extract displayed a more favorable IC50 of 14.30 µg/ml, outperforming diclofenac (Figure 15). This emphasizes the remarkable effectiveness of the n-hexane extract in inhibiting BSA denaturation. The n-hexane extract demonstrated a significant, dose-dependent inhibition of denatured protein compared to methanol extract. Moreover, the n-hexane extract displayed a higher percentage of inhibition of BSA denaturation than diclofenac, suggesting its potential to inhibit the release of lysosomalmaterial by neutrophils at the inflammation site (Khan *et al.*, 2023).

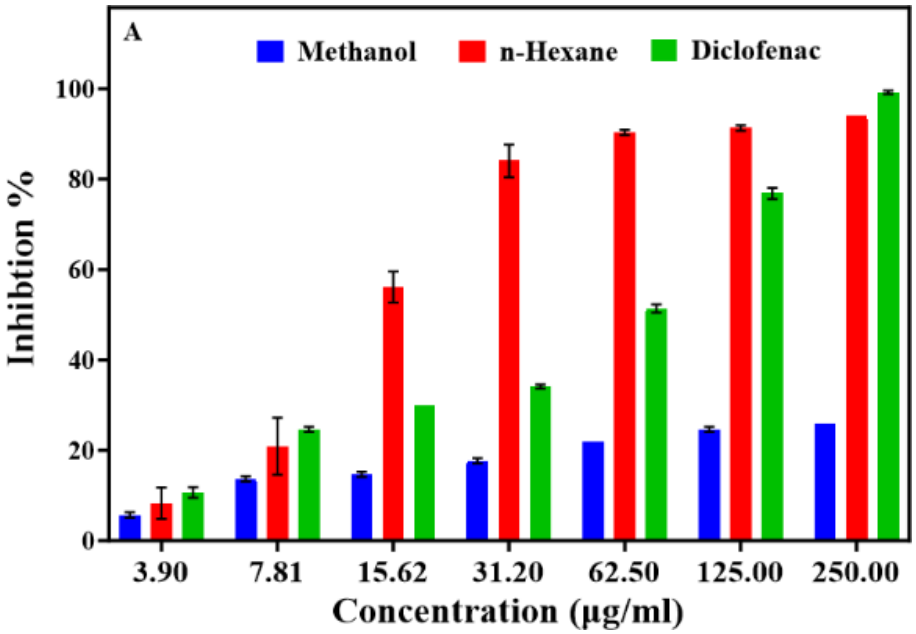

Figure 15: Effect of different concentrations of the *Ammodaucus leucotrichus* seed methanol and n-hexane extracts on BSA denaturation. Comparison of the extracts with diclofenac in a protein denaturation assay. Data are the mean ± standard deviation (n=3)

.

3.2. Proteinase inhibitory activity

Both the methanol and n-hexane extracts demonstrate significant trypsin inhibition at various concentrations, suggesting their potential in addressing rheumatoid arthritis. Notably, both extracts and diclofenac achieve 100% inhibition at 250 µg/ml. The n- hexane extract exhibits slightly reduced but significant inhibition at the same concentration, reaching 51%. present the ascending order of IC_{50} values for the extracts and the reference standard as follows: methanol (IC_{50} = 82.97 µg/ml), Diclofenac (IC_{50} = 97.04 µg/ml), and n-hexane (IC_{50} = 202.7 µg/ml) (figure 16). The methanol extracts showcase considerable anti- inflammatory effects through protease inhibition, aligning with studies by Saleem *et al.* (2020) and Mane *et al.* (2022). Given the involvement of

serine proteases (including trypsin) in arthritic joints, inhibiting these enzymes could alleviate joint discomfort and inflammation (Lucena *et al.*, 2021). Protease inhibitors have demonstrated efficacy in various clinicaldiseases, including cancer, AIDS, RA, pancreatitis, and thrombosis (Saldanha *et al.*, 2018). Therefore, the methanol extract holds promise for RA by effectively inhibiting proteases, offering a natural, alternative approach to diclofenac, a nonsteroidal anti-inflammatory drug with important side effect.

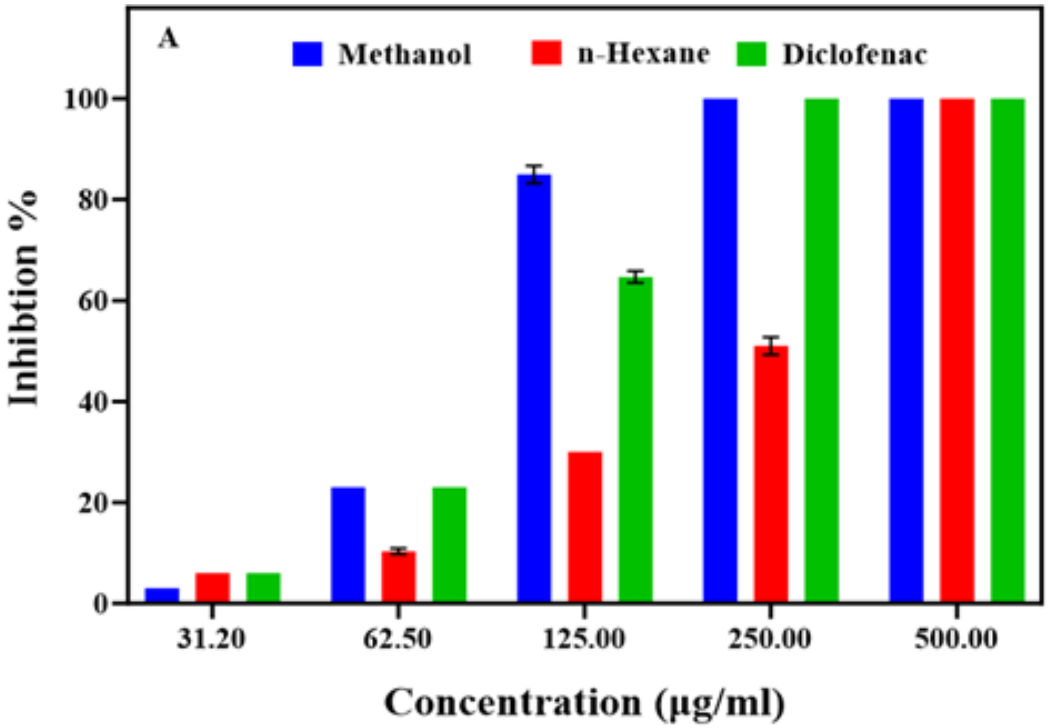

Figure 16: Influence of various concentrations of the methane and n-hexane extracts from *Ammodaucus leucotrichus* seeds on protease (trypsin) inhibition. Percentage of trypsin inhibition compared with diclofenac, the reference drug. Data are the mean ± standard deviation (n=3).

4. *In vivo* acute toxicity test

Before proceeding with the *in vivo* assessment of the *A. leucotrichus* seed extract anti-arthritic

effect, an acute toxicity test was carried out to determine the appropriate extract concentrations to be used. Male rats received one dose of the extract (2000 mg/kg/day) by oral gavage and then they were monitored for 14 days. No rat died and no sign of acute toxicity (e.g. excessive salivation, diarrhea, or respiratory problems) was observed. The LD50, whichdenotes the dose at which 50% of the tested subjects die, was not reached at the tested dose. This indicates that the extract is relatively safe even at high doses (Roumili *et al.*, 2022).

5. In vivo anti-arthritic effect of the extract

To assess its potential anti-arthritic effect, three doses of the *A. leucotrichus* seed extract (150, 300, and 600 mg/kg) were used in twowell-established rat models of arthritis (CII-induced arthritis and CFA-induced arthritis). These models closely mimic the clinical features of human rheumatoid arthritis.

5.1. Arthritic score and body weight

Rheumatoid arthritis is characterized by visible sign of joint inflammation, such as redness, swelling, and edema (Seixas *et al.*, 2020), that are indicators of the disease severity. In our experiments, these parameters were closely monitored in rats with CII-induced and CFA-induced arthritis (Figure 17): paw swelling, body weight changes, and arthritis index. Starting from day 0; the arthritis index progressively increased in both CII-induced and CFA-induced arthritis models (from 0 to 8), accompanied by paw swelling (Figure 17A-B, compared with healthy controls.

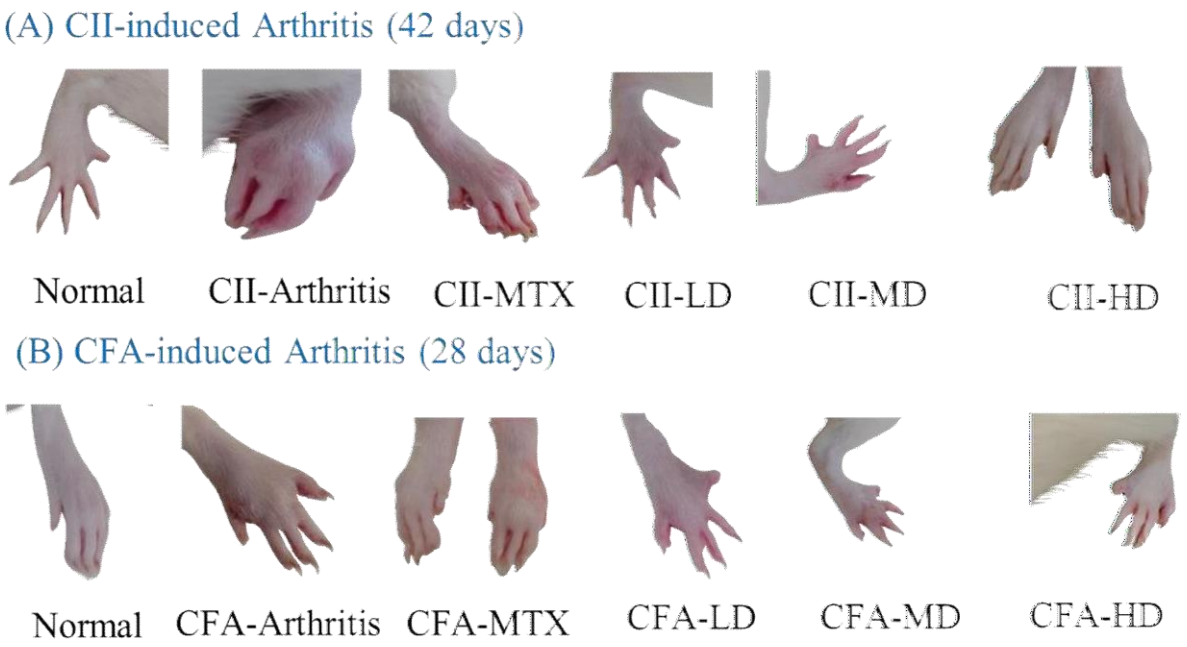

Figure 17: Paw swelling in healthy controls (normal) and untreated and treated rats with CII-induced (A) and CFA-induced arthritis (B) at the end of the experiment (day 42 and day 28, respectively). MTX, methotrexate (0.2 mg/kg); LD, 150 mg/kg of the extract; MD, 300 mg/kg of the extract; HD, 600 mg/kg of the extract.

Weight gain slowed from day 21 to day 42 in CII-induced arthritis rats and from day 14 to day 28 in CFA-induced arthritis rats compared with healthy controls (Figure 18C-D).

These results confirmed the development of arthritis following injection of CII and CFA. In treated rats (extract or MTX), paw swelling, arthritis index and body weight were less affected compared with untreated rats. This suggests that treated rats displayed signs of recovery, from day 28 to day 42 in the CII-induced arthritis group and from day 21 to day 28 in the CFA-induced arthritis group. These findings suggest that the *A. leucotrichus* seed extract and MTX limited arthritis progression and improved the overall condition of the animals.

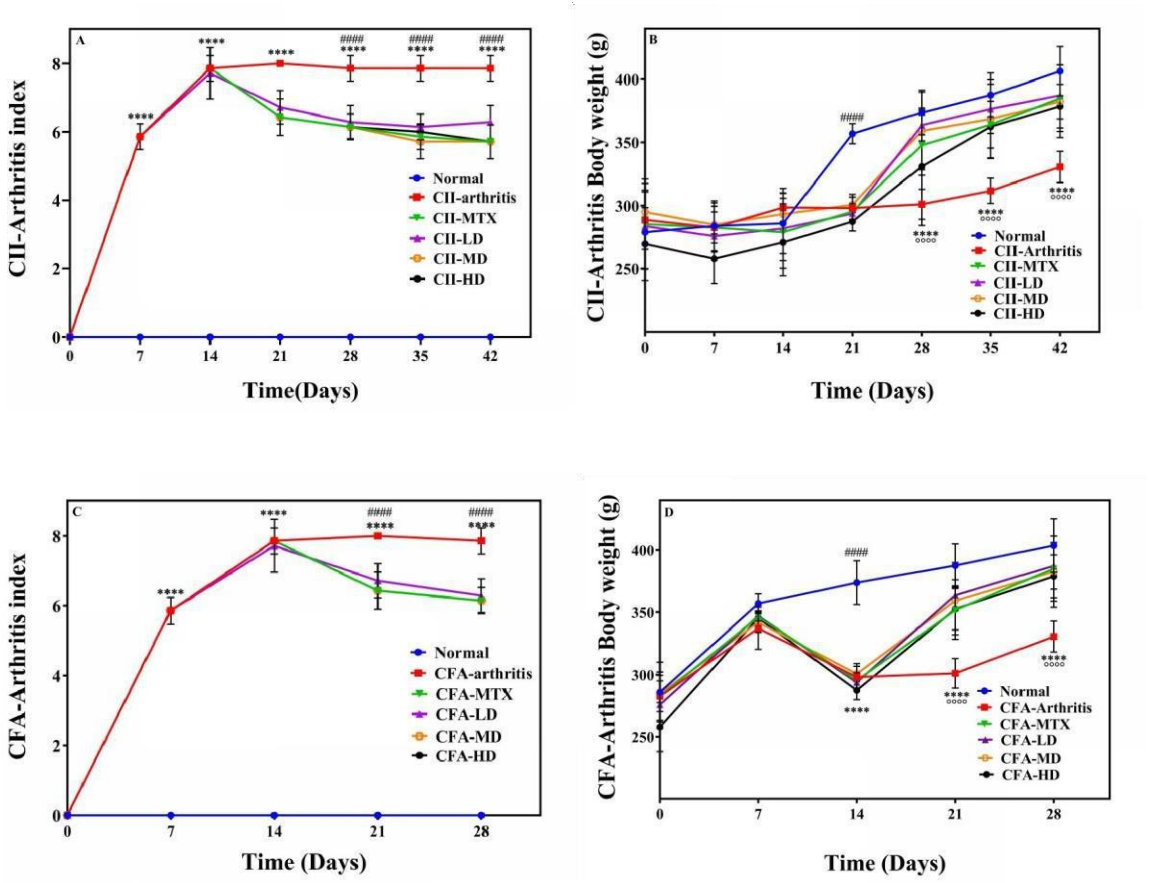

Figure 18: Effect of the extract (different doses) on the arthritis index (extent of joint redness and swelling) (A, C) and body weight (B, D) compared with methotrexate (MTX; 0.2 mg/kg). (A, B) CII-induced arthritis and (C, D) CFA-induced arthritis. Data are the mean ± SD (n=7 rats/group) (two-way repeated measures ANOVA, followed by the Tukey's multiple comparisons test. ****P<0.0001 vs normal group; $^{\#\#\#\#}$P<0.0001 vs arthritic group for both experiments.

5.2. Walking analysis of arthritic rat

At the end of the experiment (day 42 for the CII-induced arthritis model and day 28 for the CII-induced arthritis model), the following walking parameters were measured in healthy rats (normal) and in the different groups of rats with arthritis: gait distance, intra-step distance, step length, and pawprint area (Kamal *et al.*, 2021), (Figure 19). Compared with the healthy

control groups, the gait distance increased in the CII-induced- arthritis and CFA-induced arthritis groups (2.17 ± 0.23 cm versus 4.54 ± 0.34 cm and 3.99 ± 0.34 cm, respectively).

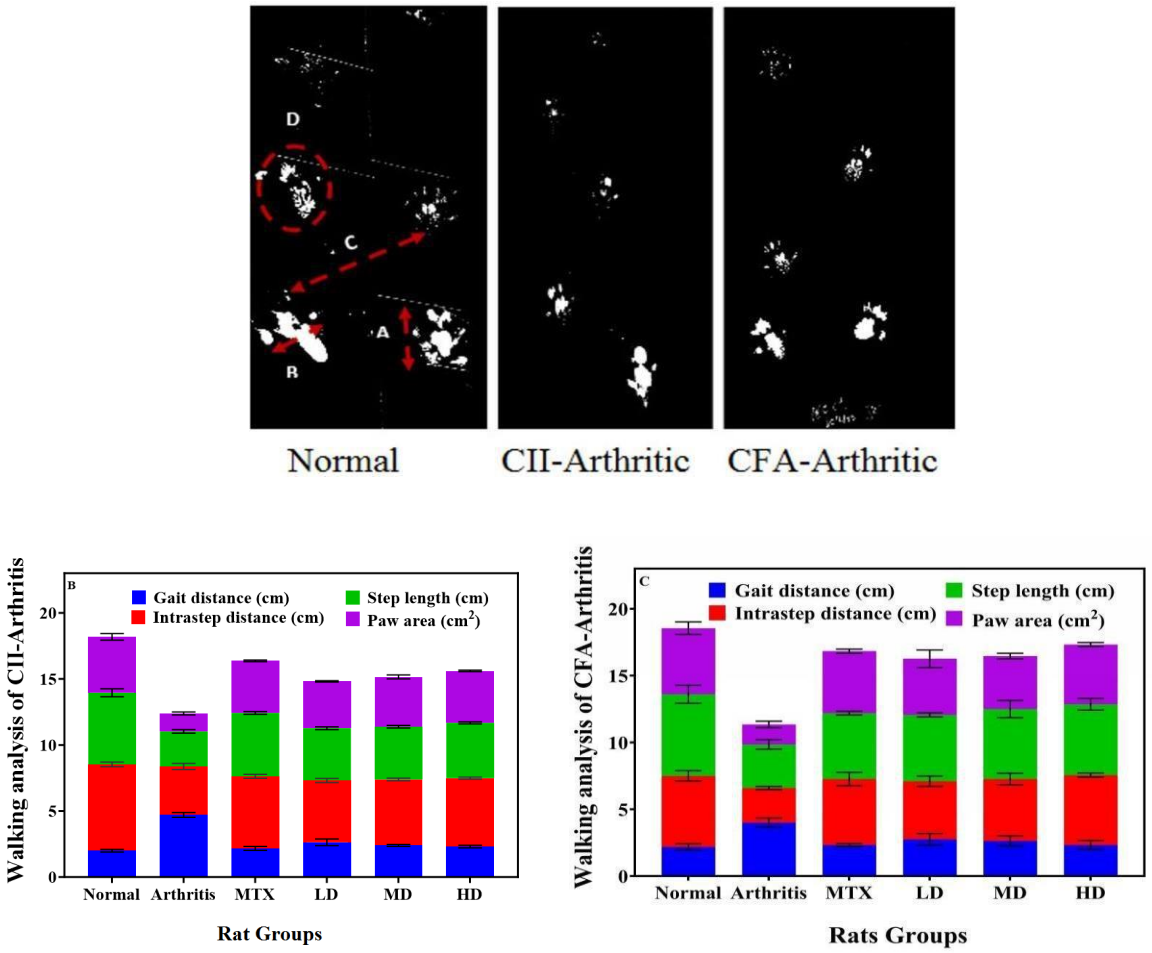

Figure 19: Walking parameter analysis at the study end. (A) Comparison of hind paw prints in healthy controls (normal) and rats with CII-induced arthritis and CFA-induced arthritis. Effects of the extract on gait distance, intra-step distance, step length, and paw print area of rats with (B) CII-induced and (C) CFA-induced arthritis. Data are the mean ± SD (n=7/group).

In animals treated with MTX or the extract, gait distance decreased compared with untreated rats. In both CII- and CFA-induced arthritis groups, treatment with the different doses of the extract (LD, MD, and HD) suggested a dose-dependent impact on locomotor activity.

Compared with the healthy control group, intra-step distance decreased in the CII-induced-

arthritis group and CFA-induced arthritis groups (5.31 ± 0.38 cm versus 3.20 ± 0.36 cm and 2.59 ± 0.11 cm, respectively). In rats treated with MTX or the extract (LD, MD, and HD), intra-step distance increased, and the strongest effect was observed in the HD group for both models.

Step length (i.e. the distance between successive placements of the same foot) also was reduced in the CII-induced arthritis group (2.86 ± 0.20 cm) and CFA-induced arthritis groups (3.26 ± 0.35 cm) compared with the healthy control group (6.11 ± 0.67 cm). Both treatments improved step length.

Paw print area (i.e. the surface area of paw imprints) was reduced in both CII- and CFA-induced arthritis groups compared with the healthy control group (1.87 ± 0.20 cm^2 and 1.49 ± 0.24 cm^2 versus 4.94 ± 0.46 cm^2, respectively). This reduction was limited by treatment with MTX and the extract (all three doses).

The findings suggest that the extract, especially at higher doses, may have a dose-dependent ameliorative effect on the tested walking parameters, and may be a candidate molecule to improve the locomotor function and motor coordination impairment caused by arthritis. These findings are consistent with the effects reported in previous studies (de Medinaceli *et al.*, 1984, Möller *et al.*, 2020).

5.3. Relative weights of spleen and thymus

In the supplementary information outlines the in vivo therapeutic effects of the extract on the relative weights of the thymus and spleen in various rat groups, encompassing normal rats, MTX-treated arthritic rats, and extract-treated arthritic rats administered with differing extract doses in both CII-induced arthritis and CFA-induced arthritis models.

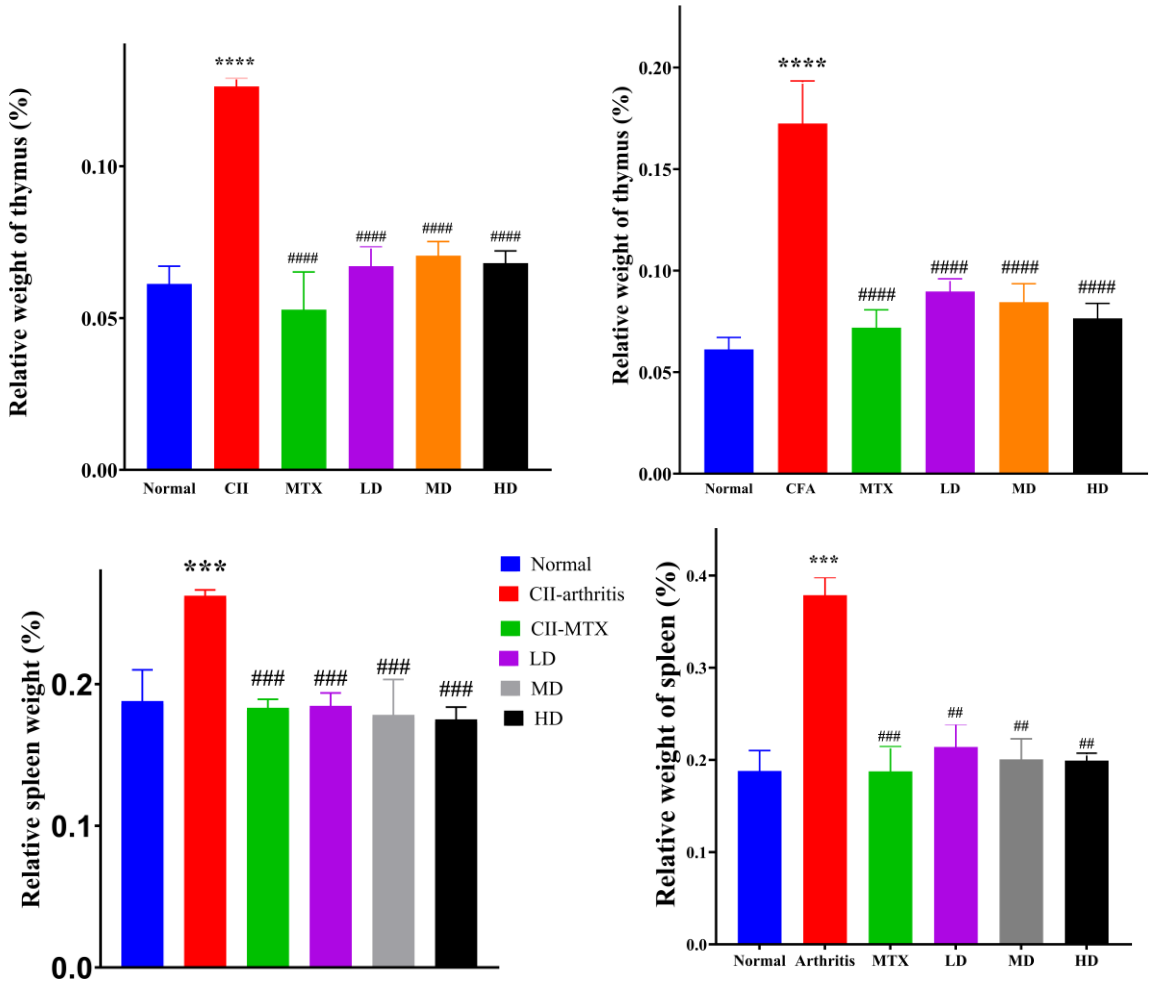

Figure 20: *In vivo* therapeutic effect of the *A. leucotrichus* seed extract on (A) thymus and (B) spleen relative weights in rats with CII-induced (blue) and CFA-induced (red) arthritis. Data are the mean (%) ± SD (n=7/group); (one-way ANOVA, followed by Tukey's multiple comparisons test). $^{****}p<0.0001$ vs normals and: $^{####}p<0.0001$,$^{###}p<0.001$,$^{##}p<0.01$ vs CII-arthritic/CFA-arthritic group.

The relative weights of the thymus and spleen (% of body weight) serve as key indicators of the immune system's functionality and, when altered, may suggest variations in immune responses due to pathological conditions or therapeutic interventions (Del Barco *et al.*, 2011). In the CII-induced arthritis group, the relative weights of both the thymus and spleen notably

increased in comparison to the normal group. The thymus showed a considerable increase to 0.120 ± 0.002% from the normal group's 0.061 ± 0.005%, while the spleen's weight increased to 0.262 ± 0.004% from the normal group's 0.188 ± 0.022% (figure 20). Additionally, the CFA-induced arthritis group displayed even more substantial increases in both thymus and spleen weights, demonstrating a significant immune system response to the arthritic conditions. These observations align with prior research (Rao *et al.*, 2018; Chen *et al.*, 2022). Conversely, the MTX group and the extract-treated groups exhibited varying responses. The MTX-treated groups displayed reduced thymus and spleen weights in both CII and CFA-induced arthritis models, indicating a possible suppression of the immune response through MTX treatment. Notably, the extract-treated groups (LD, MD, and HD) showcased varied effects on the thymus and spleen weights. While some groups displayed alterations in relative organ weights, the high-dose (HD) groups in both the CII- and CFA-induced arthritis models exhibited consistent trends towards normalized organ weights more closely aligned with the normal group, hinting at a potential restoration of immune system function with high-dose extract treatment. The findings suggest that the extract treatments, particularly at higher doses, may exert varying regulatory effects on the immune system, potentially influencing the relative weights of the thymus and spleen.

5.4. Effect of the extract on the inflammation biomarkers

The inflammation markers C3, GSH, MDA, and MPO were measured at the study end (day 42 for CII-induced arthritis and day 28 for CFA-induced arthritis). Serum C3 levels, a marker of inflammation in rheumatic diseases (Cavalli *et al.*, 2022; Arias-de la Rosa *et al.*, 2023), (Figure 21A), was increased in both CII- and CFA-induced arthritis groups (0.40±0.01 and 0.27±0.01) compared with the normal group (0.20±0.01 g/l), (Figure 21A). In the CII-induced arthritis group, only MTX significantly decreased C3 concentration, but not the extract (all three doses), (Cavalli *et al.*, 2022).

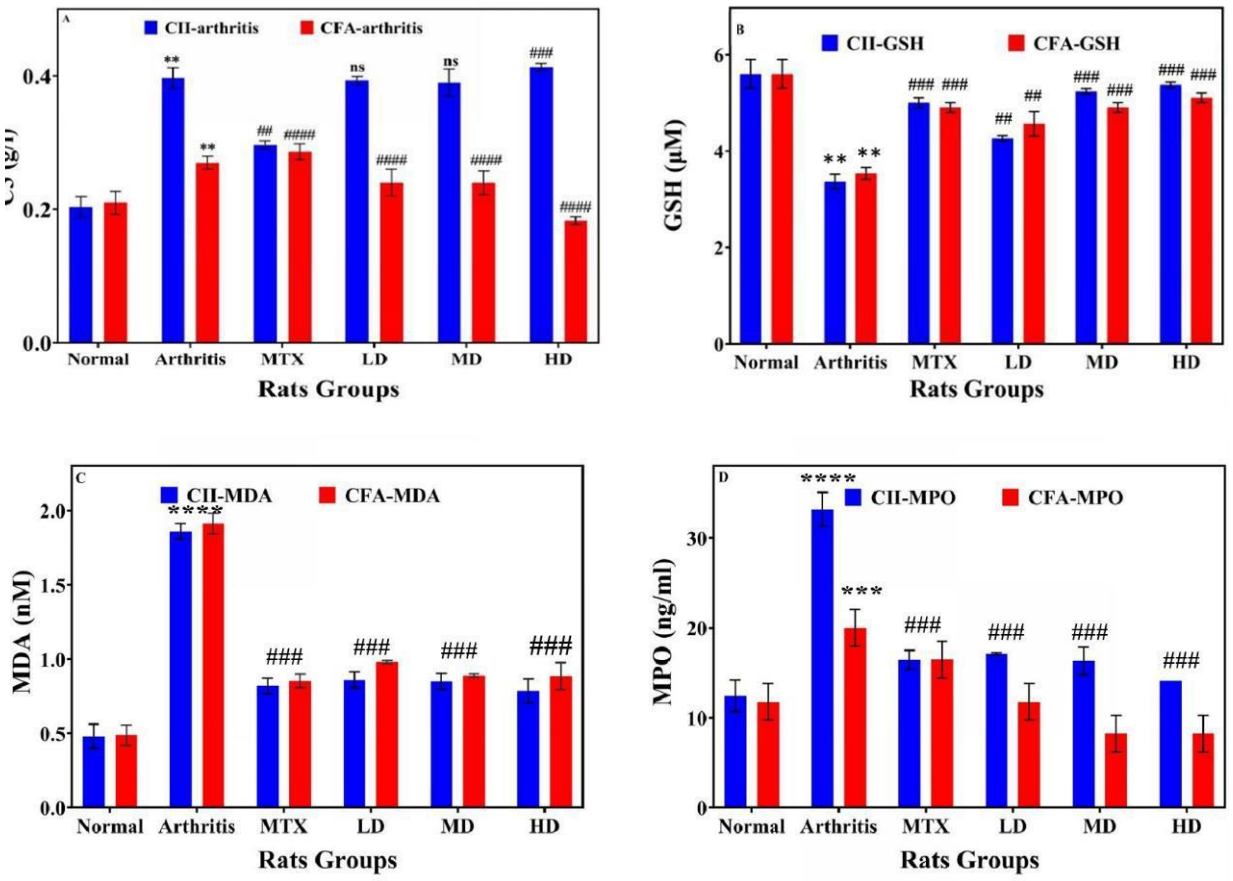

Figure 21: Effect of the extract on the serum concentration of the following inflammatory biomarkers in CII-induced arthritis and CFA-induced arthritis: (A) C3, (B) GSH, (C) MDA and (D) MPO. Values are the mean ± SD (n=7 rats/group). $^{**}p<0.01$,$^{****}p<0.0001$ vs normal; $^{###}p<0.001$ vs CII-arthritic/CFA-arthritic group.

Conversely, in the CFA-induced arthritis group, the HD extract reduced C3 concentration to 0.18±0.01 g/l. Conversely, MTX did not have any effect, in line with the findings of Paoliello-Paschoalato *et al.* (2011) and Marchi *et al.* (2018).

GSH concentration in serum decreased in the CII- and CFA-untreated groups compared with the normal group (3.36±0.15 µM and 3.56±0.20 µM versus 5.70±0.50 µM, respectively) (Figure 21B). Treatment with the extract and MTX increased GSH concentration almost to normal levels in bothmodels, consistent with previous findings (Liu et al 2022; Sun *et al.*, 2023; Alsaffar *et al.*, 2023). Specifically, GSH concentrations were 5.00±0.55 µM and

5.03±0.15 μM in the CII-MTXinduced and CFA-MTX groups, respectively. In both models, GSH increased progressively with the extract dose: from 4.26±0.75 μM (CII-LD) to 5.33±0.30 μM (CII-HD) and from 4.50±0.40 μM (CFA-LD) to 5.16 ± 0.25 μM (CFA-HD).

The examination of Figure 21C and the comprehensive data outlined in Table S9 reveal a significant increase in MDA and MPO levels within both CII-induced arthritis and CFA-induced arthritis groups when compared to the normal rat group. Serum MDA and MPO levels considered significant inflammatory markers for rheumatoid arthritis (Strzepa *et al.*, 2017; Badawi *et al.*, 2022), were notably higher in both the CII-induced and CFA-induced arthritic groups compared to the treated groups. The concentrations of MDA measured 1.86±0.05 and 1.93±0.06 nM, while MPO concentrations were recorded at 32.85±4.0 and 20±2 ng/ml, respectively (Figure 21D). However, the administration of various doses of the extract and MTX demonstrated substantial reductions in MDA levels across all treated groups in both experiments. Particularly, the CII-HD group exhibited a significant decrease in MPO levels to 14.12±0.01 ng/ml, followed by reductions in the groups treated with CII-MTX, CII-LD, CII-MD, CFA-MD, and CFA-HD, showing concentrations of 16.44±0.16, 17.13±0.11, 16.33±0.15, 8.23±0.2, and 8.24±0.25 ng/ml, respectively. This indicates the potential of both the extract and MTX in reducing these inflammatory markers, suggesting their role in attenuating oxidative stress and inflammation associated with rheumatoid arthritis.

5.5. X-ray analysis of joint space and erosion

X-ray imaging was used to assess leg swelling, a characteristic sign of inflammation in arthritic conditions, in the different groups at the study end (Figure 22A). The CII- and CFA-induced arthritis exhibited substantial joint erosion (3.33±0.57 in both groups) compared with negative controls (no swelling; 0.00±0.00).

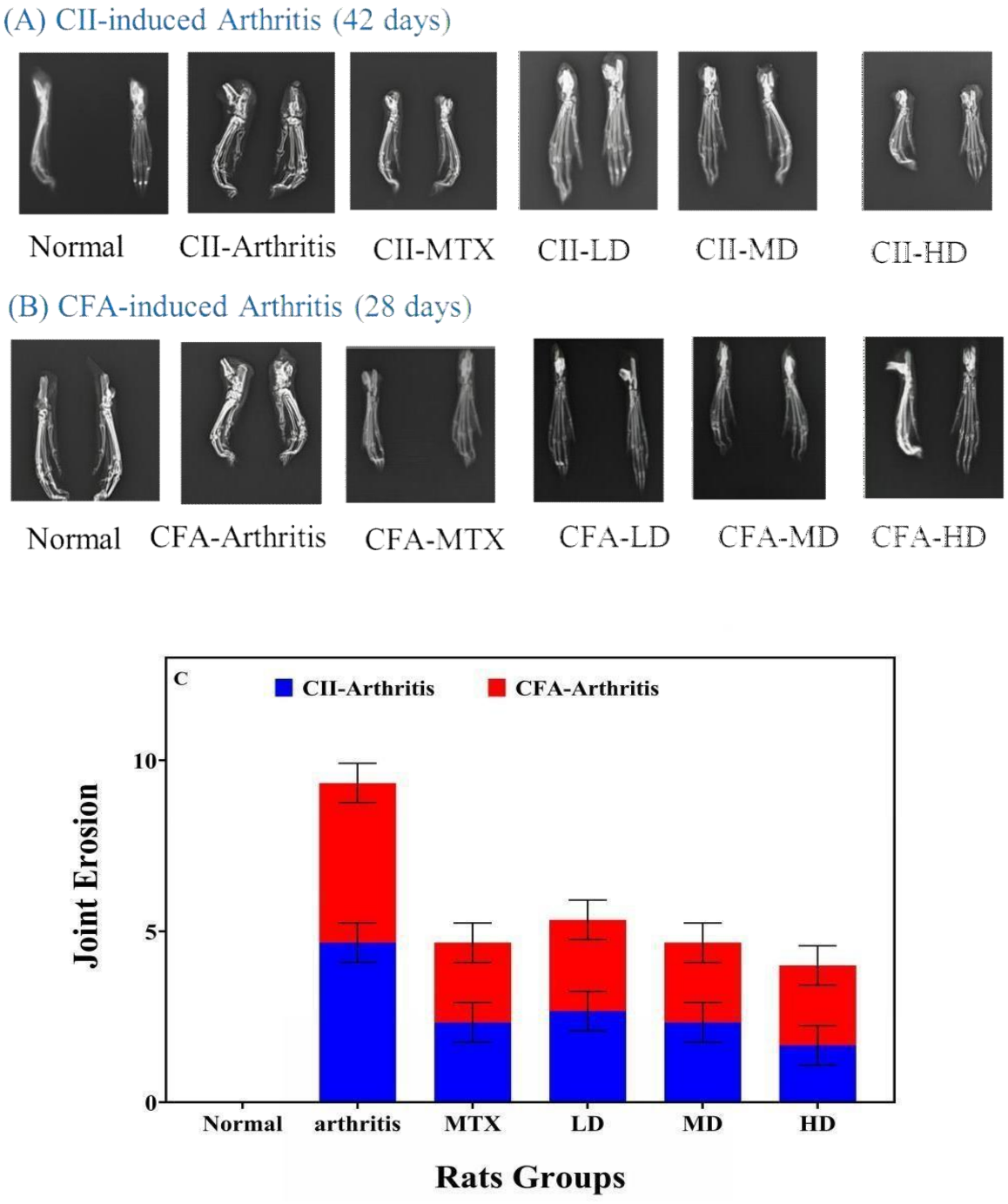

Figure 22: X-ray images of the hind paws in rats with (A) CII-induced arthritis, and (B) CFA-induced arthritis at the study end. Explain what these images show. (C) Joint erosion (mean ± SD; n=7 rats/group).

Following treatment with MTX or the extract, joint erosion decreased in both models. CFA-induced arthritis MTX group and 1.00±0.01 in the CII-HD group and 1.33±0.56 in the compared with untreated animals: 2.33±0.53 in the CII-MTX group and 2.33±0.56 in the CFA-HD group, indicating a reduction in joint erosion due to MTX treatment. The extract- treated groups (LD, MD, HD) in both arthritis conditions showcase a decreasing trend in joint erosion. In the CII-induced arthritis model, the high-dose (HD) group presents the most considerable reduction, measuring 1.00±0.01, while in the CFA-induced arthritis model, the HD group exhibits a measurement of 1.33±0.56. These observations are in line with previous studies (Zabotti *et al.*, 2020; Yao *et al.*, 2022; Zhao *et al.*, 2023). The reduction in joint erosion observed in extract-treated groups, particularly in the HD groups, suggests potential anti-inflammatory effects of the extract that may alleviate swelling associated with arthritic conditions.

5.6. Effect of the extract on joint histology

Histological analysis of hind leg joint tissue samples after hematoxylin-eosin staining did not highlight any change in the healthy control groups (score = 0 for synovial inflammation, cell infiltration, and cartilage damage). Joints of CII- and Arthritis and CFA-Arthritis) exhibited significant histopathological alterations (score = 3 for synovial inflammation, cell infiltration, and cartilage damage). In the MTX-treated groups, the scores for synovial inflammation (CII- MTX: 1.17±0.03, CFA-MTX: 1.20±0.06), cell infiltration (CII-MTX: 1.13±0.04, CFA-MTX:
1.06±0.01), and cartilage damage (CII-MTX: 0.73±0.02, CFA-MTX: 0.76±0.03) were reduced, indicating a considerable improvement compared with the arthritis groups. In the extract-treated groups, score reduction was dose-dependent. Particularly, in the HD groups thescores for synovial inflammation (CII-HD: 0.10±0.05, CFA-HD: 0.16±0.05), cell infiltration (CII-HD: 0.16±0.02, CFA-HD: 0.40±0.03), and cartilage damage (CII-HD: 0.16±0.03, CFA-
HD: 0.23±0.02) were significantly decreased in both models. These results are consistent with the current literature (Gao *et al.*, 2020; de Sousa *et al.*, 2023; Obeidat *et al.*, 2023), (Figure 23).This

emphasizes the potential efficacy of the extract in mitigating joint inflammation and damage, particularly at higher doses, similar to the effects observed with MTX.

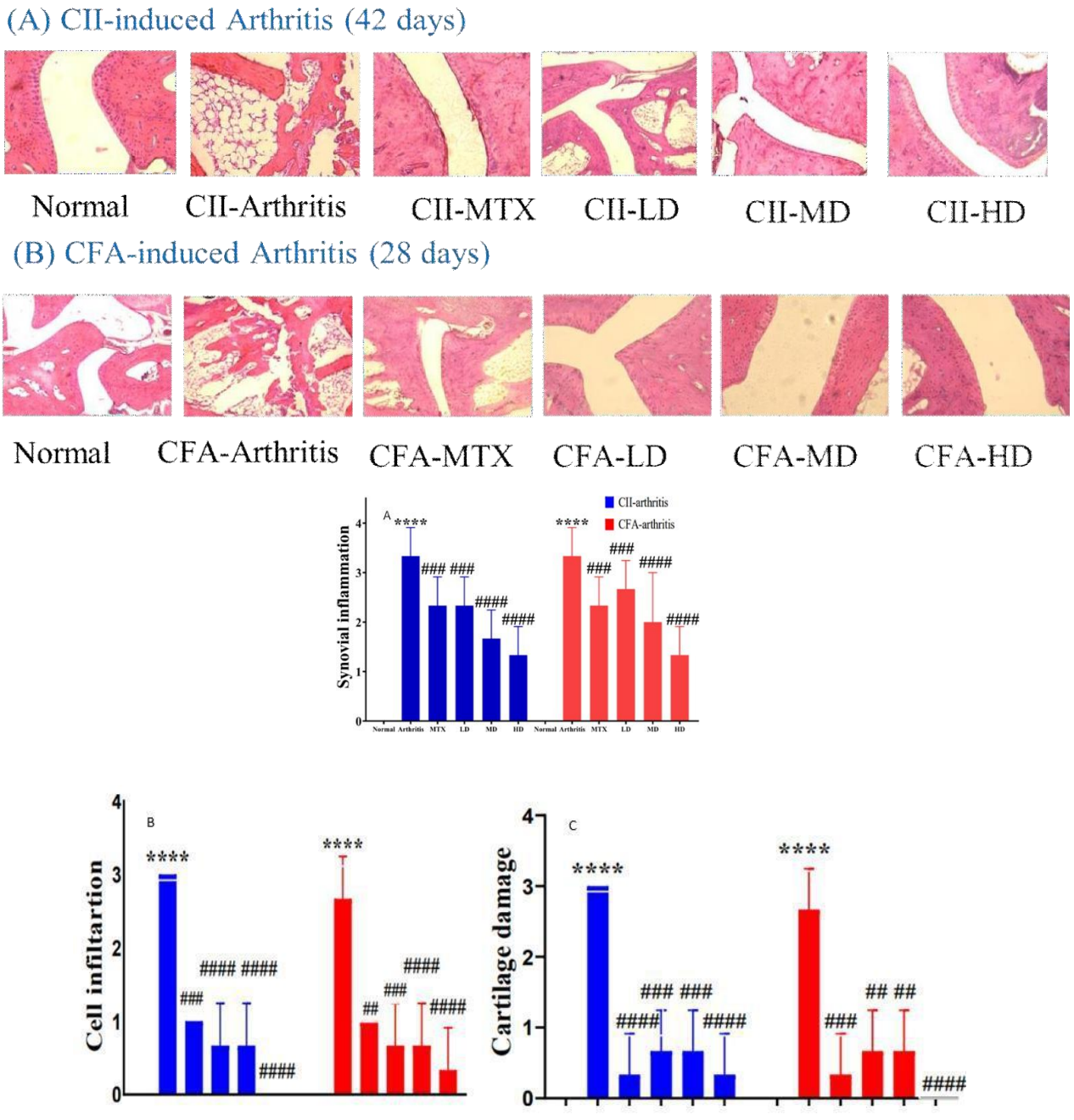

Figure 23: Histopathological changes in rats with (A) CII-induced arthritis and (B) CFA-induced arthritis at the study end. Quantification of (C) Synovial inflammation, (D) Cell infiltration, and (E) Cartilage damage in the different groups. For comparison between the Normal group vs treated groups :˙p<0.1 and¨p<0.01.Comparison with the Normal group and CII-arthritic/CFA-arthritic group:****p<0.0001 and comparison of the CII-arthritic/CFA-arthritic group with the treated groups:$^{\#\#}$p<0.01 , $^{\#\#\#}$p<0.001 and $^{\#\#\#\#}$p<0.0001.

6. *In silico* anti-arthritic effect of the extract

6.1. Molecular docking

Based on the investigation into the synergistic effects of phytocompounds within the methanol and n-hexane extracts of *Ammodaucus leucotrichus* seeds, we observed that only the methanol extract exhibits a potent anti-protease effect. Subsequently, in silico studies were conducted to individually assess the phytocompounds identified within the methanol extract. Utilizing drug design tools like FlexX 2.1.8, following essential standards, played a crucial role in expediting drug development (Abbotto *et al.*, 2023). The study involved molecular docking of phytocompounds in methanol extract with trypsin, a protein associated with rheumatoid arthritis. Figure 24 illustrates the outcomes, showing that out of the 59 compounds studied, 28 displayed negative binding energies (Table 4), suggesting potential inhibitory effects on trypsin.

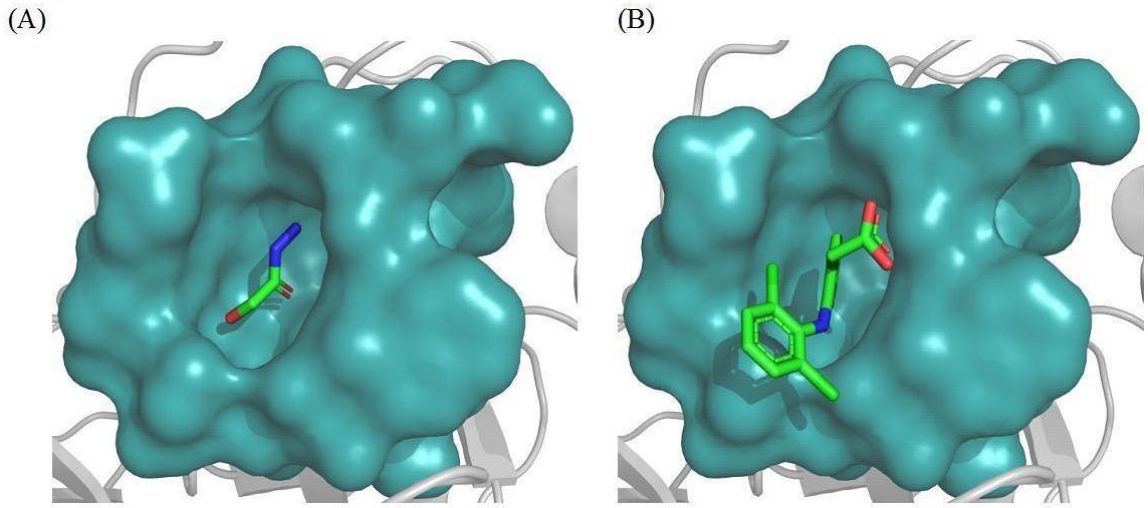

Figure 24: Placement of (A) hydroxyacetic acid hydrazide and (B) diclofenac within trypsin active site. The most plausible conformation of each compound, obtained by FlexX, is illustrated. The active site is represented in cyan as a 'surface mode,' with the ligand atoms color-coded: carbon in green, oxygen in red, and nitrogen in blue.

Table 4 Binding energies (in kJ/mol) of the 59 key compounds identified in the methanol extract from *Ammodaucus leucotrichus* seeds and of diclofenac during their interactions with trypsin. The different binding energy values reflect variations in the inhibitory potential of the compounds against trypsin.

N°	Compound	PubChem CID	Binding energy (KJ/mol)
S1	2-Pentanone, 4,4-dimethyl-	11546	-2.00
S2	1-Propanol, 2-amino-, (.+/-.)-	5126	-8.28
S3	Hydroxyacetic acid, hydrazide	350536	-17.13
S4	4H-Pyran-4-one,2,3-dihydro-3,5-dihydroxy-6-methyl	119838	-12.41
S5	5-Hydroxymethylfurfural	237332	-11.21
S6	1-Cyclohexene-1-carboxaldehyde, 4-(1-methylethenyl)-	16441	0
S7	Thymol	6989	-5.51
S8	2-Butene-1,4-diol, methanesulfonate t-butoxycarbonylaminoacetate	5365168	-4.17
S9	Cyclopentanol	7298	-5.83
S10	1-Cyclohexene-1-carboxylic acid, 4-(1-methylethenyl)-	1256	-4.82
S11	Formic acid, undecyl ester	229382	-4.19
S12	5-Oxatricyclo[8.2.0.04,6]dodecane,4,12,12-trimethyl-9-methylene-, (1R,4R,6R,10S)-	1742210	-5.99
S13	Isospathulenol	102303030	-5.17
S14	2,2-bis(oxidanylidene)-1,5-dihydroimidazo[4,5-c][1,2,6]thiadiazin-4-one	12413165	-14.39
S15	Thunbergol	5363523	-1.39
S16	3beta-Trimethylsiloxy-5alpha,6alpha-epoxycholestane	16082384	0
S17	Spiro[5.6]dodecan-7-one	282264	-7.27
S18	Silane, trichlorododecyl	20568	0
S19	3-Isopropyl-6,7-dimethyltricyclo[4.4.0.0(2,8)]decane-9,10-diol	565273	0
S20	4'-Hydroxybutyrophenone oxime	135822598	-13.45
S21	Spiro[5.5]undeca-1,7-diene	590470	0
S22	Bicyclo[2.2.1]heptane, 2-ethylidene-1,7,7-trimethyl	143908	-1.51
S23	Tetradecanoic acid	11005	0
S24	7,8-Epoxylanostan-11-ol, 3-acetoxy-	541562	0
S25	Fumaric acid, 3,5-dimethylphenyl cyclohexylmethyl ester	91711292	-4.87
S26	2H-Quinolizine-1-methanol, octahydro-	297272	-4.67
S27	1H-Cycloprop[e]azulen-7-ol, decahydro-1,1,7-trimethyl-4-methylene-, [1ar-(1a.alpha.,4a.alpha.,7.beta.,7a.beta.,7b.alpha.)]-	6432640	-8.01
S28	Longifolenaldehyde	565584	0
S29	Methyl 16-R/S-hydroxy-cleroda-3,13(14)-Z-dien-15,16-olide	16042541	-0.56
S30	3-Hydroxy-3-methyl-butyric acid, hydrazide	299142	-14.44
S31	Neophytadiene	10446	0
S32	8-Isopropyl-1,5-dimethyltricyclo[4.4.0.02,7]dec-4-en-3-	12313013	-4.74

	one		
S33	Isospathulenol	102303030	-5.17
S34	2,4,7,14-Tetramethyl-4-vinyl-tricyclo[5.4.3.0(1,8)]tetradecan-6-ol	590916	0
S35	Benzo - octahydro -acephenanthrylene	155017	0
S36	Phthalic acid, tetradecyl trans-dec-3-enyl ester	91719824	0
S37	Cyclononasiloxane, octadecamethyl-	11172	0
S38	1,2,3,4,5-Penta-O-acetyl-D-xylitol	219891	0
S39	1,3-Isobenzofurandione, 5-nitro-	230976	-9.89
S40	3,7,11,15-Tetramethyl-2-hexadecen-1-ol	5366244	0
S41	Longifolenaldehyde	103883460	0
S42	Cyclopropanebutanoic acid, 2-[[2-[[2-[(2-pentylcyclopropyl)methyl]cyclopropyl]methyl]cyclopropyl]methyl]-, methyl ester	554084	0
S43	Hexadecanoic acid, methyl ester	8181	0
S44	Phthalic acid, butyl hept-4-yl ester	91720764	-3.19
S45	n-Hexadecanoic acid	985	0
S46	Disparlure	205983	0
S47	Heptadecanoic acid	10465	0
S48	Bicyclo[4.4.0]dec-2-ene-4-ol, 2-methyl-9-(prop-1-en-3-ol-2-yl)-	535256	-11.44
S49	9,12-Octadecadienoic acid (Z,Z)-, methyl ester	5284421	0
S50	9-Octadecenoic acid, methyl ester, (E)-	5280590	0
S51	Kauren-19-yl-acetate	5284421	0
S52	2-(trans-2,6,6-Trimethylbicyclo[3.3.1]heptan-3-yl)buta-1,3-diene	5280590	0
S53	Tetradecanoic acid, 5,9,13-trimethyl-, methyl ester	554056	0
S54	9,12-Octadecadienoic acid (Z,Z)-	5280450	0
S55	9-Octadecenoic acid	637517	0
S56	Octadecanoic acid	5281	0
S57	Tetracontane	20149	0
S58	trans-(R,R)-chrysanthemyl (R)-2-methylbutanoate	91693481	-2.10
S59	Trichothec-9-ene-3,4,8,15-tetrol, 12,13-epoxy-, 15-acetate 8-(3-methylbutanoate), (3.alpha.,4.beta.,8.alpha.)-	520286	0
Diclofenac		3033	-13.01

Hydroxyacetic acid hydrazide stood out with a remarkable inhibitory effect, exhibiting a lower binding energy (-17.13 kJ/mol) compared to Diclofenac (-13.01 kJ/mol). Figure 25 further emphasizes the rational orientation of hydroxyacetic acid hydrazide and Diclofenac within the trypsin active site, highlighting their inhibitory potency. Hydroxyacetic acid

hydrazide formed seven hydrogen bonds, including crucial residues (Cys191, Ser195, Ser190, and Gly219), showcasing strong inhibitory potential. In contrast, Diclofenac formed only two hydrogen bonds with Ser214 and Gly216 amino acids.

(A)

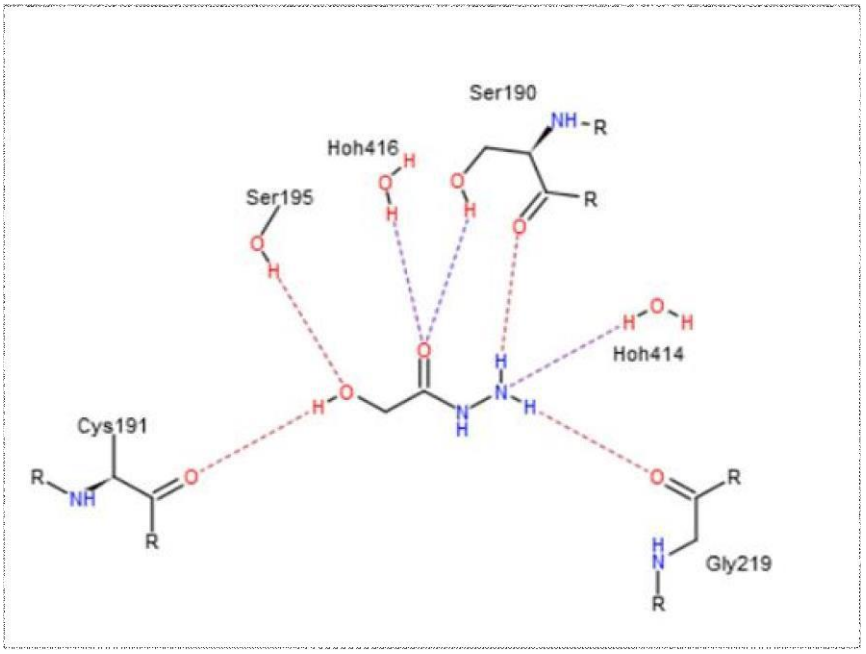

(B)

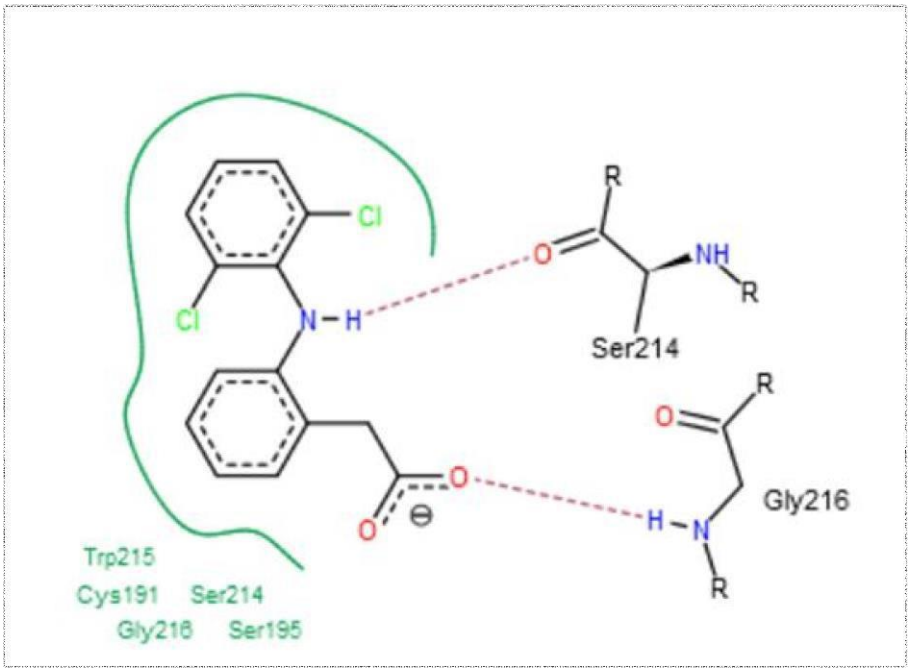

Figure 25: Binding mode interactions of (A) hydroxyacetic acid hydrazide from the extract and (B) diclofenac (reference drug) within trypsin active site (inflammation-related enzyme); hydrogen bonds depicted by broken lines.

Table 4 presents the binding energies of 59 key compounds against trypsin, highlighting the diverse range of affinities. Hydroxyacetic acid hydrazide exhibits the most negative binding energy (-17.13 kJ/mol), surpassing Diclofenac's binding energy (-13.01 kJ/mol), suggesting stronger inhibitory potential. Conversely, compounds like 1-Cyclohexene-1-carboxaldehyde, 4-(1-methylethenyl)-, 3beta-Trimethylsiloxy-5alpha, 6alpha-epoxycholestane, Silane, trichlorododecyl, and others show binding energies of 0 kJ/mol, indicating no binding affinity or potential lack of inhibitory activity. This diversity underscores hydroxyacetic acid hydrazide as a promising candidate for further exploration.

Furthermore, the integrity of bone and cartilage relies significantly on balanced proteolytic activity, with various enzymes contributing to pro-inflammatory functions in arthritis **(**Oikonomopoulou *et al.*, 2018). Serine proteinases, like trypsin, are implicated in the complement cascade, expanding the understanding beyond traditional roles of human collagenases in collagen breakdown (Fisch, A. 2019). The molecular docking results suggest that hydroxyacetic acid hydrazide from Ammodaucusleucotrichus is more tightly bound to the target protein trypsin than diclofenac, offering potential as a reference for future rheumatoid arthritis research using the *Ammodaucus leucotrichus* seeds.

6.2. Prediction of Potential Protein Targets and Drug-Likeness Analysis

Several compounds, such as 2-pentanone, 4,4-dimethyl- (S1), 1-propanol, 2-amino- (S2), and 5-hydroxymethylfurfural (S5) exhibited significant anti-inflammatory potential. The prediction outcome highlighted the complexity of the extract. Specifically, tetradecanoic acid (S23), heptadecanoic acid (S47), hexadecanoic acid, methyl ester (S43), and 9-octadecenoic acid (S55) were predicted to be potent sphinganine kinase inhibitors. Additionally, 1-propanol, 2-amino- (S2), 3-hydroxy-3-methyl-butyric acid, hydrazide (S30) and 3,7,11,15-tetramethyl-2-hexadecen-1-ol (S40) could be G-protein-coupled receptor kinase inhibitors.

The PASS tool also predicted that 4H-pyran-4-one,2,3-dihydro-3,5-dihydroxy-6-methyl (S4), thymol (S7) and 3-isopropyl-6,7-dimethyltricyclo[4.4.0.0(2,8)]decane-9,10-diol (S19) were Janus kinase 2 (JAK2) expression inhibitors, while 1-cyclohexene-1-carboxylic acid (S10), 8-isopropyl-1,5-dimethyltricyclo[4.4.0.02,7]dec-4-en-3-one (S32) and thunbergol (S15) were activators of the transcription factor NF-kB. Isospathulenol (S13), 3beta-trimethylsiloxy-5alpha, 6alpha-epoxycholestane (S16), and longifolenaldehyde (S28, S41, S58) may have immunosuppressant effects. Phthalic acid, tetradecyl trans-dec-3-enyl ester (S36) and cyclononasiloxane, octadecamethyl- (S37) were identified as potential complement factor D inhibitors (Bu *et al.,* 2022). These findings highlight the intricate network of bioactivities present in the methanol extract and their therapeutic potential. This comprehensive analysis of the predicted bioactivities is a valuable guide for future experimental study of this *Ammodaucus leucotrichus* seed extract as a potential source of anti-RA agents (table 5).

Sphinganine kinase was targeted by several of the identified phytochemicals with Pa values ranging from 0.814 to 0.935. This enzyme plays a key role in the conversion of sphingosine to sphingosine 1-phosphate and influences the regulation of inflammatory factors and immune responses in different immune cell types (Cohen *et al.*, 2010; Zhao *et al.*, 2022). G-protein-coupled receptors also were targeted by several of the identified phytochemicals with Pa values from 0.722 to 0.926. These receptors are implicated in RA mechanisms, providing a theoretical foundation for novel drug development (Nakayamada *et al.*, 2016; Stegen *et al.*, 2022; Taylor *et al.*, 2023). Several compounds inhibited JAKs (Pa values ranging from 0.730 to 0.840). JAK inhibitors represent a novel class of targeted synthetic disease-modifying antirheumatic drugs with promising results in terms of safety and efficacy (Pieta *et al.*, 2023; Radu & Bungau, 2023). Immunosuppressant agents (S6, S12, S15, S16; Pa values from 0.613 to 0.758), designed to modulate the immune system, are useful in RA by reducing chronic inflammation and pain (Li *et al.*, 2022). Matrix metalloproteinases (MMPs), including MMP9

(predicted to be inhibited by S13 with a Pa value of 0.729), play a crucial role in joint destruction, suggesting potential benefits of MMP inhibitors in RA treatment (Brown *et al.*, 2008; Nejatbakhsh *et al.*, 2020). The transcription factor NF-κB (predicted to be inhibited with Pa values ranging from 0.713 to 0.733) is pivotal in RA inflammation regulation, highlighting its significance in disease pathogenesis (Li *et al.*, 2023). Notably, the hydrazide of hydroxyacetic acid is an exception, as it is not predicted, likely due to its shorter carbon chain of one carbon.

Most of the compounds present in our extract have never been tested for RA treatment. Our *in vitro* and *in silico* results and the PASS prediction results suggest a potent effect on different RA therapeutic targets. Therefore, the pharmacokinetic properties of some of these phytochemicals were evaluated with the online tool SwissADME and with ProTox-II, a virtual laboratory for predicting the toxicity of small molecules (Banerjee *et al.*, 2018). For this analysis, six phytochemicals were selected based on the previous results: hydroxyacetic acid hydrazide (docking results) and n-hexadecanoic acid, hexadecanoic acid methyl ester, 9-octadecenoic acid methyl ester (E)-, and 9,12-octadecadienoic acid (Z,Z)-,(E) 9-octadecenoic acid (compounds with predicted activity against key RA targets: sphinganine kinase, G-protein-coupled receptor kinases, JAK2 expression, and NF-kB) transcription factor stimulants (Li *et al.*, 2023). This meticulous compound selection underscores our commitment to explore potent and multifaceted candidates for effective RA treatment. The results of SwissTargetPrediction allow us to examine the predicted macromolecular targets for selected compounds identified in the methanol extract of Ammodaucusleucotrichus. These compounds include n-hexadecanoic acid, hexadecanoic acid methyl ester, 9-octadecenoic acid methyl ester (E)-, 9,12-octadecadienoic acid (Z,Z)-, 9-octadecenoic acid and hydroxyacetic acid hydrazide. The most likely targets with which these molecules interact are enzymes, the family of fatty acid-binding proteins, G protein-coupled receptors and nuclear receptors. This

information may help us to understand the biological activity of these compounds (Figure 26) and the toxicity prediction indicated that n-hexadecanoic acid, hexadecanoic acid methyl ester, 9-octadecenoic acid methyl ester (E)-, and 9,12-octadecadienoic acid (Z,Z)- fall into the low toxicity category, with median lethal dose (LD_{50}) values of 900, 5000, 3000, and 10000 mg/kg, respectively. Conversely, 9-octadecenoic acid and hydroxyacetic acid hydrazide exhibited higher toxicity (LD_{50} values of 48 and 139 mg/kg), indicating potential harm (Figure 27).

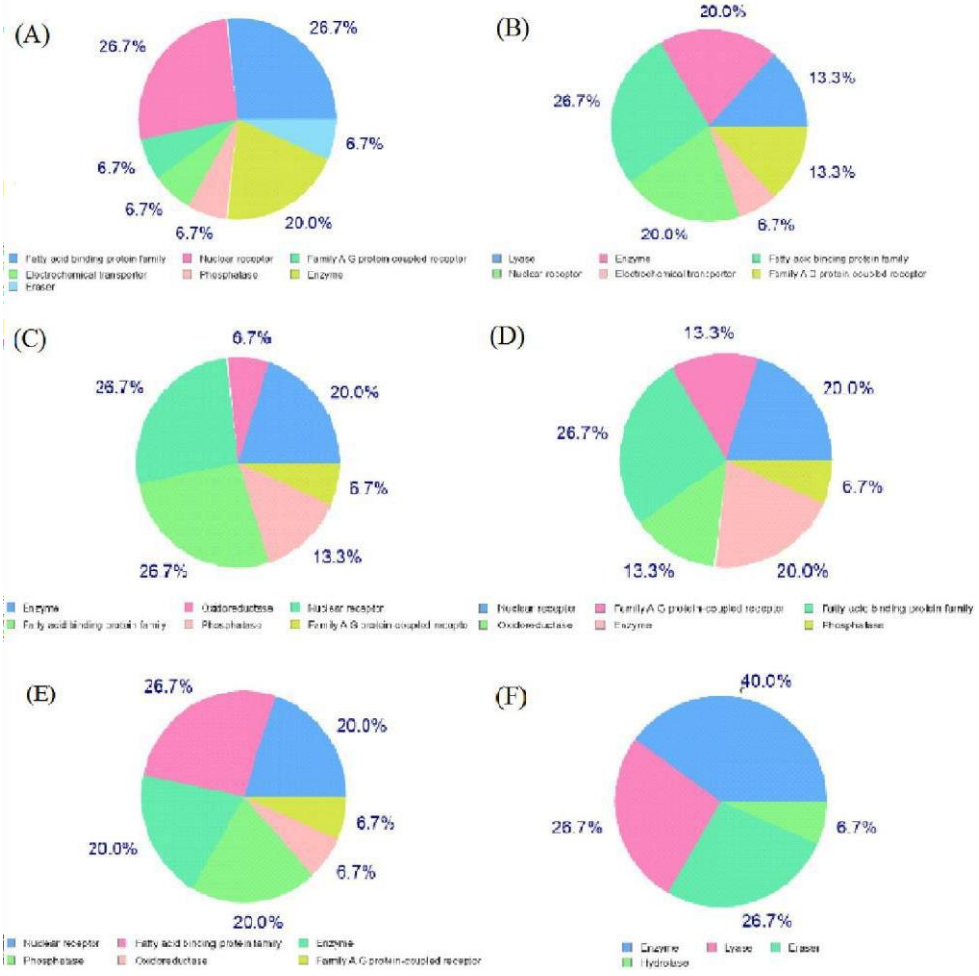

Figure 26: Data of the predicted Target of the selected compounds identified in the *Ammodaucus leucotrichus* methanol extract. The compounds include (A) n-hexadecanoicacid, (B) hexadecanoicacidmethyl ester, (C) 9-octadecenoic acidmethyl ester (E)-, (D) 9,12-octadecadienoic acid (Z,Z)-,(E) 9-octadecenoic acid, and (F) hydroxyaceticacid hydrazide interactwithThe mostlikelytargets for thesemolecules to interactwith are enzymes, the fattyacid binding proteinfamily, G-protein-coupledreceptors, and nuclearreceptors

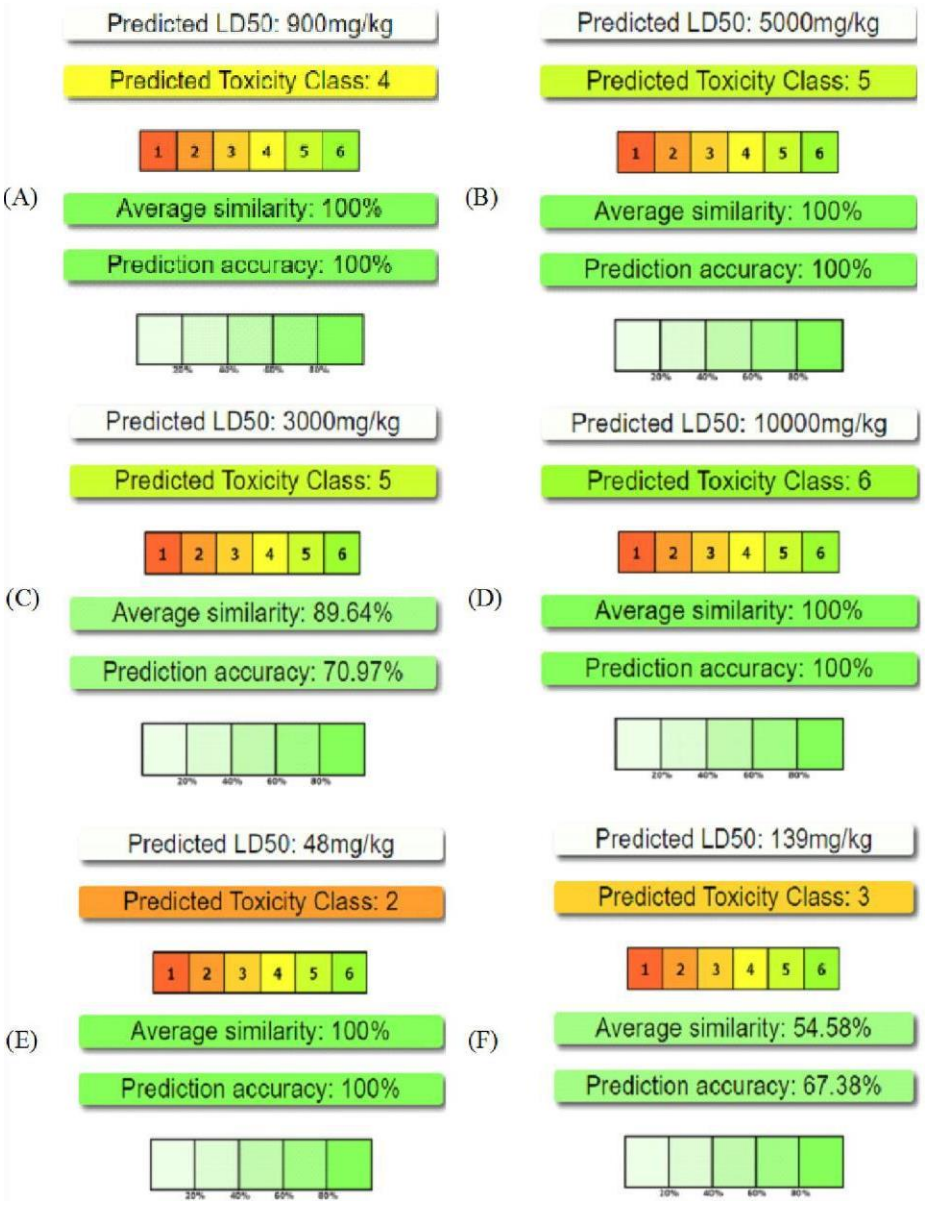

Figure 27: Toxicity, calculated by ProTox-II, of key compounds identified in the *Ammodaucus leucotrichus* seed methanol extract. The compounds include (A) n-hexadecanoic acid, (B) hexadecanoic acid methyl ester, (C) 9-octadecenoic acid methyl ester (E)-, (D) 9,12-octadecadienoic acid (Z,Z)-,(E) 9-octadecenoic acid, and (F) hydroxyacetic acid hydrazide.

Table 5: PASS prediction bioactivities of 59 constituents of the methanol extract

N°	Campound	Anti-inflammatory effects		Therapeutic Agents for RA
		Pa	Pi	
S1	2-Pentanone, 4,4-dimethyl-	0.867	0.004	Sphinganine kinase inhibitor
S2	1-Propanol, 2-amino-, (.+/-.)-	0.926	0.003	G-protein-coupled receptor kinase inhibitor
S3	Hydroxyacetic acid, hydrazide			Carbons 1 < 3
S4	4H-Pyran-4-one,2,3-dihydro-3,5-dihydroxy-6-methyl	0.730	0.014	JAK2 expression inhibitor
S5	5-Hydroxymethylfurfural	0.749	0.018	G-protein-coupled receptor kinase inhibitor
S6	1-Cyclohexene-1-carboxaldehyde, 4-(1-methylethenyl)-	0.722	0.014	Immunosuppressant
S7	Thymol	0.737	0.014	JAK2 expression inhibitor
S8	2-Butene-1,4-diol, methanesulfonate t-butoxycarbonylaminoacetate	0.840	0.006	Glutathione S-transferase
S9	Cyclopentanol	0.860	0.004	JAK2 expression inhibitor
S10	1-Cyclohexene-1-carboxylic acid, 4-(1-methylethenyl)-	0.733	0.004	Transcription factor NF kappa B stimulant
S11	Formic acid, undecyl ester	0.819	0.012	Sphinganine kinase inhibitor
S12	5-Oxatricyclo[8.2.0.04,6]dodecane,4,12,12-trimethyl-9-methylene-, (1R,4R,6R,10S)-	0.758	0.010	Immunosuppressant
S13	Isospathulenol	0.729	0.005	MMP9 expression inhibitor
S14	2,2-bis(oxidanylidene)-1,5-dihydroimidazo[4,5-c][1,2,6]thiadiazin-4-one	0.675	0.032	Methylenetetrahydrofolate reductase (NADPH) inhibitor
S15	Thunbergol	0.613	0.027	Immunosuppressant
S16	3beta-Trimethylsiloxy-5alpha,6alpha-epoxycholestane	0.727	0.014	Immunosuppressant
S17	Spiro[5.6]dodecan-7-one	0.684	0.019	JAK2 expression inhibitor
S18	Silane, trichlorododecyl	0.814	0.012	Sphinganine kinase inhibitor
S19	3-Isopropyl-6,7-dimethyltricyclo[4.4.0.0(2,8)]decane-9,10-diol	0.571	0.037	JAK2 expression inhibitor
S20	4'-Hydroxybutyrophenone oxime	0.619	0.034	Complement factor D inhibitor
S21	Spiro[5.5]undeca-1,7-diene	0.707	0.017	JAK2 expression inhibitor
S22	Bicyclo[2.2.1]heptane, 2-ethylidene-1,7,7-trimethyl	0.724	0.015	JAK2 expression inhibitor
S23	Tetradecanoic acid	0.935	0.003	Sphinganine kinase inhibitor
S24	7,8-Epoxylanostan-11-ol, 3-acetoxy-	0.795	0.005	Immunosuppressant
S25	Fumaric acid, 3,5-dimethylphenyl cyclohexylmethyl ester	0.402	0.065	Immunosuppressant
S26	2H-Quinolizine-1-methanol, octahydro-	0.680	0.025	G-protein-coupled receptor kinase inhibitor
S27	1H-Cycloprop[e]azulen-7-ol, decahydro-1,1,7-trimethyl-4-methylene-, [1ar-(1a.alpha.,4a.alpha.,7.beta.,7a.beta.,7b.alpha.)]-	0.713	0.015	Immunosuppressant
S28	Longifolenaldehyde	0.713	0.015	Immunosuppressant
S29	Methyl 16-R/S-hydroxy-cleroda-3,13(14)-Z-dien-15,16-olide	0.675	0.020	Immunosuppressant

S30	3-Hydroxy-3-methyl-butyric acid, hydrazide	0.656	0.027	G-protein-coupled receptor kinase inhibitor
S31	Neophytadiene	0.620	0.008	Transcription factor NF kappa B stimulant
S32	8-Isopropyl-1,5-dimethyltricyclo[4.4.0.02,7]dec-4-en-3-one	0.735	0.004	Transcription factor NF kappa B stimulant
S33	Isospathulenol	0.658	0.022	Immunosuppressant
S34	2,4,7,14-Tetramethyl-4-vinyl-tricyclo[5.4.3.0(1,8)]tetradecan-6-ol	0.563	0.013	Transcription factor NF kappa B stimulant
S35	Benzo - octahydro -acephenanthrylene	0.715	0.016	JAK2 expression inhibitor
S36	Phthalic acid, tetradecyl trans-dec-3-enyl ester	0.866	0.007	Sphinganine kinase inhibitor
S37	Cyclononasiloxane, octadecamethyl-	0.852	0.004	Complement factor D inhibitor
S38	1,2,3,4,5-Penta-O-acetyl-D-xylitol	0.819	0.012	Sphinganine kinase inhibitor
S39	1,3-Isobenzofurandione, 5-nitro-	0.878	0.004	Glutathione S-transferase
S40	3,7,11,15-Tetramethyl-2-hexadecen-1-ol	0.694	0.023	G-protein-coupled receptor kinase inhibitor
S41	Longifolenaldehyde	0.730	0.004	Transcription factor NF kappa B stimulant
S42	Cyclopropanebutanoic acid, 2-[[2-[[2-[(2-pentylcyclopropyl)methyl]cyclopropyl]methyl]cyclopropyl]methyl]-, methyl ester	0.388	0.057	Transcription factor NF kappa B stimulant
S43	Hexadecanoic acid, methyl ester	0.845	0.009	Sphinganine kinase inhibitor
S44	Phthalic acid, butyl hept-4-yl ester	0.754	0.018	Sphinganine kinase inhibitor
S45	n-Hexadecanoic acid	0.935	0.003	Sphinganine kinase inhibitor
S46	Disparlure	0.818	0.012	Sphinganine kinase inhibitor
S47	Heptadecanoic acid	0.935	0.003	Sphinganine kinase inhibitor
S48	Bicyclo[4.4.0]dec-2-ene-4-ol, 2-methyl-9-(prop-1-en-3-ol-2-yl)-	0.759	0.010	Immunosuppressant
S49	9,12-Octadecadienoic acid (Z,Z)-, methyl ester	0.648	0.029	Sphinganine kinase inhibitor
S50	9-Octadecenoic acid, methyl ester, (E)-	0.905	0.004	Sphinganine kinase inhibitor
S51	Kauren-19-yl-acetate	0.613	0.027	Immunosuppressant
S52	2-(trans-2,6,6-Trimethylbicyclo[3.3.1]heptan-3-yl)buta-1,3-diene	0.868	0.002	Transcription factor NF kappa B stimulant
S53	Tetradecanoic acid, 5,9,13-trimethyl-, methyl ester	0.641	0.032	Glutathione S-transferase
S54	9,12-Octadecadienoic acid (Z,Z)-	0.873	0.005	Sphinganine kinase inhibitor
S55	9-Octadecenoic acid	0.905	0.002	Sphinganine kinase inhibitor
S56	Octadecanoic acid	0.935	0.003	Sphinganine kinase inhibitor
S57	Tetracontane	0.915	0.004	Sphinganine kinase inhibitor
S58	trans-(R,R)-chrysanthemyl (R)-2-methylbutanoate	0.473	0.048	Immunosuppressant
S59	Trichothec-9-ene-3,4,8,15-tetrol, 12,13-epoxy-, 15-acetate 8-(3-methylbutanoate), (3.alpha.,4.beta.,8.alpha.)-	0.858	0.002	Immunosuppressant

The bioavailability radar charts generated by Swiss ADME (Lagorce *et al.*, 2017) stressed the favorable characteristics of the compounds: high scores for size, polarity, solubility and saturation, and low scores for flexibility and lipophilicity. Hydroxyacetic acid hydrazide was within the optimal range for all tested characteristics (Figure 28 Table 6). Utilizing the BOILED-Egg model to predict blood-brain barrier (BBB) permeation and gastrointestinal absorption (Daina *et al.*, 2016), Key compounds (n-hexadecanoic acid, hexadecanoic acid methyl ester, and 9-octadecenoic acid) were inside the yolk, suggesting high BBB permeation. Only hydroxyacetic acid hydrazide was in the white part, suggesting favorable gastrointestinal absorption due to its lower WLOGP value (a lipophilicity indicator) and higher Total Polar Surface Area (TPSA) value compared with the other compounds. The outer gray region indicates molecules with low absorption and limited BBB penetration: 9-octadecenoic acid methyl ester (E)- and 9,12-octadecadienoic acid (Z,Z)-. The SwissADME results suggested minimal impact of P-glycoproteins (P-gp) in the central nervous system on the main substances present in the methanol extract, as indicated by the red dots. SwissADME also predicted that most compounds, but n-hexadecanoic acid and 9-octadecenoic acid, should not inhibit major cytochrome P450 (CYP) isoforms (CYP2C19, CYP2D6, CYP3A4, and CYP2C9). Conversely, all tested compounds, but hydroxyacetic acid hydrazide, should inhibit CYP1A2 (Table 6).The physicochemical properties, crucial for efficacy, safety, and metabolism, were assessed using six rule-based methods, including Lipinski's rule of five (RO5), confirming the full compliance with molecular mass <500 daltons, hydrogen-bond donors (HBD) <5, hydrogen-bond acceptors (HBA) <10, and octanol-water partition coefficient (Clog *P*) ≤5 for all selected molecules (Table 6).

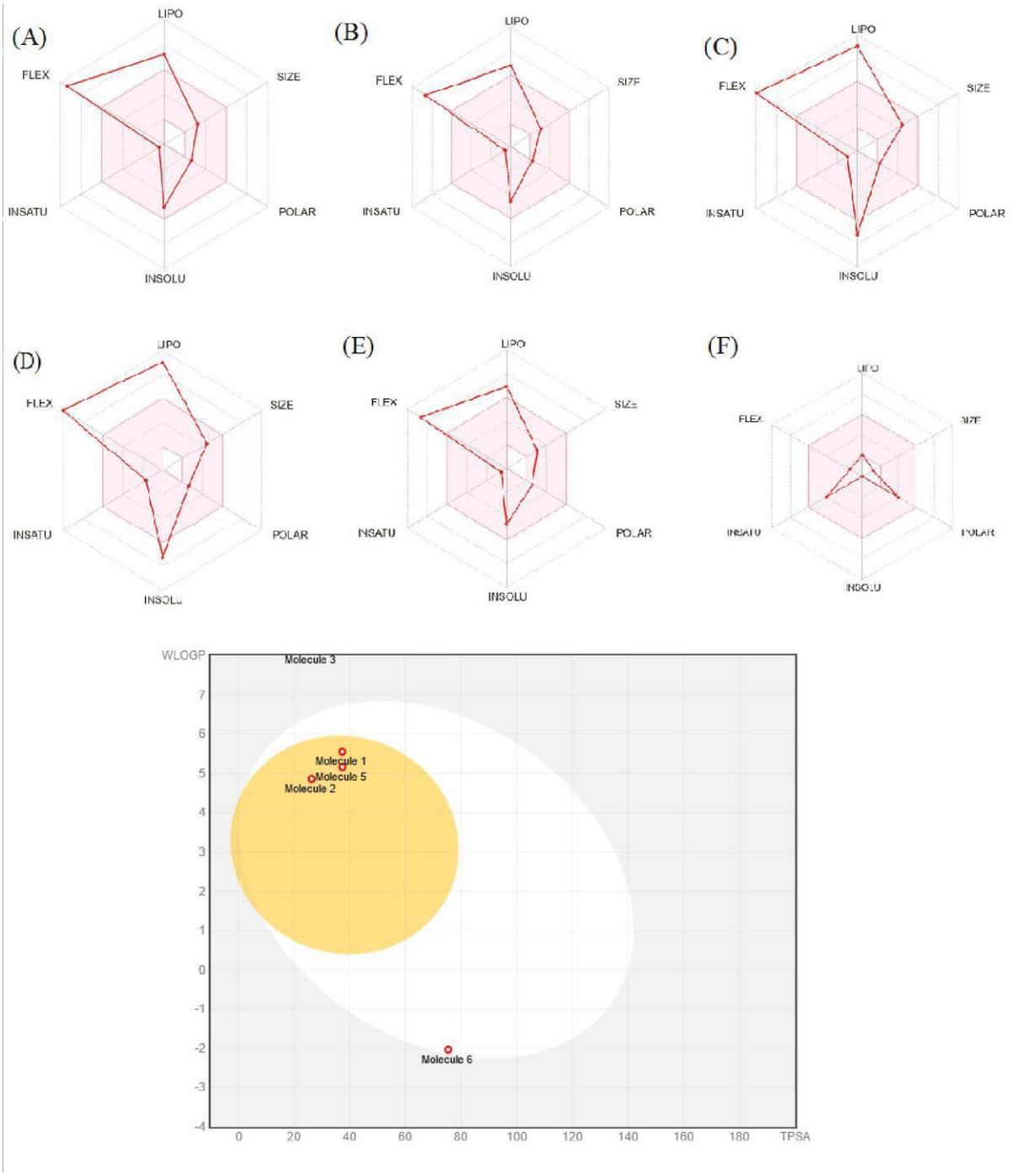

Figure 28: Bioavailability radar charts within the ADME property domain borders, calculated by SwissADME, for the key compounds identified in the methanol extract of *Ammodaucus leucotrichus* seeds: (A) n-hexadecanoic acid, (B) hexadecanoic acid methyl ester, (C) 9-octadecenoic acid methyl ester (E)-, (D) 9,12-octadecadienoic acid (Z,Z)-, (E) 9-octadecenoic acid, and (F) hydroxyacetic acid hydrazide. (G) BOILED-Egg model. The pink area in the radar charts shows the optimal range for the following features: lipophilicity (LIPO), size, polarity (POLAR), solubility (INSOLU), saturation (INSATU) and flexibility (FLEX).

Table 6 provides the comprehensive in silico ADMET profile of the six key compounds identified in the methanol extract of *Ammodaucus leucotrichus* seeds. The TPSA values rangedfrom 26.30 to 75.35 Å², and hydroxyacetic acid hydrazide had the highest TPSA. The consensus log Po/w, an indicator of lipophilicity, varied between 5.20 and -1.51; n-hexadecanoic acid displayed the highest lipophilicity and hydroxyacetic acid hydrazide was hydrophilic. All compounds were predicted to have substantial gastrointestinal absorption and complied with the Lipinski's Rule of Five, indicating their drug-like properties. BBB penetration was predicted for n-hexadecanoic acid and hexadecanoic acid methyl ester, but not for hydroxyacetic acid hydrazide. Importantly, the lack of P-gp substrate prediction suggests favorable bioavailability. Although some compounds were predicted to inhibit specific CYP isoforms, the majority of them displayed interesting characteristics for effective drug development and therapeutic applications, underscoring their potential as promising drug candidates that deserve further exploration and experimental validation.

Table 6: *In silico* ADMET profiles of six phytocompounds identified in the methanol extract

Entry	n-Hexadecanoic acid	Hexadecenoic acid, methyl ester	9-Octadecenoicacid, methyl ester, (E)-	9,12-Octadecadienoicacid(Z,Z)-	9-Octadecenoicacid	Hydroxyacetic acid, hydrazide
TPSA (Å²)	37.30	26.30	26.30	37.30	37.30	75.35
Consensus Log Po/w	5.20	5.54	5.95	5.95	5.71	-1.51
GI absorption	High	High	High	High	High	High
Bioavailability Score	0.85	0.55	0.55	0.55	0.85	0.55
BBB permeant	Yes	Yes	No	No	No	No
P-gp substrate	No	No	No	No	No	No
CYP1A2 CYP2C19 CYP2C9 CYP2D6 CYP3A4 inhibitor	Yes No Yes No No	Yes No No No No	Yes No No No No	Yes No No No No	Yes No Yes No No	No No No No No
Lipinski	Yes	Yes	Yes	Yes	Yes	Yes

In our groundbreaking evaluation of the anti-arthritic effects of methanol and n-hexane extracts from the *A. leucotrichus* plant, we observed a potent 100% inhibitory effect on trypsin at 250 µg/ml, indicating the methanolic extract's anti-protease effect with potential implications for rheumatoid arthritis (Dahal *et al.*, 2022). These promising results prompted further investigations, including in vivo testing on an animal model and in silico analysis to identify the specific compounds responsible for the observed therapeutic effects.

The curative treatment of arthritic rats with the methanol extract revealed a significant improvement in joint conditions compared to the untreated group induced with collagen and complete Freund's adjuvant (CFA). The extract demonstrated a pronounced anti-inflammatory effect, leading to almost complete suppression of inflammation, surpassing the efficacy of methotrexate. Dose-dependent responses (150, 300, 600 mg/kg/day) highlighted the extract's potential against joint damage induced by collagen and CFA injection.

Consistent results were observed through walking analysis tests and the examination of inflammatory markers C3, GSH, MDA, and MPO, crucial in the context of rheumatoid arthritis. Elevated complement C3 levels in arthritic groups were notably reduced, especially with the high dose (HD) of the extract (600 mg/kg), in contrast to methotrexate's limited impact on C3 levels (Cavalli *et al.*, 2022).

Distinct decreases in GSH levels in arthritic rat groups were mitigated by the extract and methotrexate, aligning with previous findings. Furthermore, substantial reductions in MDA and MPO levels across all treated groups indicated the potential of both the extract and methotrexate in attenuating oxidative stress and inflammation associated with rheumatoid arthritis, consistent with earlier research (Chakraborty *et al.*, 2021; de Sousa *et al.*, 2023).

Radiographic changes in arthritic rats revealed a significant progression of soft tissue swelling and joint space narrowing in the untreated groups, indicating severe bone destruction. The

extract-treated groups exhibited a tendency towards decreased leg swelling, less joint space narrowing, and absence of soft tissue edema compared to the untreated arthritic groups. MTX treatment also showed a reduction in leg swelling, with the HD group exhibiting the most significant reduction, consistent with prior research (Zabotti *et al.*, 2020; Yao *et al.*, 2022; Zhao *et al.*, 2023).

Rheumatoid arthritis progression involves morphological alterations in the synovium, leading to rheumatoid synovitis, granulomatous tissue formation (pannus), and eventual damage to cartilage and bone. The histological sections of arthritic rats confirmed these changes, indicating that the methanolic extract exerts its therapeutic effects, particularly during the early stages of pannus formation, a crucial phase in joint destruction. This effect may be attributed to the extract's significant anti-inflammatory impact, including the inhibition of pro-inflammatory molecules and NFκB activation (Fang *et al.*, 2020; Zhou *et al.*, 2022; Singh *et al.*, 2023).

To identify the compounds responsible for these therapeutic effects, GC-MS analysis highlighted a rich composition of various compounds in the *A. leucotrichus* plant. These include Ketones, Amino Alcohols, Hydrazide Derivatives, Pyranone Derivatives, Furfural Derivatives, and others known for their anti-arthritic properties. In silico molecular docking studies on 59 compounds identified 28 with potential inhibitory effects on trypsin. The hydrazide of hydroxyacetic acid emerged as a standout, exhibiting a remarkable inhibitory effect surpassing diclofenac.

This finding was further supported by predictions using PASSonline, indicating potential activities against Sphinganine kinase, G protein-coupled receptors (GPCR), Janus kinase (JAKis), Immunosuppressive drugs, Matrix metalloproteinases (MMP), and NF-κB transcription factor. Of particular note, MMP9 inhibition was highlighted as crucial in joint

destruction, suggesting potential benefits of MMP inhibitors in treating rheumatoid arthritis (Brown *et al.*, 2008; Nejatbakhsh *et al.*, 2020; Li *et al.*, 2023).

While literature research supports the anti-arthritic potential of various compounds, the docking results emphasize that only the hydrazide of hydroxyacetic acid exhibits inhibitory activity against trypsin. The ongoing exploration involves testing these compounds against other agents involved in different mechanisms responsible for triggering arthritis, providing a comprehensive understanding of the therapeutic potential of *A. leucotrichus* extracts in rheumatoid arthritis.

Conclusion and perspective

Conclusion and perspectives

In conclusion, our groundbreaking exploration into the anti-arthritic potential of methanol and n-hexane extracts from the *A. leucotrichus* plant has unveiled a promising therapeutic narrative. The unequivocal inhibition of trypsin, coupled with the profound alleviation of inflammation, oxidative stress, and histopathological changes, signifies the multifaceted prowess of *A. leucotrichus* in addressing the intricate complexities of rheumatoid arthritis. The demonstrated curative effectiveness in arthritic rats underscores the therapeutic potential of our extract.

Furthermore, identifying the hydrazide of hydroxyacetic acid as a potent trypsin inhibitor not only provides a crucial lead for future rheumatoid arthritis research but also positions it as a benchmark for innovative therapeutic investigations.

Moreover, our in silico predictions, forecasting activities against key targets pivotal in arthritis progression, augur a comprehensive impact of *A. leucotrichus* across diverse molecular pathways.The spotlight on MMP inhibition, with emphasis on MMP9, not only accentuates the potential for joint preservation but also hints at a paradigm shift in combating the underlying mechanisms of joint destruction.

Looking forward, the trajectory of this research demands an intensified focus on isolating, characterizing, and synergizing the active compounds. Transcending the confines of preclinical realms, clinical trials beckon as the next frontier, holding the promise of translating these findings into tangible therapeutic avenues for individuals grappling with the relentless challenges posed by rheumatic diseases.

Fundamentally, our research not only establishes the groundwork for the therapeutic dominance of *A. leucotrichus* in rheumatoid arthritis but also initiates an enthralling phase in the pursuit of inventive and effective interventions. While we traverse the complex terrain of rheumatological exploration, the prospective influence of *A. leucotrichus* calls upon us to delve deeper, pioneer novel approaches, and elevate our comprehension of arthritis therapeutics to unparalleled levels. Furthermore, the use of microfluidic chips could offer a new approach for studying the mechanisms and therapies of rheumatoid arthritis. This technology could allow for a more precise and detailed analysis of the cellular and molecular processes involved in arthritis, thus paving the way for more targeted and effective treatments. This is an exciting prospect that deserves thorough exploration in future research.

References

References

Abbotto E, Casini B, Piacente F, Scarano N, Cerri E, Tonelli M, & Cichero E, (2023), Novel thiazole-based SIRT2 inhibitors discovered via molecular modelling studies and enzymatic assays, Pharmaceuticals, 16(9), 1316.

Abdi Bellau ML, Chiurato MA, Maietti A, Fantin G, Tedeschi P, Marchetti N, & Guerrini A, (2022), Nutrients and main secondary metabolites characterizing extracts and essential oil from fruits of Ammodaucus leucotrichus Coss & Dur (Western Sahara), Molecules, 27(15), 5013.

Abdollahzad H, Aghdashi MA, Jafarabadi MA, & Alipour B, (2015), Effects of coenzyme Q10 supplementation on inflammatory cytokines (TNF-α, IL-6) and oxidative stress in rheumatoid arthritis patients, A randomized controlled trial, Archives of Medical Research, 46(7), 527-533.

Adu-Berchie K, & Mooney DJ, (2020), Biomaterials as local niches for immunomodulation, Accounts of Chemical Research, 53(9), 1749-1760.

Ahmad S, Saleem M, Riaz N, Lee YS, Diri R, Noor A, & Elsebai MF, (2020), The natural polypeptides as significant elastase inhibitors, Frontiers in Pharmacology, 11, 688.

Akbar M, Ali U, Khalil T, Iqbal MS, Amin A, Naeem R, & Chohan SA, (2020), Cornus macrophylla, the antibacterial activity of organic leaf extracts and the characterization of the more lipophilic components by GC/MS, Molecules, 25(10), 2395.

Akram AN, & Zhang C, (2020), Extraction of collagen-II with pepsin and ultrasound treatment from chicken sternal cartilage; physicochemical and functional properties, Ultrasonics Sonochemistry, 64, 105053.

Alam MS, Gaida MM, Debnath S, Tagad HD, Miller Jenkins LM, Appella E, & Ashwell JD, (2018), Unique properties of TCR-activated p38 are necessary for NFAT-dependent T-cell activation, PLoS Biology, 16(1), e2004111.

Aljumayi H, Aljumayi A, Algarni E, Algheshairy RM, Alharbi HF, Azhar W, & Qadhi A, (2022), The effect of chia seed extracts against complete Freund's adjuvant-induced rheumatoid arthritis in rats, Journal of Food Quality.

Alsaffar RM, Ali A, Rashid SM, Ahmad SB, Alkholifi FK, Kawoosa MS, & Rehman MU, (2023), Zerumbone protects rats from collagen-induced arthritis by inhibiting oxidative outbursts and inflammatory cytokine levels, ACS Omega, 8(3), 2982-2991.

Angelini J, Talotta R, Roncato R, Fornasier G, Barbiero G, Dal Cin L, & Scaglione F, (2020), JAK-inhibitors for the treatment of rheumatoid arthritis, A focus on the present and an outlook on the future, Biomolecules, 10(7), 1002.

Anzar CA, Joseph MV, Sundaram R, Vadiraj GB, Prasad CP, & Eranimose B, (2023), Evaluation of the anti-inflammatory properties of Boswellia serrata (Boswegex®) on carrageenan-induced paw edema in albino Wister rats, An in vivo study, International Journal of Advanced Research in Biological Sciences, 10(7), 34-42.
Aparna, V., et al. (2012). Anti-Inflammatory Property of n-Hexadecanoic Acid: Structural Evidence and Kinetic Assessment. Chemical Biology & Drug Design, vol. 80, no. 3, pp. 434-439.

Arrar, L., et al. (2013). Comparison between Polyphenol Contents and Antioxidant Activities of Different Parts of Capparis Spinosa L. Pharmacognosy Communications, vol. 3, no. 2, p. 70.

Azizov, V., and M. M. Zaiss (2021). Alcohol Consumption in Rheumatoid Arthritis: A Path through the Immune System. Nutrients, vol. 13, no. 4, p. 1324.

Babaahmadi, M., et al. (2023). Rheumatoid Arthritis: The Old Issue, the New Therapeutic Approach. Stem Cell Research & Therapy, vol. 14, no. 1, p. 268.

Badawi, M. S. (2022). The Protective Effect of β-Cryptoxanthin against Cyclophosphamide-Induced Lung Injury in Adult Male Albino Rats. Bulletin of the National Research Centre, vol. 46, no. 1, pp. 1-9.

Banerjee, P., et al. (2018). ProTox-II: A Webserver for the Prediction of Toxicity of Chemicals. Nucleic Acids Research, vol. 46, no. W1, pp. W257-W263.

Baoqi, Y., et al. (2022). Effect of Anti-Rheumatic Drugs on Cardiovascular Disease Events in Rheumatoid Arthritis. Frontiers in Cardiovascular Medicine, vol. 8, p. 812631.

Bassu, S., et al. (2020). Oxidative Stress Biomarkers and Peripheral Endothelial Dysfunction in Rheumatoid Arthritis: A Monocentric Cross-Sectional Case-Control Study. Molecules, vol. 25, no. 17, p. 3855.

Batooei, M., et al. (2018). Evaluating the Effect of Oral N-Acetylcysteine as an Adjuvant Treatment on Clinical Outcomes of Patients with Rheumatoid Arthritis: A Randomized, Double-Blind Clinical Trial. Reviews on Recent Clinical Trials, vol. 13, no. 2, pp. 132-138.

Blaszczyk, K., et al. (2015). STAT2/IRF9 Directs a Prolonged ISGF3-like Transcriptional Response and Antiviral Activity in the Absence of STAT1. Biochemical Journal, vol. 466, no. 3, pp. 511-524.

Bordy, R., et al. (2018). Microvascular Endothelial Dysfunction in Rheumatoid Arthritis. Nature Reviews Rheumatology, vol. 14, no. 7, pp. 404-420.

Boualia, I., et al. (2019). Synthesis, Molecular Docking Studies, and Biological Evaluation of Novel Alkyl Bis (4-Amino-5-Cyanopyrimidine) Derivatives. Archiv der Pharmazie, vol. 352, no. 11, p. 1900027.

Boumezzourh, A., et al. (2023). Acetylcholinesterase, Tyrosinase, α-Glucosidase Inhibition by Ammodaucus Leucotrichus Coss. & Dur. Fruits Essential Oil and Ethanolic Extract and Molecular Docking Analysis. Moroccan Journal of Chemistry, vol. 11, no. 4, pp. 11-4.

Bousoik, E., and H. Montazeri Aliabadi (2018). 'Do We Know Jack' about JAK? A Closer Look at JAK/STAT Signaling Pathway. Frontiers in Oncology, vol. 8, p. 287.

Brown, K. D., et al. (2008). The Roles of the Classical and Alternative Nuclear Factor-kappaB Pathways: Potential Implications for Autoimmunity and Rheumatoid Arthritis. Arthritis Research & Therapy, vol. 10, pp. 1-14.

Cai, W. (2021). Analysis of Antibodies to Cartilage Oligomeric Matrix Protein in Rheumatoid Arthritis and in Mouse Models. Karolinska Institutet.

Cao, Y., et al. (2023). Peripheral Complement Factor-Based Biomarkers for Patients with First-Episode Schizophrenia. Neuropsychiatric Disease and Treatment, pp. 1455-1462.

Cavalli, S., et al. (2022). Beyond Systemic Lupus Erythematosus and Anti-Phospholipid Syndrome: The Relevance of Complement from Pathogenesis to Pregnancy Outcome in Other Systemic Rheumatologic Diseases. Frontiers in Pharmacology, vol. 13, p. 841785.

Chakraborty, D., et al. (2021). A Mechanistic Insight of Phytoestrogens Used for Rheumatoid Arthritis: An Evidence-Based Review. Biomedicine & Pharmacotherapy, vol. 133, p. 111039.

Chatelain, C., et al. (2021). Révision du Genre Ammodaucus (Apiaceae) en Afrique du Nord. Candollea, vol. 76, pp. 191-200.

Chen, X., et al. (2022). Far Infrared Irradiation Suppresses Experimental Arthritis in Rats by Down-Regulation of Genes Involved in Inflammatory Response and Autoimmunity. Journal of Advanced Research, vol. 38, pp. 107-118.

Chen, Y., et al. (2022). DNA Methylation and mRNA Expression of B7-H3 Gene in Ankylosing Spondylitis: A Case-Control Study. Immunological Investigations, vol. 51, no. 7, pp. 2025-2034.

Chimenti, M. S., et al. (2015). The Interplay between Inflammation and Metabolism in Rheumatoid Arthritis. Cell Death & Disease, vol. 6, no. 9, p. e1887.

Choudhary, R., et al. (2023). Anti-Inflammatory and Anti-Arthritic Potential of Methotrexate in Combination with BA-25, an Amino Analogue of β-Boswellic Acid in the Treatment of Rheumatoid Arthritis. Cytokine, vol. 172, p. 156398.

Ciaffi, J., et al. (2021). The Effect of Ketogenic Diet on Inflammatory Arthritis and Cardiovascular Health in Rheumatic Conditions: A Mini Review. Frontiers in Medicine, vol. 8, p. 2495.

Cohen, S., and R. Fleischmann (2010). Kinase Inhibitors: A New Approach to Rheumatoid Arthritis Treatment. Current Opinion in Rheumatology, vol. 22, no. 3, pp. 330-335.

Combe, B., et al. (2017). 2016 Update of the EULAR Recommendations for the Management of Early Arthritis. Annals of the Rheumatic Diseases, vol. 76, no. 6, pp. 948-959.

Correa, L. B., et al. (2022). Protective Effect of Methyl Gallate on Murine Antigen-Induced Arthritis by Inhibiting Inflammatory Process and Bone Erosion. Inflammopharmacology, vol. 30, pp. 251-266.

Dahal, A., et al. (2022). Targeting Protein–Protein Interaction for Immunomodulation: A Sunflower Trypsin Inhibitor Analog Peptidomimetic Suppresses RA Progression in CIA Model. Journal of Pharmacological Sciences, vol. 149, no. 3, pp. 124-138.

Dahmane, D., et al. (2017). Chemical Composition, Antioxidant and Antibacterial Activities of the Essential Oils of Medicinal Plant Ammodaucus Leucotrichus from Algeria. Journal of Essential Oil Research, vol. 29, no. 1, pp. 48-55.

Dai, H., et al. (2022). Recent Applications of Immunomodulatory Biomaterials for Disease Immunotherapy. Exploration, vol. 2, no. 6, p. 20210157.

Daina, A., and V. Zoete (2016). A Boiled-Egg to Predict Gastrointestinal Absorption and Brain Penetration of Small Molecules. ChemMedChem, vol. 11, no. 11, pp. 1117-1121.

De Medinaceli, L., et al. (1984). Rat Sciatic Functional Index Data Management System with Digitized Input. Computers and Biomedical Research, vol. 17, no. 2, pp. 185-192.

De Sousa, D. C., et al. (2021). Cognitive Dysfunction in Systemic Lupus Erythematosus is Associated with Disease Activity and Oxidative Stress: A Comparative Study with rheumatoid arthritis for identifying biomarkers. *BMC neuroscience*, 24(1), 66.

de Sousa, L. M., de Figueiredo Costa, A. C., Pereira, A. F., da Silva Martins, C., de Oliveira Filho, O.

V., Goes, P., & Gondim, D. V. (2023). Temporomandibular joint arthritis increases canonical Wnt pathway expression in the articular cartilage and trigeminal ganglion in rats. Bone Reports, 18, 101649.

Del Barco, S., Vazquez-Martin, A., Cufí, S., Oliveras-Ferraros, C., Bosch-Barrera, J., Joven, J., & Menendez, J. A. (2011). Metformin: multi-faceted protection against cancer. Oncotarget, 2(12), 896.

Demmak, R. G., Bordage, S., Bensegueni, A., Boutaghane, N., Hennebelle, T., Mokrani, E. H., & Sahpaz, S. (2019). Chemical constituents from solenostemma argel and their cholinesterase inhibitory activity. Natural Product Sciences, 25(2), 115-121.

Ding, Q., Hu, W., Wang, R., Yang, Q., Zhu, M., Li, M., Cai, J., Rose, P., Mao, J., & Zhu, Y. Z. (2023). Signaling pathways in rheumatoid arthritis: implications for targeted therapy. Signal Transduction and Targeted Therapy, 8(1), 68.

Dziąbowska-Grabias, K., Sztanke, M., Zając, P., Celejewski, M., Kurek, K., Szkutnicki, S., Korga, P., Bulikowski, W., & Sztanke, K. (2021). Antioxidant therapy in inflammatory bowel diseases. Antioxidants, 10(3), 412.

Ellman, G. L. (1959). Tissue sulfhydryl groups. Archives of Biochemistry and Biophysics, 82(1), 70-77.

El-Ouady, F., & Eddouks, M. (2020). Glucose lowering activity of aqueous Ammodaucus leucotrichus extract in diabetic rats. Cardiovascular & Haematological Disorders-Drug Targets, 20(2), 152-159.

Emori, T., Kasahara, M., Sugahara, S., Hashimoto, M., Ito, H., Narumiya, S., & Fujii, Y. (2020). Role of JAK-STAT signaling in the pathogenic behavior of fibroblast-like synoviocytes in rheumatoid arthritis: effect of the novel JAK inhibitor peficitinib. European Journal of Pharmacology, 882, 173238.

Es-Safi, I., Mechchate, H., Amaghnouje, A., Calarco, A., Boukhira, S., Noman, O. M., Motana, R. A., Nasr, F. A., Bekkari, H., & Bousta, D. (2020). Defatted hydroethanolic extract of Ammodaucus leucotrichus Cosson and Durieu seeds: antidiabetic and anti-inflammatory activities. Applied Sciences, 10(24), 9147.

Fang, Q., Zhou, C., & Nandakumar, K. S. (2020). Molecular and cellular pathways contributing to joint damage in rheumatoid arthritis. Mediators of Inflammation, 2020, 3830212.

Fernandes, N., Rodrigues, C. F., Moreira, A. F., & Correia, I. J. (2020). Overview of the application of inorganic nanomaterials in cancer photothermal therapy. Biomaterials Science, 8(11), 2990-3020.

Fernández, O. S. L., Viebahn-Haensler, R., Cabreja, G. L., Espinosa, I. S., Matos, Y. H., Roche, L. D., Santos, B. T., Oruu, G. T., & Vega, J. C. P. (2016). Medical ozone increases methotrexate clinical response and improves cellular redox balance in patients with rheumatoid arthritis. European Journal of Pharmacology, 789, 313-318.

Fisch, A. (2019). Elastin-derived peptides in the pathogenesis of Kawasaki disease. Doctoral dissertation, University of Toronto (Canada).

Fonseca, L. J. S. D., Nunes-Souza, V., Goulart, M. O. F., & Rabelo, L. A. (2019). Oxidative stress in rheumatoid arthritis: What the future might hold regarding novel biomarkers and add-on therapies. Oxidative Medicine and Cellular Longevity, 2019.

Gaharwar A. K, Singh I, Khademhosseini A (2020) Engineered biomaterials for in situ tissue

regeneration, Nature Reviews Materials, 5, 686–705.

Gao J, Xiao N, Wang Q, Xu Z, Xiao F, Yang Z, Wang C (2022) OAT3 mediates methotrexate resistance in the treatment of rheumatoid arthritis, Biomedicine & Pharmacotherapy, 153, 113558.

Gao Q, Qin H, Zhu L, Li D, Hao X (2020) Celastrol attenuates collagen-induced arthritis via inhibiting oxidative stress in rats, International Immunopharmacology, 84, 106527.

Gao W, Dong X, Yang Z, Mao G, Xing W (2020) Association between rs7574865 polymorphism in STAT4 gene and rheumatoid arthritis: an updated meta-analysis, European Journal of Internal Medicine, 71, 101-103.

George G, Shyni G. L, Raghu K. G (2020) Current and novel therapeutic targets in the treatment of rheumatoid arthritis, Inflammopharmacology, 28, 1457-1476.

Ghavipour M, Sotoudeh G, Tavakoli E, Mowla K, Hasanzadeh J, Mazloom Z (2017) Pomegranate extract alleviates disease activity and some blood biomarkers of inflammation and oxidative stress in rheumatoid arthritis patients, European Journal of Clinical Nutrition, 71(1), 92-96.

Gherraf N, Zellagui A, Kabouche A, Lahouel M, Salhi R, Rhouati S (2017) Chemical constituents and antimicrobial activity of essential oils of Ammodaucus leucotrichus, Arabian Journal of Chemistry, 10, S2476-S2478.

Gligorić E, Igić R, Čonić B. S, Kladar N, Teofilović B, Grujić N (2023) Chemical profiling and biological activities of “green” extracts of willow species (Salix L., Salicaceae): Experimental and chemometric approaches, Sustainable Chemistry and Pharmacy, 32, 100981.

Gnanasundaram I, Balakrishnan K (2017) Characterization of bioactive compounds in ethanolic extract of Cissus vitiginea leaves using GC-MS Technique, IOSR Journal of Applied Chemistry, 10(9), 3.

Griffin D. R, Archang M. M, Kuan C. H, Weaver W. M, Weinstein J. S, Feng A. C, Ruccia A, Sideris E, Ragkousis V, Koh J, Plikus M. V, Di Carlo D, Segura T, Scumpia P. O (2021) Activating an adaptive immune response from a hydrogel scaffold imparts regenerative wound healing, Nature Materials, 20(4), 560-569.

Guemmaz T, Zerargui F, Boumerfeg S, Arrar L, Aouachria S, Khennouf S, Baghiani A (2018) Anti-hemolytic, anti-lipid peroxidation, antioxidant properties and acute toxicity of Xanthium strumarium leaves extracts, Annual Research & Review in Biology, 1-12.

Gunassekaran G. R, Vadevoo S. M. P, Baek M. C, Lee B (2021) M1 macrophage exosomes engineered to foster M1 polarization and target the IL-4 receptor inhibit tumor growth by reprogramming tumor-associated macrophages into M1-like macrophages, Biomaterials, 278, 121137.

Guo Q, Wang Y, Xu D, Nossent J, Pavlos N. J, Xu J (2018) Rheumatoid arthritis: pathological mechanisms and modern pharmacologic therapies, Bone Research, 6(1), 15.

Gurram S, Anchi P, Panda B, Tekalkar S. S, Mahajan R. B, Godugu C (2022) Amelioration of experimentally induced inflammatory arthritis by intra-articular injection of visnagin, Current Research in Pharmacology and Drug Discovery, 3, 100114.

Han K, Nam J, Xu J, Sun X, Huang X, Animasahun O, Achreja A, Jeon JH, Pursly B, Kamada N, Chen GY, Nagrath D, Moon J. J. (2021) Generation of systemic antitumour immunity via the in situ modulation of the gut microbiome by an orally administered inulin gel, Nature Biomedical

Engineering, 5(11), 1377-1388.

He W, Xing X, Wang X, Wu D, Wu W, Guo J, Mitragotri S. (2020) Nanocarrier-mediated cytosolic delivery of biopharmaceuticals, Advanced Functional Materials, 30(37), 1910566.

Hirvonen H, Kautiainen H, Moilanen E, Mikkelsson M, Leirisalo-Repo M. (2017) The effect of cryotherapy on total antioxidative capacity in patients with active seropositive rheumatoid arthritis, Rheumatology International, 37, 1481-1487.

Hoffmann M, Kleine-Weber H, Schroeder S, Krüger N, Herrler T, Erichsen S, Pöhlmann S. (2020) SARS-CoV-2 cell entry depends on ACE2 and TMPRSS2 and is blocked by a clinically proven protease inhibitor, Cell, 181(2), 271-280.

Holl E. K, Shumansky K. L, Borst L. B, Burnette A. D, Sample C. J, Ramsburg E. A, Sullenger B. A. (2016) Scavenging nucleic acid debris to combat autoimmunity and infectious disease, Proceedings of the National Academy of Sciences, 113(35), 9728-9733.

Huang J, Fu X, Chen X, Li Z, Huang Y, Liang C. (2021) Promising therapeutic targets for treatment of rheumatoid arthritis, Frontiers in Immunology, 12, 686155.

Idm'hand E, Msanda F, Cherifi K. (2020) Medicinal uses, phytochemistry and pharmacology of Ammodaucus leucotrichus, Clinical Phytoscience, 6(1), 1-8.

Jaswal S, Mehta H. C, Sood A. K, Kaur J. (2003) Antioxidant status in rheumatoid arthritis and role of antioxidant therapy, Clinica Chimica Acta, 338(1-2), 123-129.

Ju J. H, Heo Y. J, Cho M. L, Jhun J. Y, Park J. S, Lee S. Y, Kim H. Y. (2012) Modulation of STAT-3 in rheumatoid synovial T cells suppresses Th17 differentiation and increases the proportion of Treg cells, Arthritis & Rheumatism, 64(11), 3543-3552.

Júnior E. B. A, de Oliveira Formiga R, de Lima Serafim C. A, Araruna M. E. C, de Souza Pessoa M. L, Vasconcelos R. C, Batista L. M. (2020) Estragole prevents gastric ulcers via cytoprotective, antioxidant and immunoregulatory mechanisms in animal models, Biomedicine & Pharmacotherapy, 130, 110578.

Kamal R. M, Sabry M. M, Aly Z. Y, Hifnawy M. S. (2021) Phytochemical and in-vivo anti-arthritic significance of Aloe thraskii Baker in combined therapy with methotrexate in adjuvant-induced arthritis in rats, Molecules, 26(12), 3660.

Kamaly N, Xiao Z, Valencia P. M, Radovic-Moreno A. F, Farokhzad O. C. (2012) Targeted polymeric therapeutic nanoparticles: design, development and clinical translation, Chemical Society Reviews, 41(7), 2971-3010.

Karthik K, Kumar B. R. P, Priya V. R, Kumar S. K, Rathore R. S. B. (2013) Evaluation of anti-inflammatory activity of Canthium parviflorum by in-vitro method, Indian Journal of Research in Pharmacy and Biotechnology, 1(5), 729.

Kaur G, Sharma A, Bhatnagar A. (2021) Role of oxidative stress in pathophysiology of rheumatoid arthritis: Insights into NRF2-KEAP1 signalling, Autoimmunity, 54(7), 385-397.

Kavitha R, Uduman M. A. M. (2017) Identification of bioactive components and its biological activities of Abelmoschus moschatus flower extract-a GC-MS study, IOSR Journal of Applied Chemistry, 10(11), 19-22.

Khadim R. M, Al-Fartusie F. S. (2023) Evaluation of some trace elements and antioxidants in sera of

patients with rheumatoid arthritis: a case–control study, Clinical Rheumatology, 42(1), 55-65.

Khaldi A, Meddah B, Moussaoui A, Sonnet P. (2017) Anti-mycotoxin effect and antifungal properties of essential oil from Ammodaucus leucotrichus Coss. & Dur. on Aspergillus flavus and Aspergillus ochraceus, Journal of Essential Oil Bearing Plants, 20(1), 36-44.

Khaldi A, Moussaoui A, Meddah B. (2019) Phytochemical characterization, in-vitro antioxidant and antibacterial activities of some extracts of Ammodaucus leucotrichus Coss. & Dur. from Bechar, Algeria, South Asian Journal of Experimental Biology, 9(5), 166-172.

Khan A. U, Khan A, Khan A, Shal B, Aziz A, Ahmed M. N, Khan S. (2021) Inhibition of NF-κB signaling and HSP70/HSP90 proteins by newly synthesized hydrazide derivatives in arthritis model, Naunyn-Schmiedeberg's Archives of Pharmacology, 394, 1497-1519.

Khan Z. U. R, Assad N, Naeem-ul-Hassan M, Sher M, Alatawi F. S, Alatawi M. S, Rahimi M. (2023) Aconitum lycoctonum L. (Ranunculaceae) mediated biogenic synthesis of silver nanoparticles as potential antioxidant, anti-inflammatory, antimicrobial and antidiabetic agents, BMC Chemistry, 17(1), 128.

Khong N. M, Yusoff F. M, Jamilah B, Basri M, Maznah I, Chan K. W, Nishikawa J. (2018) Improved collagen extraction from jellyfish (Acromitus hardenbergi) with increased physical-induced solubilization processes, Food Chemistry, 251, 41-50.

Köhler B. M, Günther J, Kaudewitz D, Lorenz H. M. (2019) Current therapeutic options in the treatment of rheumatoid arthritis, Journal of Clinical Medicine, 8(7), 938.

Kralike L. (1859) Plantea Algerienses selectine. Ammodaucus leucotrichus, Bulletin de la Société Botanique de France, 6: 393-394.

Kurowska-Stolarska M, Alivernini S. (2022). Synovial tissue macrophages in joint homeostasis, rheumatoid arthritis and disease remission. Nat Rev Rheumatol. 18(7):384–97.

Laemmli UK. (1970). Cleavage of structural proteins during the assembly of the head of bacteriophage T4. Nature. 227:680–685.

Lagorce D, Douguet D, Miteva MA, Villoutreix BO. (2017). Computational analysis of calculated physicochemical and ADMET properties of protein-protein interaction inhibitors. Scientific Reports. 7(1):46277.

Lasmari S, Ikhlef S, Boulcina R, Mokrani EH, Bensouici C, Gürbüz N, Debache A. (2021). New silver N-heterocyclic carbenes complexes: Synthesis, molecular docking study and biological activities evaluation as cholinesterase inhibitors and antimicrobials. Journal of Molecular Structure. 1238:130399.

Lei Z, Ouyang L, Gong Y, Wang Z, Yu B. (2020). Effect of eriodictyol on collagen-induced arthritis in rats by Akt/HIF-1α pathway. Drug Design, Development and Therapy. 14:1633-1639.

Lenzi M, Turrini E, Catanzaro E, Cocchi V, Guerrini A, Hrelia P, Fimognari C. (2022). In vitro investigation of the anticancer properties of Ammodaucus leucotrichus Coss. & Dur. Pharmaceuticals. 15(12):1491.

Li M, Wang M, Wen Y, Zhang H, Zhao GN, Gao Q. (2023). Signaling pathways in macrophages: Molecular mechanisms and therapeutic targets. Med Comm. 4(5)

Li R L, Duan H X, Liang Q, Huang Y L, Wang L Y, Zhang Q, Peng W. (2022). Targeting matrix

metalloproteases: A promising strategy for herbal medicines to treat rheumatoid arthritis. Frontiers in Immunology. 13:1046810.

Liang H, Peng B, Dong C, Liu L, Mao J, Wei S, Chen Y. (2018). Cationic nanoparticle as an inhibitor of cell-free DNA-induced inflammation. Nature Communications. 9(1):4291.

Liu C, Li Y, Wen C, Yan Z, Olatunji O J, Yin Z. (2022). Dehydrozingerone alleviates hyperalgesia, oxidative stress and inflammatory factors in complete Freund's adjuvant-induced arthritic rats. Drug Design, Development and Therapy. 16:3015-3022.

Liu P, Li Y, Wang R, Ren F, Wang X. (2021). Oxidative stress and antioxidant nanotherapeutic approaches for inflammatory bowel disease. Biomedicines. 10:85.

Liu Y T, Ding H H, Lin Z M, Wang Q, Chen L, Liu S S, Zuo J P. (2021). A novel tricyclic BTK inhibitor suppresses B cell responses and osteoclastic bone erosion in rheumatoid arthritis. Acta Pharmacologica Sinica. 42(10):1653-1664.

Louail Z, Kameli A, Benabdelkader T, Bouti K, Hamza K, Krimat S. (2016). Antimicrobial and antioxidant activity of essential oil of Ammodaucus leucotrichus Coss. & Dur. seeds. J Mater Environ Sci. 7(7):2328-2334.

Luo M, Wang H, Wang Z, Cai H, Lu Z, Li Y, Gao J. (2017). A STING-activating nanovaccine for cancer immunotherapy. Nature Nanotechnology. 12(7):648-654.

Majid R, Al Talebi Z A, Al-Kawaz H S, Alta'ee A H, Alsalman A R S, Hadwan A M, Hadwan M H. (2023). Novel fluorometric protocol for assessing myeloperoxidase activity. Enzyme and Microbial Technology. 171:110320.

Marchi L F, Paoliello-Paschoalato A B, Oliveira R D, Azzolini A E C, Kabeya L M, Donadi E A, Lucisano-Valim Y M. (2018). Activation status of peripheral blood neutrophils and the complement system in adult rheumatoid arthritis patients undergoing combined therapy with infliximab and methotrexate. Rheumatology International. 38:1043-1052. McInnes I B, Schett G. (2011). The pathogenesis of rheumatoid arthritis. New England Journal of Medicine. 365(23):2205-2219.

Meng Q F, Zhao Y, Dong C, Liu L, Pan Y, Lai J, Rao L. (2021). Genetically programmable fusion cellular vesicles for cancer immunotherapy. Angewandte Chemie International Edition. 60(50):26320-26326.

Mobasheri A, Biesalski H K, Shakibaei M, Henrotin Y. (2014). Antioxidants and osteoarthritis. In: Laher I (eds) Systems Biology of Free Radicals and Antioxidants. Springer, Berlin, Heidelberg.

Mohammedi H, Idjeri-Mecherara S, Menaceur F, Azine K, Hassani A. (2018). Chemical compositions of extracted volatile oils of Ammodaucus leucotrichus L. fruit from different geographical regions of Algeria with evaluation of its toxicity, anti-inflammatory and antimicrobial activities. Journal of Essential Oil Bearing Plants. 21(6):1568-1584.

Möller K Ä, Aulin C, Baharpoor A, Svensson C I. (2020). Pain behaviour assessments by gait and weight bearing in surgically induced osteoarthritis and inflammatory arthritis. Physiology & Behavior. 225:113079.

Myasoedova E, Davis J, Matteson E L, Crowson C S. (2020). Is the epidemiology of rheumatoid arthritis changing? Results from a population-based incidence study, 1985-2014. Annals of the Rheumatic Diseases. 79:440–444.

Naito K, Sawadaishi K, Kawasaki M. (2022). Photobiochemical mechanisms of biomolecules relevant to germicidal ultraviolet irradiation at 222 and 254 nm. Scientific Reports. 12(1):18217.

Najah Z, Alshawish M. (2023). GC-MS Analysis of Rhus Tripartita Roots Extract. Journal of Humanitarian and Applied Sciences. 8(16):331-339.

Nakayamada S, Kubo S, Iwata S, Tanaka Y. (2016). Recent progress in JAK inhibitors for the treatment of rheumatoid arthritis. BioDrugs. 30(5):407-419.

Nash P, Kerschbaumer A, Dörner T, Dougados M, Fleischmann R M, Geissler K, Smolen J S. (2021). Points to consider for the treatment of immune-mediated inflammatory diseases with Janus kinase inhibitors: a consensus statement. Annals of the Rheumatic Diseases. 80(1):71-87.

Nejatbakhsh Samimi L, Farhadi E, Tahmasebi M N, Jamshidi A, Sharafat Vaziri A, Mahmoudi M. (2020). NF-κB signaling in rheumatoid arthritis with focus on fibroblast-like synoviocytes. Autoimmunity Highlights. 11:1-10.

Nordberg L B, Lillegraven S, Lie E, Aga A B, Olsen I C, Hammer H B, Haavardsholm E A. (2017). Patients with seronegative RA have more inflammatory activity compared with patients with seropositive RA in an inception cohort of DMARD-naïve patients classified according to the 2010 ACR/EULAR criteria. Annals of the Rheumatic Diseases. 76(2):341-345.

Obeidat A M, Kim S Y, Burt K G, Hu B, Li J, Ishihara S, Scanzello C. (2023). Recommendations for a standardized approach to histopathologic evaluation of synovial membrane in murine models of experimental osteoarthritis. bioRxiv. 10.14.562259.

OECD. (2008). Guidelines for the testing of chemicals. Acute oral toxicity. Up and down procedure. 425:27.

Oikonomopoulou K, Diamandis E P, Hollenberg M D, Chandran V. (2018). Proteinases and their receptors in inflammatory arthritis: an overview. Nature Reviews Rheumatology. 14(3):170-180.

Pan H, Zheng M, Ma A, Liu L, Cai L. (2021). Cell/bacteria-based bioactive materials for cancer immune modulation and precision therapy. Advanced Materials. 33(50):2100241.

Paoliello-Paschoalato A B, Moreira M R, Azzolini A E C S, Cavenaghi A A, Marzocchi-Machado C M, Donadi E A, Lucisano-Valim Y M. (2011). Activation of complement alternative pathway in rheumatoid arthritis: implications in peripheral neutrophils functions. The Open Autoimmunity Journal. 3:1-9.

Phull A R, Nasir B, ul Haq I, Kim S J. (2018). Oxidative stress, consequences and ROS mediated cellular signaling in rheumatoid arthritis. Chemico-biological interactions. 281:121-136.

Pieta A, Venetsanopoulou A I, Kittas C, Christaki E, Voulgari P V. (2023). Recurrent Scedosporium apiospermum cutaneous infection in a patient with rheumatoid arthritis: the potent role of IL-6 signaling pathway blockade: a case-based review. Journal of Fungi. 9(6):683.

Prasad P, Verma S, Surbhi, Ganguly N K, Chaturvedi V, Mittal S A. (2023). Rheumatoid arthritis: advances in treatment strategies. Molecular and Cellular Biochemistry. 478(1):69-88.

Pushpalatha D S S S, Kumaraswamy S, Selvaraj G K, Narayanaswamy R, Prabhakaran V S, Sivakumar T, Kesavan A. (2023). Plant-derived bioactive compounds: promising prospective uses in chronic inflammation. In: Natural products as cancer therapeutics. IGI Global. 254-274.

Qayyum S, Mehdi A. (2023). Potential efficacy of turmeric as an anti-inflammatory agent and

antioxidant in the treatment of osteoarthritis. Khyber Medical University Journal. 15(3):190-197.

Qiang R, Huang H, Chen J, Shi X, Fan Z, Xu G, Qiu H. (2023). Carbon quantum dots derived from herbal medicine as therapeutic nanoagents for rheumatoid arthritis with ultrahigh lubrication and anti-inflammation. ACS Applied Materials & Interfaces. 15(32):38653-38664.

Quiñonez-Flores C M, González-Chávez S A, Del Río Nájera D, Pacheco-Tena C. (2016). Oxidative stress relevance in the pathogenesis of rheumatoid arthritis: a systematic review. BioMed Research International. 2016:6097417.

Obeidat A M, Kim S Y, Burt K G, Hu B, Li J, Ishihara S, Scanzello C. (2023). Recommendations for a standardized approach to histopathologic evaluation of synovial membrane in murine models of experimental osteoarthritis. bioRxiv. 10.14.562259.

OECD. (2008). Guidelines for the testing of chemicals. Acute oral toxicity. Up and down procedure. 425:27.

Oikonomopoulou K, Diamandis E P, Hollenberg M D, Chandran V. (2018). Proteinases and their receptors in inflammatory arthritis: an overview. Nature Reviews Rheumatology. 14(3):170-180.

Pan H, Zheng M, Ma A, Liu L, Cai L. (2021). Cell/bacteria-based bioactive materials for cancer immune modulation and precision therapy. Advanced Materials. 33(50):2100241.

Paoliello-Paschoalato A B, Moreira M R, Azzolini A E C S, Cavenaghi A A, Marzocchi-Machado C M, Donadi E A, Lucisano-Valim Y M. (2011). Activation of complement alternative pathway in rheumatoid arthritis: implications in peripheral neutrophils functions. The Open Autoimmunity Journal. 3:1-9.

Phull A R, Nasir B, ul Haq I, Kim S J. (2018). Oxidative stress, consequences and ROS mediated cellular signaling in rheumatoid arthritis. Chemico-biological interactions. 281:121-136.

Pieta A, Venetsanopoulou A I, Kittas C, Christaki E, Voulgari P V. (2023). Recurrent Scedosporium apiospermum cutaneous infection in a patient with rheumatoid arthritis: the potent role of IL-6 signaling pathway blockade: a case-based review. Journal of Fungi. 9(6):683.

Prasad P, Verma S, Surbhi, Ganguly N K, Chaturvedi V, Mittal S A. (2023). Rheumatoid arthritis: advances in treatment strategies. Molecular and Cellular Biochemistry. 478(1):69-88.

Pushpalatha D S S S, Kumaraswamy S, Selvaraj G K, Narayanaswamy R, Prabhakaran V S, Sivakumar T, Kesavan A. (2023). Plant-derived bioactive compounds: promising prospective uses in chronic inflammation. In: Natural products as cancer therapeutics. IGI Global. 254-274.

Qayyum S, Mehdi A. (2023). Potential efficacy of turmeric as an anti-inflammatory agent and antioxidant in the treatment of osteoarthritis. Khyber Medical University Journal. 15(3):190-197.

Qiang R, Huang H, Chen J, Shi X, Fan Z, Xu G, Qiu H. (2023). Carbon quantum dots derived from herbal medicine as therapeutic nanoagents for rheumatoid arthritis with ultrahigh lubrication and anti-inflammation. ACS Applied Materials & Interfaces. 15(32):38653-38664.

Quiñonez-Flores C M, González-Chávez S A, Del Río Nájera D, Pacheco-Tena C. (2016). Oxidative stress relevance in the pathogenesis of rheumatoid arthritis: a systematic review. BioMed Research International. 2016:6097417.

Radu, A. F., & Bungau, S. G. (2023). Nanomedical approaches in the realm of rheumatoid arthritis. *Ageing Research Reviews*, 101927.

Radu A F, Bungau S G. (2023). Nanomedical approaches in the realm of rheumatoid arthritis. Ageing Research Reviews. 101927.

Ralph J A, Morand E F. (2008). MAPK phosphatases as novel targets for rheumatoid arthritis. Expert Opinion on Therapeutic Targets. 12(7):795-808.

Rankin L C, Artis D. (2018). Beyond host defense: emerging functions of the immune system in regulating complex tissue physiology. Cell. 173(3):554-567.

Rao K, Roome T, Aziz S, Razzak A, Abbas G, Imran M, Shah M R. (2018). Bergenin loaded gum xanthan stabilized silver nanoparticles suppress synovial inflammation through modulation of the immune response and oxidative stress in adjuvant induced arthritic rats. Journal of Materials Chemistry B. 6(27):4486-4501.

Rao L, Xia S, Xu W, Tian R, Yu G, Gu C, Chen X. (2020). Decoy nanoparticles protect against COVID-19 by concurrently adsorbing viruses and inflammatory cytokines. Proceedings of the National Academy of Sciences. 117(44):27141-27147.

Rarey M, Kramer B, Lengauer T, Klebe G. (1996). A fast flexible docking method using an incremental construction algorithm. Journal of Molecular Biology. 261(3):470-489.

Release S. (2015). 1: Maestro, version 10.1, Schrödinger, LLC, New York.

Rezvantalab S, Drude N I, Moraveji M K, Güvener N, Koons E K, Shi Y, Kiessling F. (2018). PLGA-based nanoparticles in cancer treatment. Frontiers in Pharmacology. 9:1260.

Roumili I, Mayouf N, Charef N, Arrar L, Baghiani A. (2022). HPLC analysis, acute toxicity and anti-inflammatory effects of Salix alba L. barks extracts on experimental animal models. Indian Journal of Experimental Biology. 60(11):842-850.

Sadaoui N, Bec N, Barragan-Montero V, Kadri N, Cuisinier F, Larroque C, Khettal B. (2018). The essential oil of Algerian Ammodaucus leucotrichus Coss. & Dur. and its effect on the cholinesterase and monoamine oxidase activities. Fitoterapia. 130:1-5.

Saferding V, Blüml S. (2020). Innate immunity as the trigger of systemic autoimmune diseases. Journal of Autoimmunity. 110:102382.

Samarpita S, Rasool M. (2021). Cyanidin attenuates IL-17A cytokine signaling mediated monocyte migration and differentiation into mature osteoclasts in rheumatoid arthritis. Cytokine. 142:155502.

Saparbekova A A, Kantureyeva G O, Kudasova D E, Konarbayeva Z K, Latif A S. (2023). Potential of phenolic compounds from pomegranate (Punica granatum L.) by-product with significant antioxidant and therapeutic effects: A narrative review. Saudi Journal of Biological Sciences. 30(2):103553.

Schepetkin I A, Plotnikov M B, Khlebnikov A I, Plotnikova T M, Quinn M T. (2021). Oximes: Novel therapeutics with anticancer and anti-inflammatory potential. Biomolecules. 11(6):777.

Scherer H U, Häupl T, Burmester G R. (2020). The etiology of rheumatoid arthritis. Journal of Autoimmunity. 110:102400.

Sebaa A, Marouf A, Kambouche N, Derdour A. (2018). Phytochemical composition, antioxidant and antimicrobial activities of Ammodaucus leucotrichus fruit from Algerian Sahara. Oriental Journal of Chemistry. 34(1):519.

Seixas M J, Martins E, Reis R L, Silva T H. (2020). Extraction and characterization of collagen from elasmobranch byproducts for potential biomaterial use. Marine Drugs. 18(12):617.

Shan X, Zhang C, Mai C, Hu X, Cheng N, Chen W, Xie Y. (2021). The biogenesis, biological functions, and applications of macrophage-derived exosomes. Frontiers in Molecular Biosciences. 8:715461.

Sheela D, Uthayakumari F. (2013). GC-MS analysis of bioactive constituents from coastal sand dune taxon-Sesuvium portulacastrum (L.). Bioscience Discovery. 4(1):47-53.

Singh A, Anang V, Kumari K, Kottarath S K, Verma C. (2023). Role of lymphocytes, macrophages and immune receptors in suppression of tumor immunity. Progress in Molecular Biology and Translational Science. 194:269-310.

Soares M P, Teixeira L, Moita L F. (2017). Disease tolerance and immunity in host protection against infection. Nature Reviews Immunology. 17(2):83-96.

Solomon D H, Glynn R J, Karlson E W, Lu F, Corrigan C, Colls J, Ridker P M. (2020). Adverse effects of low-dose methotrexate: a randomized trial. Annals of Internal Medicine. 172(6):369-380.

Sorushanova A, Delgado L M, Wu Z, Shologu N, Kshirsagar A, Raghunath R, Zeugolis D I. (2019). The collagen suprafamily: from biosynthesis to advanced biomaterial development. Advanced Materials. 31(1):1801651.

Stegen M, Frey U H. (2022). The role of G protein-coupled receptor kinase 6 regulation in inflammation and pain. International Journal of Molecular Sciences. 23(24):15880.

Stump K L, Lu L D, Dobrzanski P, Serdikoff C, Gingrich D E, Dugan B J, Seavey M M. (2011). A highly selective, orally active inhibitor of Janus kinase 2, CEP-33779, ablates disease in two mouse models of rheumatoid arthritis. Arthritis Research & Therapy. 13(2):1-15.

Sujitha S, Rasool M. (2017). MicroRNAs and bioactive compounds on TLR/MAPK signaling in rheumatoid arthritis. Clinica Chimica Acta. 473:106-115.

Sun Y, Liu J, Xin L, Wen J, Zhou Q, Chen X, Zhang X. (2023). Xinfeng capsule inhibits inflammation and oxidative stress in rheumatoid arthritis by up-regulating LINC00638 and activating Nrf2/HO-1 pathway. Journal of Ethnopharmacology. 301:115839.

Tang F, Li L, Chen D. (2012). Mesoporous silica nanoparticles: synthesis, biocompatibility and drug delivery. Advanced Materials. 24(12):1504-1534.

Taylor P C, Atzeni F, Balsa A, Gossec L, Müller-Ladner U, Pope J. (2021). The key comorbidities in patients with rheumatoid arthritis: a narrative review. Journal of Clinical Medicine. 10(3):509.

Taylor P C, Laedermann C, Alten R, Feist E, Choy E, Haladyj E, Tanaka Y. (2023). A JAK inhibitor for treatment of rheumatoid arthritis: The Baricitinib experience. Journal of Clinical Medicine. 12(13):4527.

Taylor S R, Ramsamooj S, Liang R J, Katti A, Pozovskiy R, Vasan N, Goncalves M D. (2021). Dietary fructose improves intestinal cell survival and nutrient absorption. Nature. 597(7875):263-267.

Thalhamer T, McGrath M A, Harnett M M. (2008). MAPKs and their relevance to arthritis and inflammation. Rheumatology. 47(4):409-414.

Islam M T, Quispe C, Herrera-Bravo J, Rahaman M M, Hossain R, Sarkar C, Calina D. (2022). Activities and molecular mechanisms of diterpenes, diterpenoids, and their derivatives in rheumatoid arthritis. Evidence-Based Complementary and Alternative Medicine. 2022:4787643.

Tukiran T, Salma N A, Sutoyo S, Sabila F I. (2023). Anti-arthritic activity of combination of Caesalpinia sappan and Zingiber officinale extracts in complete Freund's adjuvant-induced arthritic in rats. Tropical Journal of Natural Product Research. 7(11):5164-5171.

Türk S M, Cansu D Ü, Teke H Ü, Kaşifoğlu T, Meltem Akay O, Bilgin M, Korkmaz C. (2018). Can we predict thrombotic tendency in rheumatoid arthritis? A thromboelastographic analysis (with ROTEM). Clinical Rheumatology. 37:2341-2349.

Usman M, Cheng S, Boonyubol S, Cross J S. (2023). Evaluating green solvents for bio-oil extraction: advancements, challenges, and future perspectives. Energies. 16(15):5852.

Wang H J, Su C P, Lai C C, Chen W R, Chen C, Ho L Y, Lien C Y. (2022). Deep learning-based computer-aided diagnosis of rheumatoid arthritis with hand X-ray images conforming to modified total Sharp/van der Heijde score. Biomedicines. 10(6):1355.

Watanabe Y, Tsuchiya A, Terai S. (2021). The development of mesenchymal stem cell therapy in the present, and the perspective of cell-free therapy in the future. Clinical and Molecular Hepatology. 27(1):70.

Weyand C M, Goronzy J J. (2021). The immunology of rheumatoid arthritis. Nature Immunology. 22(1):10-18.

Whitaker R H, Cook J G. (2021). Stress relief techniques: p38 MAPK determines the balance of cell cycle and apoptosis pathways. Biomolecules. 11(10):1444.

Xu L, Chang C, Jiang P, Wei K, Zhang R, Jin Y, He D. (2022). Metabolomics in rheumatoid arthritis: advances and review. Frontiers in Immunology. 13:961708.

Xu L, Xiang J, Liu Y, Xu J, Luo Y, Feng L, Peng R. (2016). Functionalized graphene oxide serves as a novel vaccine nano-adjuvant for robust stimulation of cellular immunity. Nanoscale. 8(6):3785-3795.

Yang Y, Guo Z, Chen W, Wang X, Cao M, Han X, Qiu Z. (2021). M2 macrophage-derived exosomes promote angiogenesis and growth of pancreatic ductal adenocarcinoma by targeting E2F2. Molecular Therapy. 29(3):1226-1238.

Yang Y, Liu Y, Yu H, Xie Q, Wang B, Jiang S, Wang W. (2022). Sesquiterpenes from Kadsura coccinea attenuate rheumatoid arthritis-related inflammation by inhibiting the NF-κB and JAK2/STAT3 signal pathways. Phytochemistry. 194:113018.

Yao Y, Cai X, Zheng Y, Zhang M, Fei W, Sun D, Zheng C. (2022). Short-chain fatty acids regulate B cell differentiation via the FFA2 receptor to alleviate rheumatoid arthritis. British Journal of Pharmacology. 179(17):4315-4329.

Zabotti A, Finzel S, Baraliakos X, Aouad K, Ziade N, Iagnocco A. (2020). Imaging in the preclinical phases of rheumatoid arthritis. Clinical and Experimental Rheumatology. 38(3):536-542.

Zamani B, Farshbaf S, Golkar H R, Bahmani F, Asemi Z. (2017). Synbiotic supplementation and the effects on clinical and metabolic responses in patients with rheumatoid arthritis: a randomized, double-blind, placebo-controlled trial. British Journal of Nutrition. 117(8):1095-1102.

Zampeli E, Vlachoyiannopoulos P G, Tzioufas A G. (2015). Treatment of rheumatoid arthritis: unraveling the conundrum. Journal of Autoimmunity. 65:1-18.

Zamudio-Cuevas Y, Martínez-Flores K, Martínez-Nava G A, Clavijo-Cornejo D, Fernández-Torres J, Sánchez-Sánchez R. (2022). Rheumatoid arthritis and oxidative stress. Cellular and Molecular Biology. 68(6):174-184.

Zeng F, Li S, Yang G, Luo Y, Qi T, Liang Y, Xu X. (2021). Design, synthesis, molecular modeling, and biological evaluation of acrylamide derivatives as potent inhibitors of human dihydroorotate dehydrogenase for the treatment of rheumatoid arthritis. Acta Pharmaceutica Sinica B. 11(3):795-809.

Zhang Q, Dehaini D, Zhang Y, Zhou J, Chen X, Zhang L. (2018). Neutrophil membrane-coated nanoparticles inhibit synovial inflammation and alleviate joint damage in inflammatory arthritis. Nature Nanotechnology. 13(12):1182-1190.

Zhang Q, Peng W, Wei S, Wei D, Li R, Liu J, Pu X. (2019). Guizhi-Shaoyao-Zhimu decoction possesses anti-arthritic effects on type II collagen-induced arthritis in rats via suppression of inflammatory reactions, inhibition of invasion and migration, and induction of apoptosis in synovial fibroblasts. Biomedicine & Pharmacotherapy. 118:109367.

Zhao J, Wei K, Jiang P, Chang C, Xu L, He D. (2022). G-protein-coupled receptors in rheumatoid arthritis: recent insights into mechanisms and functional roles. Frontiers in Immunology. 13:907733.

Zhao W, Zheng L, Yang J, Li Y, Zhang Y, Ma T, Wang Q. (2023). Dissolving microneedle patches-mediated percutaneous delivery of tetramethylpyrazine for rheumatoid arthritis treatment. European Journal of Pharmaceutical Sciences. 184:106409.

Zhou C, Dowlatshah S, Hansen F A, Pedersen-Bjergaard S. (2024). Generic conditions for electromembrane extraction of polar bases. Talanta. 267:125215.

Zhou J, Wang F, Qu Y, Sun H, Liu Z, Sun H. (2022). Lesions of bones and joints associated with rheumatism. In: Radiology of Infectious and Inflammatory Diseases- Volume 5: Musculoskeletal System (pp. 285-332). Singapore: Springer Nature Singapore.

Zhu L, Zhang Z, Xia N, Zhang W, Wei Y, Huang J, Yang L. (2020). Anti-arthritic activity of ferulic acid in complete Freund's adjuvant-induced arthritis in rats: JAK2 inhibition. Inflammopharmacology. 28:463-473.

Ziani B E, Rached W, Bachari K, Alves M J, Calhelha R C, Barros L, Ferreira I C. (2019). Detailed chemical composition and functional properties of Ammodaucus leucotrichus Cross & Dur. and Moringa oleifera Lamarck. Journal of Functional Foods. 53:237-247.

الملخص

بحثت هذه الدراسة في إمكانات مستخلصات بذور الكمون الصوفي *Ammodaucus leucotrichus* كعامل علاجي لالتهاب المفاصل الروماتويدي والتهاب المفاصل. تم اختبار مستخلصات الميثانول والهكسان لخصائصها المضادة للالتهابات والمضادة لالتهاب المفاصل. أظهر مستخلص الميثانول قدرة كبيرة على تثبيط التربسين، وأظهر مستخلص الهكسان n قدرة ملحوظة على منع تمسخ ألبومين المصل البقري. تم إحداث التهاب المفاصل الروماتويدي في نماذج الفئران باستخدام طريقتين: التحصين باستخدام مساعد فرويند الكامل ومحلول الكولاجين من النوع الثاني المشتق من غضروف الدجاج. تم تقييم الفعالية العلاجية للمستخلصات بجرعات مختلفة ومقارنتها مع الميثوتريكسيت، وهو علاج قياسي لالتهاب المفاصل الروماتويدي لدى البشر. أدت كل من المستخلصات والميثوتريكسيت إلى تحسين حركة الفئران، كما يتضح من زيادة مسافة المشي، وطول الخطوة، والمسافة داخل الخطوة، ومنطقة البصمة. كما أنها أثرت بشكل إيجابي على العلامات البيوكيميائية للالتهاب. في دراسات الالتحام السيليكو حددت عدة مركبات ذات نشاط مثبط محتمل للتربسين: - 2هيدروكسي أسيتو هيدرازيد يظهر تأثيرات مثبطة متفوقة مقارنة بالديكلوفيناك. في الختام، تقدم هذه الدراسة أدلة دامغة تشير إلى إمكانات بذور *Ammodaucus leucotrichus*

Abstract

This study investigated the potential of *Ammodaucus leucotrichus* seed extracts as a therapeutic agent for rheumatoid arthritis and joint inflammation. Methanol and n-hexane extracts were tested for their anti-inflammatory and anti-arthritic properties. The methanol extract demonstrated a significant ability to inhibit trypsin, and the n-hexane extract showed a remarkable ability to prevent the denaturation of bovine serum albumin. Rheumatoid arthritis was induced in rat models using two methods: immunization with Freund's complete adjuvant and a solution of type II collagen derived from chicken cartilage. The therapeutic efficacy of the extracts was evaluated at varying doses and compared with methotrexate, a standard treatment for rheumatoid arthritis in humans. Both the extracts and methotrexate improved the mobility of the rats, as evidenced by increased walking distance, stride length, intra-step distance, and footprint area. They also positively influenced biochemical markers of inflammation. *In silico* docking studies identified several compounds with potential trypsin inhibitory activity: 2-hydroxyaceto hydrazide showing superior inhibitory effects compared to diclofenac. In conclusion, this study provides compelling evidence that suggests the potential of *Ammodaucus leucotrichus* seed

Résumé

Cette étude a examiné le potentiel des extraits de graines d'*Ammodaucus leucotrichus* en tant qu'agent thérapeutique contre la polyarthrite rhumatoïde et l'inflammation des articulations. Les extraits de méthanol et de n-hexane ont été testés pour leurs propriétés anti-inflammatoires et anti-arthritiques. L'extrait au méthanol a démontré une capacité significative à inhiber la trypsine, et l'extrait au n-hexane a montré une capacité remarquable à empêcher la dénaturation de l'albumine sérique bovine. La polyarthrite rhumatoïde a été induite chez des modèles de rats à l'aide de deux méthodes : l'immunisation avec l'adjuvant complet de Freund et une solution de collagène de type II dérivée du cartilage de poulet. L'efficacité thérapeutique des extraits a été évaluée à différentes doses et comparée au méthotrexate, un traitement standard de la polyarthrite rhumatoïde chez l'homme. Les extraits et le méthotrexate ont amélioré la mobilité des rats, comme en témoigne l'augmentation de la distance de marche, de la longueur des foulées, de la distance intra-pas et de la surface de l'empreinte. Ils ont également influencé positivement les marqueurs biochimiques de l'inflammation. Des études d'amarrage in silico ont identifié plusieurs composés ayant une activité potentielle d'inhibition de la trypsine : le 2-hydroxyacéto hydrazide présentant des effets inhibiteurs supérieurs à ceux du diclofénac. En conclusion, cette étude fournit des preuves convaincantes suggérant le potentiel des graines d'*Ammodaucus leucotrichus*